EUROPEAN COMMISSION

European Research Area

CArbon-14 Source Term

CAST

Rates of steel corrosion and carbon-14 release from irradiated steels – state of the art review (D2.1)

Author(s):

S.W. Swanton, G.M.N. Baston and N.R. Smart **(AMEC)**

Date of issue of this report: 07/01/2015

The project has received funding form the European Union's European Atomic Energy Community's (Euratom) Seventh Framework Programme FP7/2207-2013 under grant agreement no. 604779, the CAST project.		
Dissemination Level		
PU	Public	**X**
RE	Restricted to the partners of the CAST project	
CO	Confidential, only for specific distribution list defined on this document	

EURATOM

CAST – Project Overview

The CAST project (CArbon-14 Source Term) aims to develop understanding of the potential release mechanisms of carbon-14 from radioactive waste materials under conditions relevant to waste packaging and disposal to underground geological disposal facilities. The project focuses on the release of carbon-14 as dissolved and gaseous species from irradiated metals (steels, Zircaloys), irradiated graphite and from ion-exchange materials as dissolved and gaseous species.

The CAST consortium brings together 33 partners with a range of skills and competencies in the management of radioactive wastes containing carbon-14, geological disposal research, safety case development and experimental work on gas generation. The consortium consists of national waste management organisations, research institutes, universities and commercial organisations.

The objectives of the CAST project are to gain new scientific understanding of the rate of re-lease of carbon-14 from the corrosion of irradiated steels and Zircaloys and from the leaching of ion-exchange resins and irradiated graphites under geological disposal conditions, its speciation and how these relate to carbon-14 inventory and aqueous conditions. These results will be evaluated in the context of national safety assessments and disseminated to interested stakeholders. The new understanding should be of relevance to national safety assessment stakeholders and will also provide an opportunity for training for early career researchers.

For more information, please visit the CAST website at:
http://www.projectcast.eu

CAST		
Work Package: 2	CAST Document no. :	Document type:
Task: 2.1	CAST-2015-D2.1	R
Issued by: AMEC		Document status:
Internal no. : AMEC/201265/001 Issue 4.1		Final

Document title
Rates of steel corrosion and carbon-14 release from irradiated steels – state of the art review

Executive Summary

Carbon-14 is a key radionuclide in the assessment of the safety of underground geological disposal facilities for radioactive wastes. Carbon-14 has a radioactive half-life of 5,730 years, so if it can be retained within the multi-barrier system of a disposal facility for sufficient time it will decay. However, it is possible for the carbon-14 in wastes to be released as a result of dissolution and/or waste degradation processes. Carbon-14 can be released in a variety of chemical forms, both organic and inorganic, depending on the nature of the waste materials and the chemical conditions. It may also be transported as volatile species in a bulk gas phase (primarily hydrogen from the corrosion of metal wastes and containers) if the rates of gas generation, combined with the hydrogeology of a disposal facility, are such that a bulk gas phase is able to form and migrate through the near field and geosphere to the biosphere.

The International CAST (CArbon-14 Source Term) project, part-funded through the Euratom Seventh Framework Programme, aims to develop understanding of the generation and release of carbon-14 from radioactive waste materials under conditions relevant to waste packaging and disposal to underground geological disposal facilities (GDFs). Work Package 2 "Steels" (WP2) is focusing on carbon-14 releases from irradiated steel wastes, which contribute a significant proportion of the carbon-14 inventory of radioactive wastes worldwide. These wastes comprise the irradiated ferrous metal components of nuclear reactor structures and nuclear fuel assemblies. In particular, the pressure vessels of various designs of nuclear reactors have been made from low-carbon (mild) steels, and reactor internals and fuel assembly components have been manufactured from stainless steel and/or nickel alloys due to their greater resistance to general corrosion by water. Carbon-14 is formed in steels primarily by the thermal neutron activation of nitrogen-14 that is present in all steels as a trace component.

Under WP2, it is planned to undertake both experimental and modelling studies to develop further understanding of the speciation and rate of both carbon-14 and stable carbon release from the corrosion of irradiated and unirradiated steels under conditions relevant to deep geological repositories. The objective of this report is to review the current state of understanding of steel corrosion rates and carbon-14 releases from irradiated steels under conditions relevant to the storage and long-term disposal of radioactive wastes and thereby incorporate information available from outside the CAST project into CAST WP2.

Corrosion data

The review of corrosion data has extended a previous compilation of data for carbon and stainless steels, undertaken in 2006/07, to include new information in the published literature as well as recent information, some of it as yet unpublished, from national programmes supplied by partners in WP2. This review identifies the various environments that could be experienced by waste packages containing cement-encapsulated irradiated metal wastes during their long-term management (i.e. during surface storage and transportation, and then in a geological disposal facility (GDF), both before and after resaturation with a groundwater that could have a high chloride concentration). For each environment, relevant corrosion rate data for carbon steel and stainless steels have been compiled and reviewed critically. The literature review has focused on metal loss and gas generation as a result of general corrosion rather than localised corrosion. The effects of a number of variables (including oxygen concentration, temperature and chloride concentration) on corrosion rates have been considered.

A number of additional datasets have been identified and summarised in this review. In general, they have not changed the view of the likely corrosion rates for carbon steel in the conditions expected during waste disposal, developed previously. In the case of stainless steel, however, a recent paper by Yoshida *et al.* has provided data for the very low corrosion rates experienced by stainless steels under anoxic alkaline conditions, and these results are important in relation to the issue of carbon-14 release from stainless steels in the longer term post-closure phase of a GDF. The data are all below 0.01 μm yr^{-1}, which was the value recommended as an upper limit in the previous review. The new data indicate a mean anaerobic corrosion rate of 0.0008 μm yr^{-1} for 18/8 stainless steel at 30°C after 2 years exposure. The Japanese data also show a decrease of the anaerobic corrosion rate under alkaline conditions with time (the significance of which is not yet clear), and a temperature dependence, neither of which could be discriminated previously.

It is noted that all of the corrosion data compiled in this review were obtained for unirradiated materials. It is known that neutron irradiation can change the microstructure of steels, in particular radiation-induced segregation of alloy components can arise at grain boundaries. However, the overall impact of irradiation on the long-term corrosion rates of waste steels is unknown.

Carbon and carbon-14 releases from iron and steels

The review of carbon-14 releases from steels has sought to include all available information on the releases of stable carbon (carbon-12 and carbon13) from irons and steels to supplement the very limited information available on carbon-14 releases from irradiated steels. In fact, the review has found that information on the chemical forms of carbon released from steels by corrosion is also limited and the processes involved are not well understood.

The speciation of carbon releases from steels on corrosion is likely to be determined both by the chemical form of the carbon in the steel and the corrosion conditions, in particular the availability of oxygen. In this report, the range of possible carbon-14 species in irradiated steels has been considered to evaluate the range of carbon-14 species that could be released from irradiated steels by corrosion.

In the low carbon-content steel wastes of interest in CAST WP2 (generally <0.3wt% carbon), carbon may be present in steels in the form of interstitial carbides, dissolved in the principal iron phase of the steel (ferrite in carbon steel or austenite in 300–series stainless steel), as a distinct carbide phase with other alloying components (e.g. niobium, manganese) and/or as carbonitride phases. The distribution of carbon between dfferent species will depend on the steel composition and its production process.

The reactivity of the different carbon species that may be present in a steel on contact with water varies considerably. Some alloying components (e.g. niobium, titanium) form very stable interstitial carbide phases that react only slowly with acids releasing methane and hydrogen. In contrast, the electropositive metals (e.g. aluminium) form reactive carbides that are essentially ionic in character, rapidly releasing hydrocarbons related to the nature of the carbide ion present (acetylene in the case of calcium carbide, CaC_2) on contact with water. The smaller-sized transition metal elements (e.g. iron, manganese) form so-called intermediate carbides in which carbon atoms may form chains through a distorted metal lattce; multiple carbide stoichiometries are possible and these carbides may be hydrolysed by water and dilute acids releasing a range of hydrocarbon species and hydrogen. In general, carbonitride phases tends to be more resistant to hydrolysis than the equivalent carbide phase.

There is considerable uncertainty whether carbon-14 produced by activation of nitrogen-14 will be present in the same chemical forms in irradiated steels as the carbon present in the steels at the time of their production; radiation-induced segregation of alloying components of steel may also contribute to a redistribution of the carbon species.

On the basis of the known information on the reactions of metal carbides and carbonitrides with water, the following carbon-14 release behaviour might be expected on leaching an irradiated steel.

- As the steel slowly corrodes, the carbon-14 in its different chemical forms will be exposed to the waste disposal environment; different forms of carbon-14 may be expected to be released in different ways.
- Dispersed ionic and intermediate carbide phases and interstitial carbon present in the iron phase may be hydrolysed over relatively short time periods to form methane, and other hydrocarbons.
- Intermediate carbonitrides may be hydrolysed at a much slower rate than the equivalent carbides to yield a range of products that may include hydrocarbons and compounds containing C-N bonds such as amines and cyanides.
- Stable carbides and carbonitride phases may react only very slowly (if at all) and may be released in particulate form.

Experiments on inactive iron-water systems have shown clear evidence for the release of carbon as hydrocarbon species as a result of the hydrolysis of carbide species in the iron. A variety of species ranging from C1 to C5 hydrocarbons have been identified in the gas phase in separate studies, and quantitative conversion of carbide carbon to hydrocarbons has been reported. The mechanism of hydrocarbon formation is proposed to occur through processes similar to those occurring in Fischer-Tropsch (FT) synthesis (hydrocarbon formation from CO/H_2 mixtures over a metal catalyst). It is suggested that the carbide species exposed at

the iron surface may be similar to the intermediates formed on the surfaces of metal catalysts in the FT synthesis.

In contrast, in Japanese experiments on inactive carbon steel and iron carbide, which focused on releases to solution, carbon releases were presented as arising primarily as soluble organic species, with some of the dissolved carbon being inorganic. A range of low-molecular weight organic species were identified on the basis of high performance liquid chromatography, although these identifications must be treated as tentative. Carbon releases from iron carbide were identified as both inorganic and organic, apparently at odds with the results of iron-water studies. These findings remain to be corroborated.

The information on carbon-14 release from irradiated steels is sparse; only three experimental studies have been performed to date, all in Japan. Unfortunately, a lack of reports available in English, providing sufficient details of the materials and the experimental methodologies used, hinders a proper evaluation of these studies. The findings of these studies are outlined below, but again require corroboration:

- In an experiment in which a sample of irradiated stainless steel from the upper grid of a BWR was leached in a pH 10 cement-equilibrated water, carbon-14 was reported to be released to the solution phase as a mixture of inorganic (25-34%) and organic (66-75%) species. No measurements were made of gas phase releases, and no information is available concerning the amount of carbon-14 released.
- In experiments with irradiated metals where the sample was first acid-cleaned to remove the passivating oxide film, carbon-14 is reported to be released from irradiated stainless steel, nickel alloy and zirconium alloy into solution at rates that are consistent with metal corrosion rates.
- In the most recent experiment reported, a small amount of carbon-14 was reported to be released to the gas phase on leaching irradiated stainless steel in alkaline solution for 42 months; the distribution of the 4.76 Bq released was reported to be 25% to the gas phase with a ratio of organic to inorganic carbon-14 of nearly one in the solution phase. Organic species in solution were reported to be predominantly in anionic forms (i.e. carboxylates) rather than neutral species (e.g. alcohols).

This review has highlighted the current lack of well-documented inactive studies of the release of stable carbon from low-carbon and stainless steels that include measurements of carbon releases to both the gas phase and to the solution phase under anaerobic alkaline conditions. Such studies, which are planned under CAST WP2, are expected to throw light onto the apparent discrepancy in the observed speciation of carbon release from iron and those performed on the Japanese programme. A clearer understanding of the speciation of carbon releases from steels undergoing corrosion will aid the development of advanced methods for determining the speciation of much smaller quantities of carbon-14 released from irradiated steels in the corrosion experiments planned under CAST WP2.

List of Contents

Executive Summary i
List of Contents v
1 Introduction 1
1.1 Context 1
1.2 Objectives and scope of this review 4
1.2.1 Scope 6
1.3 Sources of information 7
1.4 Structure of this report 8
2 Overview of steel wastes containing carbon-14 9
2.1 Carbon steels 9
2.2 Stainless steels 9
2.3 Chemical form of carbon-14 in steels 12
2.4 Reactor steel wastes 16
3 Mechanisms of corrosion 20
3.1 Types of corrosion 20
3.2 Corrosion processes affecting carbon steel 21
3.3 Corrosion processes affecting stainless steel 25
3.4 Effect of irradiation on corrosion 26
3.5 Measurement of corrosion rates 27
4 Environmental conditions during the storage and disposal of steel wastes 28
4.1 Use of cements in the storage and disposal of steel wastes 28
4.2 Environmental conditions during waste management 30
4.2.1 Conditions pre-backfilling 31
4.2.1.1 Atmospheric exposure 31
4.2.1.2 Aqueous exposure 32
4.2.2 Conditions post-backfilling 33
4.2.2.1 Atmospheric exposure 34
4.2.2.2 Aqueous exposure 34
4.3 Oxygen and water availability 34
5 Corrosion rates of carbon steels during waste management 36
5.1 Neutral solutions 36
5.1.1 Aerobic neutral solutions 36
5.1.1.1 Effect of temperature 36
5.1.1.2 Effect of oxygen concentration 37
5.1.1.3 Effect of chloride concentration 43
5.1.1.4 Effect of dissolved gases 43
5.1.1.5 Effect of surface condition 44
5.1.1.6 Effect of radiation 44
5.1.1.7 Effect of hydrodynamics 44
5.1.1.8 Effect of corrosion product build up and scaling 44
5.1.2 Anaerobic neutral solutions 45
5.2 Alkaline solutions 47
5.2.1 Aerobic alkaline solutions 47
5.2.2 Anaerobic alkaline solutions 49

5.3 Corrosion in concrete 52
5.3.1 Aerobic 52
5.3.2 Anaerobic 52
5.4 Atmospheric corrosion 53
5.5 Overview of carbon steel corrosion data 54
5.5.1 Aerobic corrosion in grout, low chloride 54
5.5.2 Anaerobic corrosion, low chloride, alkaline conditions 56
5.5.3 Anaerobic corrosion, high chloride, alkaline conditions 57
6 Corrosion rates of stainless steels during waste management 82
6.1 Neutral solutions 82
6.1.1 Aerobic neutral solutions 82
6.1.2 Anaerobic neutral solutions 85
6.2 Alkaline solutions 85
6.2.1 Aerobic alkaline solutions 85
6.2.2 Anaerobic alkaline solutions 85
6.3 Corrosion in concrete 88
6.4 Atmospheric corrosion 89
6.5 Overview of stainless steel corrosion data 90
6.5.1 Atmospheric corrosion 90
6.5.2 Aerobic corrosion in grout, low chloride 91
6.5.3 Anaerobic corrosion, low chloride 92
6.5.4 Anaerobic corrosion, high chloride 92
7 Carbon and carbon-14 release from steels 104
7.1 Studies of stable carbon release 104
7.2 Studies of carbon-14 release from irradiated steels 112
7.3 Summary of current understanding 116
8 Discussion and conclusions 120
8.1 Steel corrosion rates 120
8.1.1 Carbon steel 120
8.1.1.1 Aerobic corrosion in grout 120
8.1.1.2 Anaerobic corrosion, alkaline conditions 121
8.1.2 Stainless steel 122
8.1.2.1 Aerobic corrosion in grout 122
8.1.2.2 Anaerobic corrosion, alkaline conditions 122
8.1.3 Effects of irradiation 122
8.2 Carbon and carbon-14 release from irradiated steels 123
9 Acknowledgements 125
10 References 126
Appendix 1 147
Appendix 2 153

1 Introduction

1.1 Context

Carbon-14 is a key radionuclide in the assessment of the safety of underground disposal facilities for radioactive wastes [1, 2]. Carbon-14 has a radioactive half-life of 5,730 years, so if it can be retained within the multi-barrier system of a disposal facility for sufficient time it will decay. However, it is possible for the carbon-14 in wastes to be released as a result of dissolution and or waste degradation processes. Carbon-14 can be released in a variety of chemical forms, both organic and inorganic, depending on the nature of the waste materials and the chemical conditions. In several national programmes, carbon-14, transported as dissolved species in moving groundwater, has been identified as a key radionuclide in radiological assessments [3, 4, 5]. In addition, if a bulk gas phase can be formed in the engineered disposal facility (e.g. as a result of hydrogen production from the corrosion of metal wastes and containers), there is the potential for carbon-14 to be released and transported in the gas phase [1]. The radiological consequences of the release of gaseous carbon-14 bearing species has been identified as a potential issue from generic assessments undertaken on the UK programme [6, 7]; the impact of gas phase carbon-14 releases has also been considered in Japan [3].

Carbon-14 in wastes is produced predominantly by the thermal neutron activation of precursor species present in nuclear fuel components and reactor core structures. The principal source of production is nitrogen-14, but carbon-13 and oxygen-17 are also important contributors for certain materials. Carbon-14 is also produced in nuclear fuel from tertiary fission, but this production route makes only a very minor contribution. For example, the dominant production routes for carbon-14 in the core components of a UK Advanced Gas-cooled Reactor (AGR) and typical elemental concentrations of the target isotopes on which these estimates are based are shown in Table 1 and Table 2, respectively [8].

Table 1: Dominant nuclear production routes for carbon-14 arising from AGR operation.

Production reaction	Natural abundance of target isotope	Thermal neutron (2200 ms^{-1}) cross-section (barns)	Proportion of inventory from production route		
			AGR fuel cladding stainless steel	AGR moderator graphite	AGR fuel (UO_2)
$^{14}N(n,p)^{14}C$	99.63%	1.76	~100%	~60%	56%
$^{17}O(n,\alpha)^{14}C$	0.04%	0.226	~0%	~0%	42%
$^{13}C(n,\gamma)^{14}C$	1.10%	0.0013	~0%	~40%	0%
Tertiary Fission			0%	0%	2%

Table 2: Target element concentrations assumed in activation calculations for AGR reactor core components.

Target element	Target element concentration in material (ppm)		
	AGR fuel cladding stainless steel	AGR moderator graphite	AGR fuel (UO_2)
N	450	15	8.5
O	250	100	118,500
C	150	1,000,000	10

The International CAST (CArbon-14 Source Term) project, part-funded through the Euratom Seventh Framework Programme, aims to develop understanding of the generation and release of carbon-14 from radioactive waste materials under conditions relevant to waste packaging and disposal to underground geological disposal facilities (GDFs)[1]. The project is focusing on carbon-14 releases from irradiated metals (steels and Zircaloy),

[1] The terminology varies between national waste management organisations; the term *geological disposal facility* (GDF) is now preferred in the UK (for example), whereas *geological repository* has been used historically and remains in widespread use. The term GDF is used predominantly in this report.

irradiated graphite and spent ion-exchange materials as dissolved and gaseous species. The scientific understanding obtained from these studies will then be considered in terms of national disposal programmes and the impact on safety assessments.

Work Package 2 (WP2) of the CAST project is concerned with carbon-14 releases from irradiated steels. The main objectives of WP2 Steels are:

- to develop analytical techniques for the identification and quantification of carbon-14 species formed during corrosion of irradiated steels under conditions relevant to cement-based GDFs;
- to validate activation models by measuring carbon-14 inventories in irradiated steel;
- to carry out experiments and modelling to develop further understanding of the speciation and rate of carbon-12/carbon-13 and carbon-14 release from corrosion of irradiated and unirradiated steels under conditions relevant to GDFs;
- to incorporate information from existing and ongoing projects elsewhere on steel corrosion into this work package to make the current understanding available.

This report is designed to meet the last of these four principal objectives.

Several of the countries represented by participants in WP2 are considering or developing cement-based geological disposal concepts for the long-term management of long-lived intermediate-level radioactive wastes [e.g. 9, 10, 11, 12], such as the irradiated steel wastes that arise from reactor operations and decommissioning. For this reason, the emphasis of the work in WP2 is on the releases of carbon-14 from steel wastes under the conditions that will develop in the longer term in a cement-based facility after its closure. In particular, once the facility becomes resaturated with water and the remaining oxygen has been consumed by corrosion processes, conditions are expected to become anaerobic and highly alkaline.

The scope of the experimental programme planned under WP2 is summarised in Table 3. Two experimental parameters are being varied across the suite of planned experiments: pH and the availability of oxygen. The typical scenario for most of the planned experiments is the corrosion of irradiated steel in a reducing, highly alkaline cementitious environment

(stainless steel = AMEC/NRG, VTT, JRC and PSI, mild steel = SCK.CEN). Because pH values lower than 12 could exist in some environments (e.g. if decomposition of organic materials neutralises the alkalinity of the available cement), lower pH values will be used in some studies (stainless steel at pH 8-9 VTT, pH 5-6 JRC, and pH 1-3 KIT). In addition, Enresa and Ciemat will conduct aerobic experiments to address the non-reducing conditions that will prevail during waste storage and for a relatively short period after GDF closure. Finally, VTT will undertake supporting studies on unirradiated specimens of stainless steel, carbon steel, iron and iron carbide and RWMC will investigate unirradiated stainless steel.

1.2 Objectives and scope of this review

The objective of this report is to review the current state of understanding of steel corrosion rates and carbon-14 releases from irradiated steels under conditions relevant to the storage and long-term disposal of radioactive wastes and thereby incorporate information available from outside the CAST project into CAST WP2.

The information contained in this review can be used in two ways:

- to support the design of the experimental programme planned under CAST WP2; and
- to support the assessment of the potential radiological impact of carbon-14 released from steel wastes during storage, disposal operations and after closure of a disposal facility.

This report forms Deliverable 2.1 of CAST WP2.

Table 3: Intended scope of corrosion experiments from irradiated and unirradiated steels planned under CAST WP2 (as at June 2014).

Organisation	Samples			Conditions	pH				Other
	Material	Grade (description)	Irradiated	Anaerobic	> 12	8-11	4-7	1-3	
AMEC/NRG	Stainless	316L(N)	✓	✓	✓				Ambient
PSI	Stainless PH	1.4541 (X6CrNiTi18-10) OR 1.4550 (X6CrNiNb18-10) OR 1.4571 (X6CrNiMoTi17-12-2)	✓	✓	✓				Ambient
RWMC	Stainless	18Cr-8Ni (~304)	No	✓	✓	✓			Ambient
SCK-CEN	Carbon-steel	JRQ (BR2 PV) (0.18%C)	✓	✓	✓				80°C
VTT	Stainless	Olkiluoto core grid	✓	✓	✓	✓			Ambient
	Stainless	Loviisa pipe, Russian O8X18H10T (~321) (0.08%C)	No	✓	✓	✓			Ambient
	Carbon steel	Japanese high-C (1.2%C)							
	Stainless	Steel powder (0.01%C)							
	Iron	Iron powder with 4% C as Fe_3C							
KIT	Stainless PH	1.4568 (X7CrNiAl17-7) (0.07wt% C)	✓	✓				✓	36.8bar Ar /3.2 bar H_2
JRC-ITU	Stainless	NIMPHE fuel cladding (316-like)	✓	✓	✓		✓		
Ciemat/Enresa	Stainless	Jose Cabrera PWR internal (304)	✓	No	✓		✓	✓	20 ± 3°C

PH = Precipitation hardened steel

1.2.1 Scope

A wide variety of ferrous metals have been used in nuclear power applications ranging from fuel assemblies to reactor structures and waste containers. This review is focused on those steels that may be used in neutron radiation fields and which could therefore contain significant concentrations of carbon-14. The main categories of steel under consideration in the current report are carbon steels and stainless steels and these are introduced in Section 2.

Steels corrode under both aerobic and anaerobic[2] conditions, and will generate hydrogen under anaerobic conditions. The rate and nature of the corrosion processes depend on the composition of the steel, the temperature and the local environmental conditions.

This report identifies the various corrosive environments that could be experienced by both containers and encapsulated metal wastes during their long-term management (*i.e.* during surface storage and transportation, and then in a GDF, both before and after re-saturation with a groundwater). For each environment, relevant corrosion rate data for carbon steel and stainless steel have been compiled from the literature. The literature survey focused on metal loss and gas generation as a result of general corrosion rather than localised corrosion (the latter is unlikely to contribute significantly to gas generation). The effects on the corrosion rates of a number of variables (including oxygen concentration, temperature and chloride concentration) are considered.

A summary of corrosion rate data [13] was originally compiled to support gas generation calculations performed for the Nuclear Decommissioning Authority's Radioactive Waste Management Directorate (NDA RWMD, now Radioactive Waste Management Limited (RWM), a wholly-owned subsidiary of the NDA) for UK intermediate-level wastes. These published data on corrosion rates under relevant conditions were last reviewed in 2007 and consequently a survey of more recent literature was carried out to expand the database of available information as an input to the current report for the CAST project. It should be

[2] In this report, the terms "aerobic" and "anaerobic" are used interchangeably with "oxic" and "anoxic" respectively.

noted that the review carried out in support of the NDA RWMD gas generation calculations was focused on bulk gas generation rather than carbon-14 release. It considered only general, uniform corrosion, which is the mechanism for hydrogen production by anaerobic corrosion processes. For some metals, such as stainless steel, the rate of release of carbon-14 may depend on the location of the carbon in the metal and localised corrosion processes, such as intergranular corrosion, may have a role since carbon-14 may be concentrated near grain boundaries.

The rate of release of carbon-14 present within irradiated steel will be determined by the rate of steel corrosion as well as the distribution and concentration of carbon-14 present in the metal. Whether the carbon-14 will be released as a gaseous or dissolved species or as a solid phase will depend on the chemical form of the carbon within the metal and the reactivity of the carbon species in the corrosive environment. The possible forms of carbon-14 in irradiated steels and the chemical forms in which they may be released have therefore been considered in this review. Experimental information on the rates and speciation of both stable carbon (carbon-12 and carbon-13) releases from inactive ferrous metals and radioactive carbon-14 releases from activated ferrous metals is limited. However, the available information has been reviewed as comprehensively as possible.

1.3 Sources of information

The information provided in this report is drawn from the following main sources:

- an existing data review of carbon steel, stainless steel and Zircaloy corrosion rates that was last updated for NDA RWMD (now RWM) by Serco (now AMEC) in 2006 (and published in 2010) [13];
- recent reviews on the corrosion behaviour of different types of steels being considered as container materials in national radioactive waste programmes [14-18];
- a number of recent documents on the topic of carbon-14 from national programmes [1, 19, 20] and references therein concerned with the chemical forms of carbon in steel and the speciation of carbon and carbon-14 releases;

- an extensive literature search for new corrosion data carried out in two major bibliographic databases: INIS and Corrosion Abstracts for publications from 2006 to early 2014.
- the Dechema corrosion handbooks [21], which contained useful bibliographies, as do a number of standard text books and reviews [22-27].

Some additional draft documents and information were provided by partners in WP2 for inclusion in this review.

1.4 Structure of this report

This report is structured as follows:

Section 2 consists of an introduction to the main types of steel that may be present in the waste being handled by the waste producers and a consideration of the possible chemical forms and location of carbon-14 in the metals.

Section 3 summarises the corrosion mechanisms for carbon steel and stainless steels and outlines the main parameters that control the rates of corrosion.

Section 4 summarises the range of environmental conditions that will pertain during the waste management and disposal process.

Sections 5 and 6 present summaries of the corrosion rates of carbon steel and stainless steel in the various conditions that will apply during the waste disposal process.

Section 7 presents a summary of the published information on the release of carbon and carbon-14 from cast irons and steels.

A discussion of the results and the main conclusions drawn are presented in Section 8.

2 Overview of steel wastes containing carbon-14

2.1 Carbon steels

Carbon steels are composed predominantly of iron, with no other major metallic alloying elements, but with small concentrations of carbon, manganese and trace elements such as silicon, phosphorus, nitrogen, aluminium and sulphur. They are sometimes known as mild steels. Cast irons contain a high concentration of carbon (i.e. >2wt%), but these materials are unlikely to be present in the irradiated waste and will not therefore contain significant quantities of carbon-14. The corrosion of cast iron is not considered further in the current report.

There is a wide range of grades of carbon steel available commercially. They differ in the exact concentrations of the minor elements, particularly carbon, and the heat treatments that are applied. In this way it is possible to control the microstructure of the material and hence the mechanical properties such as the tensile strength and ductility. From the point of view of discussing the release of carbon-14 from the corrosion of carbon steel, the important consideration is the composition of the material and location and speciation of carbon in the material. It is common practice to report the carbon content of steels, but the nitrogen concentration is rarely given in carbon steel specifications or analyses.

2.2 Stainless steels

Stainless steels are iron alloys containing a minimum of approximately 11 wt% chromium [28]. This minimum chromium content prevents the formation of rust in an unpolluted atmosphere; hence the designation “stainless”. This resistance to corrosion is provided by a very thin surface film of stable chromium oxy-hydroxide, known as the passive film, which is self-healing in a wide variety of environments. The different classes of stainless steel take their name from their predominant crystal structure: austenitic (face-centred cubic), ferritic (body-centred cubic), martensitic (body-centred tetragonal) or duplex alloys containing roughly equal proportions of austenite and ferrite.

A variety of stainless steel grades are available commercially, but the most commonly used in the nuclear industry are the 300 series austenitic, nickel-containing grades[3], which represent compositional variations of the classic 18/8 (18wt% chromium and 8wt% nickel) stainless steel [28]. The two most widely used grades are type 304 (18/10), which is considered the standard grade, and type 316 [26], which has improved resistance to localised corrosion through the alloy addition of molybdenum. Type 316 is also known as marine grade stainless steel due to its increased resistance to chloride corrosion compared to Type 304. The compositions of these and some of the other stainless steel grades used in the nuclear industry are given in Table 4.

The carbon content of 300-series stainless steels is low, typically about 0.08wt% in 304 and 316 and usually less than 0.25wt%. Lower carbon (L) grade modifications of types 304 and 316 (<0.03% C) are used for applications requiring welding to improve resistance to sensitisation, the precipitation of carbides at grain boundaries, which can reduce corrosion resistance in heat-treated zones. Nitrogen is always present as a trace element (<0.1%) but may be added to improve strength; for example, nitrogen-strengthened 316LN contains 0.1-0.16wt% nitrogen.

By definition, a stainless steel must contain at least 50% iron. When the iron content falls below 50%, the alloy is named after the next major element. A range of nickel alloys have been used in nuclear applications for their resistance to corrosion and retention of strength at elevated temperatures. In particular, many nickel-based alloys show excellent resistance to pitting, crevice corrosion and stress corrosion cracking in chloride environments.

[3] Stainless steel grades are identified using several different numbering systems. In this report, the best known American Iron and Steel Institute (AISI) system, which designates the standard stainless steel grades by three digit numbers, with, in some cases, one or more suffix letters, will be used, where applicable.

Table 4: Composition ranges (wt%) of alloying components (balance iron) in common stainless steels grades used in nuclear applications (data from reference [28]).

Alloy	Cr	Ni	Mo	Mn	Si	P	N	C	S	Cu
304	18-20	8-10		2.0	1.0	0.045	<0.1	<0.08	0.03	
304L	18-20	8-10		2.0	1.0	0.045	<0.1	<0.03	0.03	
309	22-24	12-15		2.0	1.0	0.045	<0.1	<0.20	0.03	
309S	22-24	12-15		2.0	1.0	0.045	<0.1	<0.08	0.03	
316	16-18	10-14	2-3	2.0	1.0	0.045	<0.1	<0.08	0.03	
316L	16-18	10-14	2-3	2.0	1.0	0.045	<0.1	<0.03	0.03	
316L(N)	16-18	10-14	2-3	2.0	1.0	0.045	0.1-0.16	<0.03	0.03	
321	17-19	9-12		2.0	1.0	0.045		<0.08	0.03	
321S12 (EN 58B)	17-19	9-12		0.5-2.0	0.2-1.0	0.045		<0.08	0.03	
416S21 (BS970-EN56)	11.5-13.5	1.0	0.6	1.5	1.0	0.060		0.09-0.15	0.15-0.35	
904L	19-23	23-28	4-5	2.0	1.0	0.045		0.02	0.035	1-2

2.3 Chemical form of carbon-14 in steels

The possible forms of carbon-14 in metals and the chemical forms in which they may be released have been reviewed by Hicks *et al*. [29]. Additional studies on the chemical forms of carbon leached from carbon steel [30] and from steel and metal carbides [31] have been reported.

As discussed in Section 1.1, carbon-14 is generated in reactor steels by the activation of nitrogen-14 impurities; only a very small fraction of the carbon-14 is formed from the carbon-13 present. The steels under consideration in CAST WP2 have low carbon and nitrogen contents. For example, 316L(N) stainless steel (the L grade stands for low carbon) has maximum permissible carbon and nitrogen contents of 0.03 wt% and 0.1 wt%, respectively. Carbon steels used in reactor pressure vessels typically have a carbon content <0.3 wt% (see Table 5).

Carbon and nitrogen are soluble to some extent (as a solid solution) in the iron phases that comprise the bulk of the steel: austenite in 300-series stainless steels and ferrite in mild steel. Nitrogen may also be present in distinct phases as nitrides of iron and the alloying metals; carbon will also be present as metal carbides. Carbonitrides may also form with iron and many alloying elements. In general, steels with carbon contents <1.5 wt% (such as the mild and stainless steel considered in this study) do not contain carbon in graphite form [32]. If the nitrogen is originally present as nitride then the resulting carbon-14 may be present as carbide [29] and/or carbonitride. However, it is far from clear that carbon-14 produced by activation will be in the same forms as carbon present in the steels at their time of production [33].

The form and reactivity of carbides and nitrides present in transition metals depends on the ratio of the atomic radii of carbon and nitrogen to the transition metal. For the fourth, fifth and sixth series of transition elements (e.g. Ti, Zr, Nb, Mo, W, with the exception of chromium), carbon and nitrogen atoms are sufficiently small to enter the interstices of the crystal lattice without appreciably distorting the metal structure. Such interstitial carbides

and nitrides are reported to be highly stable and attacked only slowly by concentrated acids [34].

For the smaller transition metal elements of the seventh and eighth series (e.g. Fe, Ni, Co, Mn plus Cr), where the lattice interstices are also smaller than for the fourth, fifth and sixth series elements, carbon atoms may interact to form chains that run through the distorted metal lattice. Multiple carbide stoichiometries are known, such as the chromium carbides $Cr_{23}C_6$, Cr_7C_3 and Cr_3C_2 [34]. These carbides, with structures that lie between the interstitial carbides and the ionic carbides, (discussed below) are referred to as 'intermediate' carbides. The intermediate carbides may be hydrolysed by water and dilute acids to generate hydrogen, methane and a range of hydrocarbons (mainly straight-chain alkanes and alkenes) [35][4].

The most electropositive metals (group I, II and III metals) form carbides that are essentially ionic in character [39]. Theses ionic carbides are readily hydrolysed by water or dilute acids at ordinary temperatures yielding hydrocarbons corresponding to the form of the carbide anion present (e.g. C^{4-}, C_2^{2-}, C_3^{4-}). For example, aluminium carbide, Al_4C_3, which contains methide (C^{4-}) ions, hydrolyses to release methane. Calcium carbide (CaC_2) reacts with water to yield ethyne and a magnesium carbide (Mg_2C_3) reacts to yield propyne. In a similar way, ionic nitrides that are readily hydrolysed by water to release ammonia are formed with the electropositive metals (e.g. Ca_3N_2, Li_3N).

Thus, the nature of the metal carbides formed in the steel will affect not only the rate of release of carbon but also the species released. The types of carbides and nitrides present will be dependent on the steel composition, in particular the presence of carbide-forming elements (e.g. titanium, niobium) or nitride-forming elements (e.g. aluminium, titanium),

[4] There is some inconsistency in the literature concerning the ease of hydrolysis of the chromium carbides. Some sources (e.g. [36,37]) describe Cr_3C_2 as inert to water and dilute acids in common with the interstitial carbides; however, the original studies from which this conclusion was drawn are unclear. In more recent work, Cataldo [35] describes Cr_3C_2 as being "easily hydrolysable"; he reports the release of methane, hydrogen and a series of alkenes (other alkanes not being detectable with the methods employed) on contact of a commercially-available Cr_3C_2 powder with water and dilute acid at ambient and elevated temperatures. These results are similar to the hydrolysis behaviour of the intermediate carbides of Mn, Fe, Co and Ni.

the nature of the iron phase (e.g. ferrite, austenite) and the solubility of the carbon and nitrogen therein.

The solubility of both carbon and nitrogen is greater in austenite (face-centered cubic lattice) than in ferrite (body-centered cubic lattice) because of the larger interstices available in the face-centred-cubic structure. When the solubility of the carbon and nitrogen is exceeded, separate carbide and nitride phases will be produced, which can be seen as precipitates or separate phases within the microstructure of the metal. For carbon, a separate iron carbide phase called cementite, Fe_3C, is formed. Cementite forms a discrete phase, which, when alternated with ferrite in a lamellar structure, forms a phase known as pearlite, a common characteristic of structural carbon steels. In the case of low-carbon stainless steels, a higher proportion of the carbon may be present in solid solution in the austenite, rather than being present as separate carbide phases.

The low carbon content of 316L stainless steel is designed to minimise the formation of carbide phases, in particular chromium carbides. Chromium carbides may form along grain boundaries leading to depletion of chromium from the austenite grains, decreasing the steel's corrosion resistance. The addition of carbide-forming elements, such as titanium or niobium, to some stainless steels (e.g. 321 and 347 grades, and 20/25/Nb, a heat-resistant grade of stainless steel used specifically for AGR fuel cladding in the UK) is designed to minimise chromium depletion. For these grades, the principal carbides are expected to be corrosion-resistant interstitial carbides of niobium, titanium or tungsten, for example, rather than more readily hydrolysed cementite.

In iron, the nitride phase is described as Fe_4N, which is analogous to cementite [40]. Nitrogen also forms carbonitrides with iron and many alloying elements, but in the presence of strong nitride formers, such as aluminium and titanium, separate nitride phases can occur. Consequently, according to reference [40] the majority of the nitrogen in commercial carbon steels is present as aluminium nitride, since aluminium forms highly stable and inert nitrides. Thus, on activation, a proportion of the carbon-14 is expected to be present as Al_4C_3 or $Al_xC_yN_z$, which may be formed from the original aluminium nitride.

It is unclear how reactive any carbon-14-containing carbonitrides resulting from the partial conversion of nitrides may be. In the case of aluminium, there is a marked contrast between the stabilities of the inert nitride and highly reactive carbide. It is noted also that the process of "carbonitriding" or "nitrocarburising" may be applied to the surfaces of steels, producing an iron carbonitride layer, to improve their abrasion, wear and corrosion resistances [e.g. 41]. In principle, compounds containing C-N bonds such as cyanides or amines as well as hydrocarbons could result from the hydrolysis of metal carbonitrides (amines and hydrocarbons have been reported on water vapour hydrolysis of thorium and uranium carbonitrides [42]). The above information suggests that carbonitrides are likely to react more slowly than the equivalent carbide with a rate that is likely to be dependent on, and increase with, the ratio of carbon to nitrogen. Thus there is the possibility that carbon-14 generated by activation of nitride nitrogen-14 may be locked into relatively inert carbonitrides.

Interstitial nitrogen-14 might be expected to remain as interstitial carbon-14 on conversion; however, given atomic displacements on irradiation and the ready diffusion of carbon and nitrogen atoms in steels (even at room temperature), it is not clear whether this will remain the case.

On the basis of the above information, the following carbon-14 release behaviour might be expected on leaching an irradiated steel. As the steel slowly corrodes, the carbon-14 in its different forms will be exposed to the waste disposal environment. The different forms of carbon-14 may be expected to be released in different ways.

- Ionic and intermediate carbides and interstitial carbon present in the iron phase may be hydrolysed over relatively short time periods to form methane and other hydrocarbon gases.
- Intermediate carbonitrides may be hydrolysed at a much slower rate than the equivalent carbides to yield a range of products that may include hydrocarbons and compounds containing C-N bonds such as amines and cyanides.
- Stable carbides and carbonitrides may react only very slowly (if at all) and be released in particulate form.

Carbon is not expected to be present or released in graphite form from corroding stainless steel or mild steel due to their low carbon content. However, it is not clear whether this would also be true after significant irradiation.

It is noted here that previous studies related to the potential carbon-14 release mechanisms from steels have tended to focus on carbide carbons as the most likely forms of carbon-14 in irradiated steels. The potential role of carbonitrides has been relatively neglected.

There is relatively little information in the literature on the release of carbon from steels and the chemical form of the carbon species generated; see Section 7 for further discussion on this topic.

2.4 Reactor steel wastes

Carbon steels and stainless steels have been commonly used as structural materials in nuclear reactors worldwide [26]. Low carbon (mild) steels have been commonly used as the reactor pressure vessels in Boiling Water Reactors (BWRs) and Pressurised Water Reactors (PWRs) and also in gas-cooled Magnox reactors built in the UK. In general, ferritic and bainitic[5] carbon steels are used. Some examples of the compositions of the pressure vessel steels used in major nuclear countries are given in Table 5. In the UK, a range of mild steel grades was used for the pressure vessels across the Magnox fleet with trade names such as COHLO 1. More generally, carbon steels have also been used for piping and cooling systems equipment and as rebars in concrete.

Stainless steels have been preferred for some of the internal structural materials of BWRs and PWRs due to their greater resistance to general corrosion by water. Indeed, the internal surfaces of BWR and PWR pressure vessels have been clad with 308/309 stainless steel weld overlays to protect them from general corrosion [26]. According to Feron [26], types 304 and 316 stainless steels and in particular the low-carbon grade type 316L are also frequently used in commercial BWR and PWR reactors. Stainless steel is used for the fuel

[5] A fine non-lamellar structure that forms in steels at temperatures of 250–550°C (depending on alloy content), bainite commonly consists of cementite and dislocation-rich ferrite. The high concentration of dislocations in the ferrite increases the hardness of the steel.

cladding in UK Advanced Gas-cooled Reactors (AGRs) and for the structural components of AGR fuel assemblies [8]. Special grades containing niobium or titanium as minor alloying components have been selected for cladding and fuel assembly components, respectively.

A limited amount of information is available concerning the contributions of carbon-14 in steels to the radioactive waste inventories in nuclear programmes across the world.

In Switzerland, activated metal wastes consisting of stainless steel, Zircaloy and nickel alloys arising from fuel assemblies and supporting hardware in the Swiss fleet of three PWRs and two BWRs, is the most important source of carbon-14 in the Swiss inventory of ILW and L/ILW [19]. Some 85% of the total carbon-14 inventory is associated with activated stainless steels with a further 1.4% associated with activated Zircaloy (hulls and ends). The carbon-14 activities in irradiated steels are estimates based on an estimated nitrogen concentration of 800 ppm and a reactor operational lifetime of 60 years.

An assessment is made of the UK's radioactive waste inventory (RWI) on a three-year cycle. The 2013 UK RWI was published in 2014 [43] and contains a best estimate for total carbon-14 of 10,697 TBq in the UK's higher activity wastes (arising from existing and legacy reactors) that are destined for geological disposal[6]. Most of the carbon-14 is in graphite, but some of this carbon-14 is associated with steel wastes. More detailed studies of carbon-14-bearing wastes have been undertaken by RWM's Carbon-14 Project [1]. Work undertaken in 2013 and 2014 (that will be published as a project report [8]) has identified that the majority of the carbon-14 inventory in waste steels arises from seven distinct classes of reactor wastes, as summarised in Table 6 [8]. In general, the carbon-14 activities of the waste steels have been determined by activation calculations based on assumed concentrations of nitrogen-14 impurities in the steels concerned and either known or projected neutron fluxes and durations of reactor operation.

[6] The UK RWI includes details of all radioactive waste arisings in the UK, which includes low-level wastes (LLW) destined for diposal in the Low-level Waste Repository (LLWR), a near-surface disposal facility, near Drigg in Cumbria. Some of the UK's reactor wastes are classified as LLW, and this includes some carbon-14-containing mild steel wastes.

Table 5: Chemical compositions (wt %) of alloying components (balance iron) in some ferritic steels used for reactor pressure vessels [26]; note that the nitrogen contents of the steels are not included.

Steel	Country and reactor type	C	Mn	Mo	Cr	Ni	Si	P	S	Cu	Co	V
20MnMoNi5-5 (ASME SA 508 3 Cl.1)	Germany PWR	0.25	1.54		0.18	0.62		0.014	0.015			0.024
22NiMoCr3-7 (ASME SA 508 2 Cl.1)	Germany PWR	0.22	0.91		0.42	0.88		0.008	0.007			0.007
22NiMoCr 37 (ASTM 508 Cl.2)	Switzerland	0.18	0.82		0.39	0.96	0.15	0.005	0.008	0.08	0.014	<0.01
15Ch2MFA	Russia VVER 400	0.15	0.4	0.64	2.78	0.3	0.24	0.013	0.015	0.08	0.009	0.29
15Ch2NMFA	Russia VVER 1000	0.15	0.45	0.57	2.15	1.23	0.25	0.009	0.007	0.05		0.08
JRQ (ASTM 533-B Cl.1)	Japan	0.19	1.39		0.12	0.83	0.25	0.019	0.004	0.14		0.003
16 MnNiMo05 (16 MND 5)	France PWR	0.2		0.45/ 0.55	<0.25	1.15/ 1.55	0.1/ 0.34	<0.008	<0.008	<0.8	<0.03	

Table 6: Carbon-14 activity in steel wastes from existing and legacy reactors destined for geological disposal in the UK [8].

Waste stream group	Carbon-14 activity (TBq) at 2200
ILW AGR stainless steel fuel cladding	29.4
ILW AGR stainless steel fuel assembly components	38.4
ILW AGR fuel stringer debris	99.5
ILW stainless steels from legacy reactor decommissioning	97.5
ILW other stainless steel reactor wastes	1.2
ILW other ferrous metal from legacy reactor decommissioning	124.3
ILW other ferrous metal reactor wastes	23.5
Total Carbon-14	**413.8**

Notes: These figures exclude about 101 TBq of carbon 14 in Scottish Policy wastes that may not be disposed to a GDF and a further 6,664 TBq of carbon-14 in stainless steel wastes that are projected to arise from a programme of new-build nuclear reactors in the UK.

Further information concerning the UK's irradiated stainless steel wastes, gathered by the RWM Carbon-14 IPT project, is summarised in Appendix 1.

3 Mechanisms of corrosion

3.1 Types of corrosion

Corrosion processes can generally be divided in to two main categories, namely general corrosion and localised corrosion. General (or uniform) corrosion results in an even distribution of metal removal across the complete surface of the metal, whereas localised corrosion results in corrosion at very small sites, while the main part of the surface remains uncorroded. Carbon steel is not a corrosion resistant material and it is mainly affected by general corrosion, whereas stainless steel, nickel alloys and Zircaloy are corrosion resistant materials that experience very low uniform corrosion rates, due to the presence of a protective passive film. However, they can be subject to various forms of localised corrosion in the presence of aggressive species such as chloride. This localised corrosion can take the form of pitting, in which small hemispherical depressions develop at sites of breaks in the passive film, crevice corrosion which develops at mating surfaces, where locally aggressive conditions can develop, and stress corrosion cracking, which can develop in the presence of an applied stress, aggressive species or a susceptible material.

General corrosion tends to be the most significant corrosion mechanism for carbon steels, but for stainless steels, localised corrosion (e.g. pitting) may be a more important mechanism for release of a significant corroded volume of material, due to the low uniform corrosion rates.

If microbially influenced corrosion (MIC) were to occur, the corrosion rates could be significantly higher than the abiotic corrosion rate. MIC of various materials that may arise in nuclear waste has been reviewed by King *et al*. [44], who carried out a detailed review of the potential for microbial activity in a range of different disposal concepts. In all concepts, microbes will be present in the groundwater, but the backfill material will tend to reduce microbial acitivity in the vicinity of the canister. In the case of a cement-based near-field,

of principal interest here, the alkaline environment will prevent microbial activity[7] so that microbial activity at the surface of the steel wastes will be severely restricted.

3.2 Corrosion processes affecting carbon steel

The following reactions [23] are assumed to occur in oxygenated conditions:

$$4Fe + 6H_2O + 3O_2 \Rightarrow 4Fe(OH)_3$$
$$4Fe + 3O_2 \Rightarrow 2Fe_2O_3 \quad (1)$$

In anaerobic conditions, corrosion is thought to occur according to the reactions [45, 46]:

$$Fe + 2H_2O \Rightarrow Fe(OH)_2 + H_2$$
$$3Fe + 4H_2O \Rightarrow Fe_3O_4 + 4H_2$$
$$3Fe(OH)_2 \Rightarrow Fe_3O_4 + 2H_2O + H_2 \quad \text{(at higher temperatures)} \quad (2)$$

These equations are a simplified view of the complex array of reactions that are likely to occur in practice. A range of corrosion products would be formed under the many combinations of pH, chloride concentration and temperature that could occur during waste management. The remainder of this subsection discusses the composition of the films that are likely to form in the various stages of waste management. The discussion applies to stainless steel as well as to carbon steel. The composition of corrosion products and passive films has been the subject of a large number of publications (*e.g.* [47, 48]) and it is not the intention to provide a comprehensive review here.

An indication of the complex range of oxides and hydroxides that can arise through corrosion in neutral water is shown in Figure 1 [47]. According to this diagram the final reaction product from slow oxidation of iron in aerobic, neutral solutions is magnetite, Fe_3O_4. A multi-layer film containing iron in a range of oxidation states (*e.g.* FeO, Fe_3O_4 and Fe_2O_3) is often found [23]. Measurements by Kalashnikova *et al*. [49] showed that the stoichiometry of the magnetite corrosion product changed with immersion time in seawater. At higher temperatures both Fe_2O_3 and Fe_3O_4 are formed. Using Mössbauer spectroscopy,

[7] There are some alkaline-tolerant microbial species, but the upper pH limit for microbial activity is thought to be around pH 11. It is possible that lower pH niches could develop that would allow greater microbial activity.

Peev *et al*. [50] identified FeOCl, β-FeOOH and γ-FeOOH in the corrosion products of steel in seawater. Chen *et al*. [51] also identified green rust ($Fe(OH)_2/Fe(OH)_3$), $Fe(OH)_2$ and $Fe_2(OH)_3Cl$.

Sagoe-Crentsil and Glasser [52] have constructed a stability diagram for iron in cement at pH 12 and temperature 25°C, as a function of chloride concentration (Figure 2). Very detailed Pourbaix diagrams for iron in the presence of chloride have been produced by Refait and Genin [53], which also take into account the green rust phases (see reference for details).

Since many groundwaters contain some carbonate alkalinity, it is possible that corrosion product films containing carbonate would also be formed, although, if grout is present, it is likely that most of the carbonate would precipitate out as calcium carbonate before the groundwater reaches the metal surface. Jelinek and Neufeld [45] reported that a two-layer corrosion product formed on iron in de-aerated water. The outer layer was friable and the inner layer was adherent and compact. X-ray diffraction (XRD) analysis identified Fe_3O_4, but there were several other unidentified peaks. Mass spectroscopy of the gas released while heating the corrosion product revealed that some hydrogen was trapped in it.

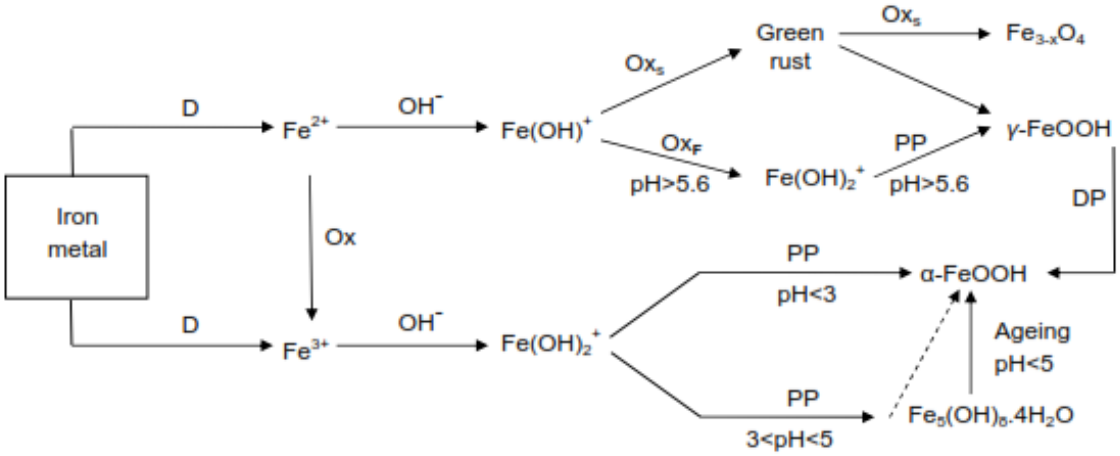

Figure 1: A schematic diagram of the formation and transformation of the solid products of corrosion under different pH conditions at room temperature: D - dissolution; Ox - aerobic oxidation in solution; Ox_s - slow oxidation; Ox_r - rapid oxidation; PP - polymerisation-precipitation; DP - dissolution-precipitation (redrawn from reference [47]).

The detailed composition and structure of the passive films formed in alkaline solutions are still a matter of debate, despite much research. It is generally agreed that Fe_2O_3 is a major component, in which Fe_3O_4 and bound water may also be present. The film may have a multi-layer structure, the exact composition of which depends on the electrochemical potential [23, 54-56]. Several workers have investigated the reduction of the oxide films using electrochemical techniques. Riley and Sykes [57], for example, used a galvanostatic technique to reduce the film formed on a NiCrMoV steel at pH 9.2 in de-aerated carbonate-bicarbonate solution at 70°C. By using a ring-disc electrode it was possible to monitor the products of the film reduction in solution. The results supported the concept of a two-layer film composed of an inner layer of Fe_3O_4 and an outer layer of Fe_2O_3. In some experiments the "auto reduction" of the passive film was observed, *i.e.* the film formed in the passive region was allowed to "float" without potential control and the film was observed to dissolve. The following reaction was postulated:

$$Fe \Rightarrow Fe^{2+} + 2e^-$$
$$\gamma\text{-}Fe_2O_3 + 6H^+ + 2e^- \Rightarrow 2Fe^{2+} + 3H_2O \qquad (3)$$

Fe^{2+} dissolved from the metal lattice provides electrons that can reduce the ferric ion in the outer layer of the oxide. The "auto reduction" or "reductive dissolution" of a film that had been grown at +0.2V (SCE) took approximately one minute and the final rest potential was approximately -0.8V (SCE).

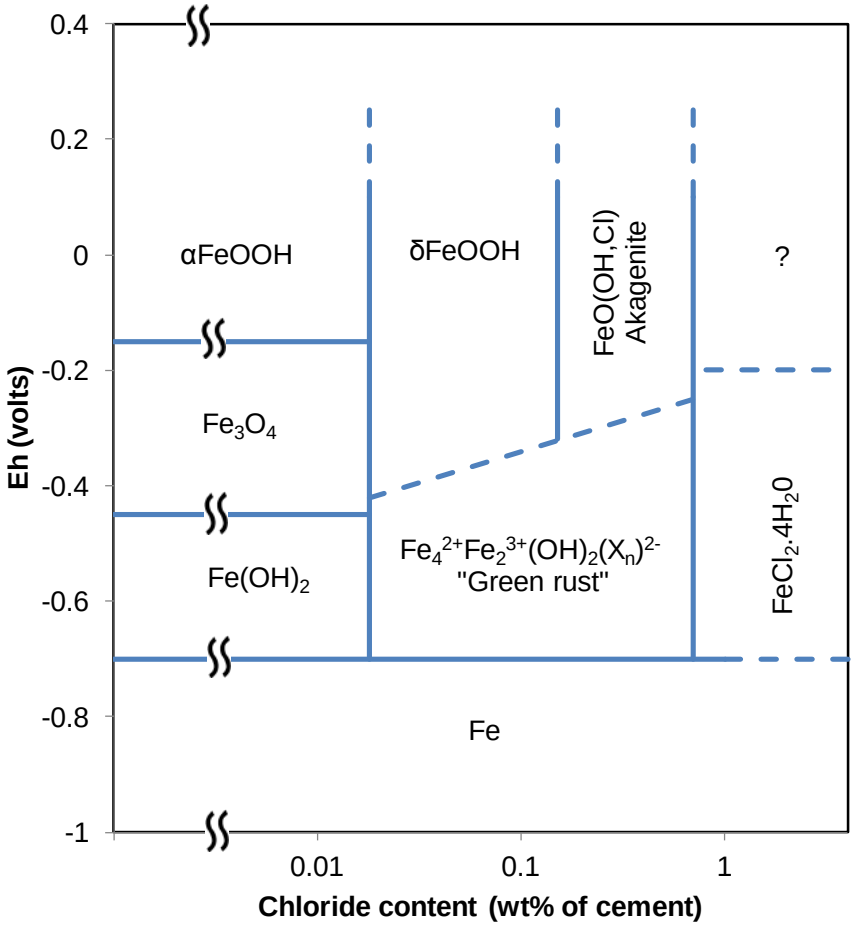

Figure 2: Eh-chloride stability diagram for iron in cement at pH~12 and 20°C (redrawn from reference [52]).

Long-term atmospheric corrosion tests on iron give corrosion products composed of a range of iron oxides and hydroxides, including α-, β- and γ-FeOOH, γ -Fe_2O_3 and Fe_3O_4 [47]. During wet cycles, the anodic dissolution of iron provides electrons for the reduction of Fe(III) oxides, *viz.*

$$Fe \Rightarrow Fe^{2+} + 2e^-$$

$$Fe^{2+} + 8FeOOH + 2e^- \Rightarrow 3Fe_3O_4 + 4H_2O \qquad (4)$$

During dry cycles, when oxygen can permeate the porous corrosion product, the magnetite (Fe_3O_4) is re-oxidised to FeOOH. These reactions involve complex solid-state processes [58, 59]. It should be noted that the dry, re-oxidation step would not be possible in an anaerobic environment.

Reductive dissolution of the oxide film, *i.e.* conversion of Fe(III) oxide to Fe(II) oxide, has been observed in the laboratory for passive films that have been produced by maintaining a positive potential using a potentiostat, and for air-formed films (*e.g.* [60, 61]), but it is not clear whether such reactions can occur for the films formed under GDF conditions and, if so, what the kinetics of reaction would be. In some cases, for example corrosion in aerobic neutral conditions or wet atmospheric conditions, the corrosion product may already be in the reduced state, *i.e.* Fe_3O_4.

The composition of the corrosion product layer is expected to evolve over time. For example, films formed in the aerobic stage at neutral pH, with low chloride concentrations, may subsequently be exposed under anaerobic conditions to high-pH, high-chloride conditions as resaturation of the grout occurs. Most published corrosion rate data refer to the corrosion behaviour of freshly prepared metal surfaces. Experiments in the UK have shown that aerobically-formed films can delay the onset of hydrogen evolution [62]; this may reflect the time required to allow film reduction. As reducing conditions develop, the stoichiometry of the oxide film formed under aerated conditions may change so that it will contain iron in a lower oxidation state. In addition the stoichiometry of the iron may change with depth through the film.

3.3 Corrosion processes affecting stainless steel

The corrosion behaviour of stainless steels is dominated by the presence of a thin passive film on the surface of the metal [28], which is commonly composed of a hydrated chromium-rich oxy-hydroxide [63]. The exact composition and structure depend on the material and the environment. It may only be of the order of a few nm thick but it is sufficient to confer a high degree of corrosion resistance, so that the uniform corrosion rates are normally very low, unless the environment is highly acidic, which is not likely to occur in the context of waste disposal in normal circumstances. There has been much

experimental research and theoretical modelling of the structure and properties of the passive film (e.g. [64]). If stainless steel does suffer from corrosion it is normally in the form of localised corrosion, as described in Section 3.1. This means that the rate of creation of new surface area from which carbon-14 could potentially be released is much smaller for corrosion resistant alloys than for low alloy materials, such as carbon steel, which suffers corrosion across a uniform front. On the other hand, if localised corrosion, such as pitting corrosion occurred at a high propagation rate, the local release rate of carbon-14 from the site of localised corrosion could be significant. Nickel-chromium alloys, such as Inconel, are also protected by a passive film which confers high corrosion resistance. Further information about the corrosion behaviour of nickel alloys is available in references [65] and [66]. These alloys are not considered in detail in the present report.

The corrosion properties of stainless steel in general are thoroughly described and summarised in reference [28] and the corrosion behaviour of austenitic and duplex stainless steels specifically during radioactive waste management has been reviewed by King *et al*. for the UK NDA [15, 16], with a focus on the 304 and 316L austenitic stainless steels and the 2304 and 2205 duplex stainless steels. Under deaerated conditions the risk of localised corrosion is very low because the corrosion potential is below the breakdown potentials for localised corrosion to occur, but in the presence of oxygen the risk of localised corrosion increases as the corrosion potential becomes more positive. In aerated conditions, the risk of localised corrosion increases with increasing temperature, increasing chloride concentration and decreasing pH.

3.4 Effect of irradiation on corrosion

Radiation can affect corrosion processes in two main ways. Firstly, radiolysis of an aqueous phase can generate reactive species such as radicals and peroxide that can affect the chemical and electrochemical processes that are involved in the corrosion reactions and hence change the corrosion rate of the material. Secondly, radiation can change the properties of the materials themselves, by for example producing segregation of trace elements in the matrix, as discussed by Was [67, 68]. This can alter the corrosion susceptibility of particular locations in the microstructure of the material. In the context of stainless steel AGR cladding material, for example, neutron irradiation can lead to the

development of radiation-induced depletion of chromium at grain boundaries, which renders the material more susceptible to intergranular corrosion [69].

3.5 Measurement of corrosion rates

In the literature, corrosion rate data are derived from investigations using both instantaneous and integrated techniques. Instantaneous techniques give a measure of the corrosion rate at any particular time, and include electrochemical methods such as: linear polarisation resistance; Tafel-slope extrapolation; and passive current measurement. They provide a value for the corrosion rate at the time of the measurement. Descriptions of instantaneous techniques may be found in a number of texts, *e.g.* [70] and [71]. Integrated techniques include measurements of dimensional change, weight loss (*e.g.* [72]) or hydrogen evolution (*e.g.* [73, 74]). The total change over a period of time is used to derive the corrosion rate. Instantaneous measurements may give misleadingly high corrosion rates, particularly in systems where a steady corrosion rate is achieved only after a long time.

4 Environmental conditions during the storage and disposal of steel wastes

4.1 Use of cements in the storage and disposal of steel wastes

Many countries (including Belgium [11], France [75], Japan [12], Sweden [76], Switzerland [9] and the UK [10, 77]) are considering or developing cement-based disposal concepts for the management of long-lived higher activity radioactive wastes, which will include irradiated steels from reactor structures and fuel assembly components[8]. Details vary between disposal concepts, but in general, most concepts envisage that the wastes will be placed into containers (typically manufactured from steel or concrete) that will be conditioned by the addition of a cementitious grout, to fill the void spaces and immobilise the waste. The waste containers are likely to be stored for an interim period (which may last for several hundred years), before being transported to a GDF, where they will be placed in disposal vaults or tunnels, deep underground (typically 100-1000m below surface). At some time prior to closure of the facility, the waste vaults and tunnels will be filled with a cementitious backfill material. The use of cementitious materials in these concepts is specifically designed to maintain an alkaline pH in the porewater, which has various benefits including reducing the rate of steel corrosion. In the context of carbon-14, cements also have a significant capacity to absorb any carbon-14 released from the waste in the form of carbonate or carbon dioxide through the precipitation of calcium carbonates.

The chemical evolution of the near field in a cement-based disposal facility will be dependent on both the disposal concept and the characteristics of the host rock and groundwater. In particular, the evolution of the pH will be determined by the initial composition of the cement backfill and its evolution with time resulting from its interactions with: the groundwater; the host rock; the wastes; the containers; and with other components of the engineered barrier system [78]. For typical candidate backfill compositions, which

[8] Not all of the irradiated steel wastes from nuclear reactors will be disposed to GDFs; lower-activity carbon-14 containing steel wastes may be disposed to near-surface facilities, such as the LLWR in the UK.

are based on formulations of Portland cement[9] (CEM-1) and may include additional lime (calcium hydroxide), the following stages of pH evolution have been identified [e.g. 77, 80]:

Stage 1 pH > 12.5 arising from the dissolution of sodium and potassium oxides, with the pH value dependent on the amounts of alkali metal oxides and on the porosity of the backfill;

Stage 2 pH ~ 12.5 buffered by equilibration of the ingressing groundwater with the calcium hydroxide component of the backfill;

Stage 3a pH falling from 12.5 to ~ 9.8 controlled by the incongruent dissolution of calcium silicate hydrate phases;

Stage 3b pH ~ 9.8 controlled by congruent dissolution of calcium silicate hydrate phases (or secondary mineral phases giving additional buffering at other pH values);

Stage 4 pH < 9 once exhaustion of the pH-buffering cementitious phases has occurred, with pH determined by the groundwater and remaining phases such as calcite.

This simple picture is summarised in Figure 3. In general, the associated timescales vary considerably, depending on factors such as the groundwater flow rate through the waste vaults, and the groundwater chemistry, but calculations [e.g. 81] suggest that Stage 1 will last for at least a few thousand years and Stage 2 considerably longer. The time spans may be even longer for a facility located in a low permeability sedimentary rock (such as an argillite formation) where diffusion is the dominant transport process in this host rock [82]. In the context of carbon-14, with a half-life of 5730 years, the relevant pH during the period of carbon-14 release is expected to be pH 12.5 or higher.

[9] Hydrated (and hardened) Portland cement comprises four main phases that make up more than 95% of the material: portlandite (calcium hydroxide, 20-30%), poorly crystalline calcium-silicate hydrate gel (C-S-H, 50-65%), ettringite (AFt, a calcium alumino/ferric tri-sulphate, 2-6%) and AFm (a calcium alumina-ferric monosulphate, 5-10%). These phases are intimately mixed. The C-S-H phase forms a rigid gel which contains bound water. Excess water from the original cement-water mix not required by cement hydration reactions is trapped in the pores and has a pH in excess of 12.5. For more information about cement chemistry see (e.g.) reference [79].

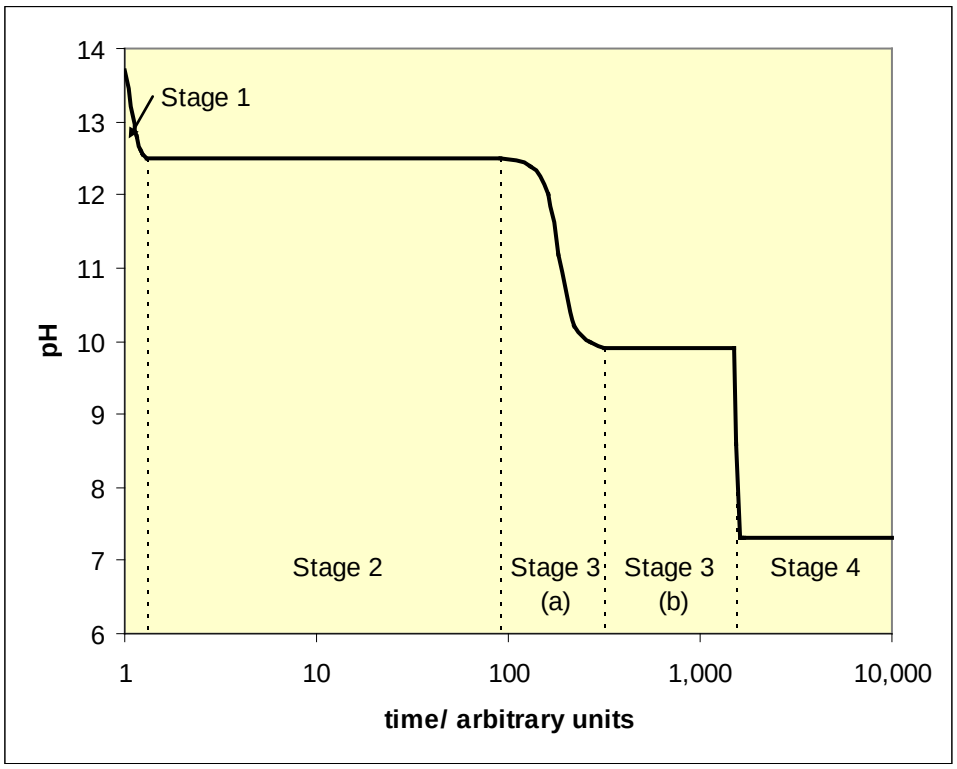

Figure 3: Schematic representation of the evolution of pH in the backfill porewater during groundwater leaching of a cement-based GDF [78].

A review of the use of cementitious materials as backfill materials in geological disposal concepts is given in reference [78].

4.2 Environmental conditions during waste management

It will be apparent from the previous section that irradiated steel wastes may be exposed to a variety of conditions during their long-term management. Therefore, in developing the safety cases for all stages of the management of these wastes, it will be necessary to consider the rates of corrosion and release of carbon-14 under the appropriate conditions. In this section, the range of environments for which corrosion data may be required in safety assessments is considered, with an emphasis on cement-based disposal concepts. Clearly, the range of conditions encountered will depend on the disposal concept and the geology of the host rock. In particular, the groundwater chemistry will determine the exposure of waste steels to solutes that may affect corrosion rates such as chloride and sulphide.

The various environments affecting the waste form can be divided into:

- those pre-backfilling of disposal vaults (including packaging, storage, transport and emplacement in a repository); and
- those post-backfilling (including GDF closure).

A further distinction is drawn between atmospheric and aqueous exposure, because corrosion is different in these two environments.

4.2.1 Conditions pre-backfilling

The environmental conditions experienced by packaged steel wastes during storage, transport and emplacement in a GDF will depend on the design of the waste container, whether the steels are segregated from other types of wastes, and any conditioning that is applied to immobilise the wastes within the container. In particular, if the container is vented, which may be required to allow the escape of gas generated by degradation of the wastes, then an aerobic environment may be maintained within the package throughout the pre-backfilling period; if a cement-based container, liner or immobilisation grout is used, then conditions will become cementitious and alkaline. If no cement is present within the waste package, then the wastes would be exposed to an aerobic, neutral[10] environment (or to an aerobic, acidic environment if acidic residues are present in the waste).

In general, waste packages will not be saturated with water and so steel wastes will be exposed to both the atmosphere within the waste package and to any free solution. If water is present within the wastes, then the wastes may also be exposed to isolated pockets of solution; in grouted containers, the wastes may be contact with the grout porewater.

4.2.1.1 Atmospheric exposure

The ambient temperature of the atmosphere in contact with the waste container during fabrication, filling, above-ground storage and transport will probably be in the range 5°C to 35°C. The internal temperature of the package will be determined by the external

[10] Throughout this report neutral pH refers to a pH in the range 6–8, *i.e.* it does not refer to a pH of exactly 7.

temperature and the small amount of heat generated by the waste form. Temperature cycling during storage may cause condensation / evaporation cycles, but radiation-induced heating will tend to counteract this effect.

The relative humidity inside a grouted waste package will be a function of the water content of the cement grout and, if the container is vented, the external relative humidity. It is conceivable that an anaerobic atmosphere may develop in closed voids or in a closed container, after a period of corrosion or microbial activity.

The external atmosphere will hold chloride-containing particulates in the form of aerosols, which will deposit on the external surfaces of waste containers and could, in principle, enter the inside of waste containers through any vents fitted in the lids. Typically, the vents would be fitted with filter materials (e.g. sintered stainless steel) to reduce the quantity of airborne particulates penetrating the interior of the waste containers. The quantity of aerosol particles penetrating would depend on the relative sizes of the particles, which are present in a range of sizes, and the pore sizes of the filters in the vents. Data on the composition, size distribution and deposition rates of such airborne particles in store environments in the UK are available [83, 84]. Deposition of hygroscopic salt particles onto the surfaces of steel containers can lead to localised corrosion. However, in unsaturated, grouted waste containers any particulates entering the container would deposit on the upper surface of the grout and would not be expected to reach the surfaces of encapsulated waste metals.

4.2.1.2 Aqueous exposure

The aqueous conditions experienced within a waste container will depend, primarily, on the pH and chloride concentration of the solution, which will depend on the composition of the waste and the presence of a cementitious grout. For segregated steel wastes, however, the chloride content would be expected to be low. During the pre-backfilling stage, corrosion can be minimised by ensuring that all waste is as dry as possible. If a concrete liner and internal grout are not used, and the waste is not dry, neutral or even acidic solutions could be present. It is possible that isolated pockets of anaerobic solution could develop as a result of corrosion or microbial activity, particularly in a sealed container. However, in a

vented container, it seems likely that most of the interior will remain oxygenated assuming air can enter through the gas vent.

4.2.2 Conditions post-backfilling

After placement, the containers may be surrounded with a cement-based backfill material. When a GDF is full, the remaining tunnels would be backfilled and the facility closed. In the early years after closure, the temperature within some parts of the facility will increase, mainly due to chemical reactions such as curing of the backfill, radioactive decay, corrosion and microbial degradation.

The maximum temperature rise and the subsequent duration and magnitude of the temperature excursion (above ambient for the host rock) will depend on the disposal concept and waste inventory.

After closure, groundwater will flow back into the engineered facility, resaturating all the excavated and backfilled spaces. The rate of resaturation will depend on the way the GDF has been operated, the permeabilities of the backfill and host rock, and the regional head gradient. The rate of resaturation of the waste container will depend on whether or not it is vented. Vented containers will be expected to resaturate as water flows back into the near field. However, resaturation of closed, metal containers would be dependent on the corrosion resistance of the waste container, and the time required for corrosion to breach the container wall.

The groundwater is expected to contain very low concentrations of oxygen and therefore will impose anaerobic conditions within the GDF. Corrosion and microbial activity will also reduce the oxygen concentration in the near field. The inflowing groundwater may contain significant concentrations of chloride ions (up to tens of thousands ppm in coastal locations), a particularly important aggressive anion with regard to the corrosion behaviour of metals (especially stainless steels), or other anionic species (such as sulphide) that may affect corrosion rates. However, the pH of the near field porewater will be controlled by the cementitious backfill materials and initially would be expected to be >12.5 (Stage 1 in Figure 3).

4.2.2.1 Atmospheric exposure

Initially regions of the package could be exposed to an aerobic atmosphere, from air trapped in voids. These voids will become anaerobic as a result of corrosion or microbial activity.

4.2.2.2 Aqueous exposure

If a concrete liner or internal grout is used, the interior of the package will be exposed already to an aerobic, alkaline aqueous phase. However, in the absence of cementitious materials in the package, and if the waste is not dry, neutral or even acidic solutions could be present initially.

For a vented container on resaturation, the interior of the package will be exposed to the aerobic, alkaline (pH 12.5–13) near-field porewater which has mixed with inflowing groundwater. The chloride concentration is expected to increase as the near field resaturates and groundwater enters the container via the gas vent or a corrosion-induced penetration. Eventually the solution in the waste container will become anaerobic. Once the GDF is completely resaturated and trapped oxygen has been consumed, the interior of the package will be exposed to an anaerobic, high-pH, aqueous phase that could contain chloride ions and a mixture of other inorganic salts (depending on the groundwater composition).

4.3 Oxygen and water availability

In general, the corrosion reactions of steels consume oxygen in oxic conditions and water in anoxic conditions. The consumption of oxygen is important because, in a closed system, its exhaustion controls the transition from aerobic to anaerobic corrosion and the onset of hydrogen production. The corrosion processes also consume or depend on the presence of water. For vented containers water may be freely available (both inside and outside the container) after resaturation (this depends on the disposal concept and the host geology), but in the early phases of operation of a disposal facility there may be limited availability of water.

During transport and storage, when the containers will be exposed to atmospheric conditions, it is assumed that air flow through a vent will ensure that the environment in waste containers will remain oxic. This is probably an oversimplification, as it is possible

that anoxic niches may be present in these circumstances. However, as long as the niches are small in size relative to the waste volumes, the assumption of aerobic conditions during these phases is a reasonable assumption overall. Post-closure, when the wastes are isolated from the atmosphere, the oxygen remaining in the vaults at closure has to be consumed before the conditions become anoxic.

During transport and storage, some water may be present in packages from the initial creation of the waste form. Some water vapour may also diffuse into packages through the vent. Following GDF closure, there will be a period of intermediate water saturation in the vaults, en route to full resaturation, which may take anything from a few years to a thousand or more years, depending on the properties of the host rock. During the period of partial saturation, the vault humidity may be at 100%, but it is not clear to what extent gas generating processes in packages into which liquid water has not yet percolated will be inhibited by water shortages.

5 Corrosion rates of carbon steels during waste management

The data presented in this section include those originally presented in reference [13], and have been supplemented with data that were either identified from recent literature searches or provided by the partners in the CAST project. The data are summarised in a tabular manner (see Table 7 to Table 13) by corrosive environment. In each table, the additional data have been appended after the data from reference [13].

5.1 Neutral solutions

5.1.1 Aerobic neutral solutions

Considerable bodies of work have been published on corrosion in drinking water, seawater and hot concentrated brines (particularly in relation to the corrosion of HLW waste packaging materials in hot geological brines, *e.g.* Q-brine, Germany, and Yucca mountain brines, U.S.A.). Other papers report corrosion rate data for a variety of chloride solutions, including simple chloride solutions, minewaters and groundwaters (which from coastal locations may have salinities similar to or greater than seawater).

A summary of data relating to the corrosion of carbon steel in aerobic neutral solutions is given in Table 7. The following subsections review how the corrosion rate depends on the main environmental variables.

5.1.1.1 Effect of temperature

The temperature can affect the corrosion rate in two main ways. Firstly, an increase in chemical reaction rates, and hence corrosion rate, is to be expected if the temperature is raised. Secondly, the temperature affects the solubility of oxygen and consequently the access of oxygen to the surface. Temperature differentials produce convection currents and so also influence the access of oxygen to the surface. In general the corrosion rate increases up to about 80°C, after which the corrosion rate declines as a result of the effect of reduced oxygen solubility at higher temperatures dominating over the increased electrochemical reaction rates and oxygen diffusion rate. This behaviour is shown in Figure 4 [22]; Figure 4

also shows that in a closed system the corrosion rate does not pass through a peak, but continues to rise with temperature because the oxygen is not allowed to escape.

5.1.1.2 Effect of oxygen concentration

In seawater the corrosion rate is normally directly proportional to the oxygen concentration. This can be seen by examining the corrosion rate of steel as a function of depth in the sea (Figure 5), and the results of corrosion tests over a range of oxygen concentrations (Figure 6). This implies that in a GDF, the corrosion rate would fall as the oxygen is consumed by corrosion, and that the approach to anaerobic conditions would decelerate.

The aerobic corrosion rate would be controlled by the supply of oxygen to the metal surfaces of the containers and waste, which in turn would depend on restrictions to the oxygen supply and the diffusion rate of oxygen through the surrounding media. As the oxygen concentration drops, the corrosion potential of iron would fall until eventually the potential at which hydrogen generation can occur would be reached, and anaerobic corrosion, by the reduction of water, would begin.

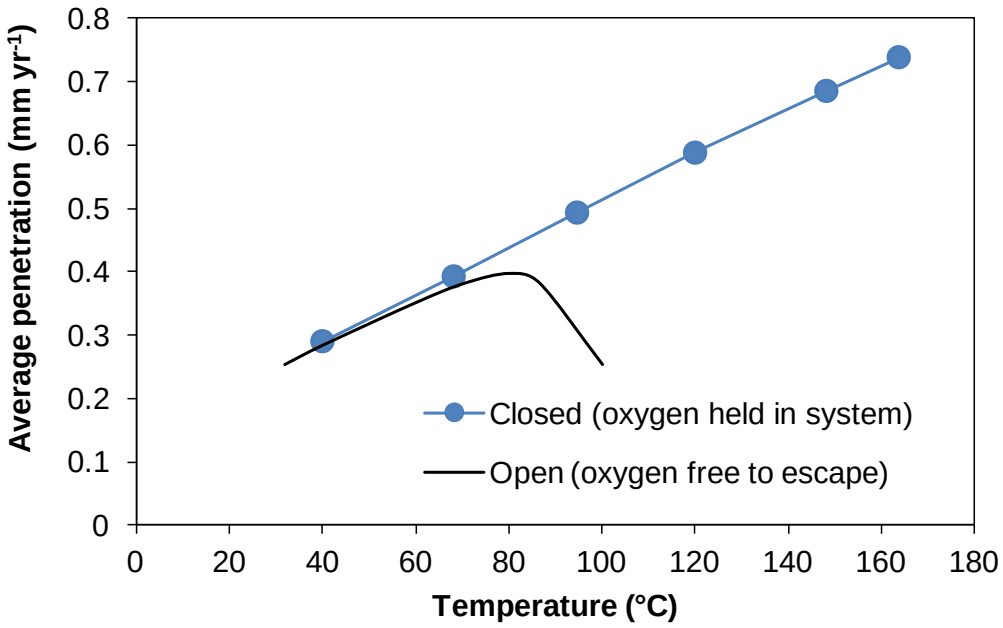

Figure 4: Comparison of the effect of temperature on corrosion in water in an open compared to a closed system (redrawn from reference [22]).

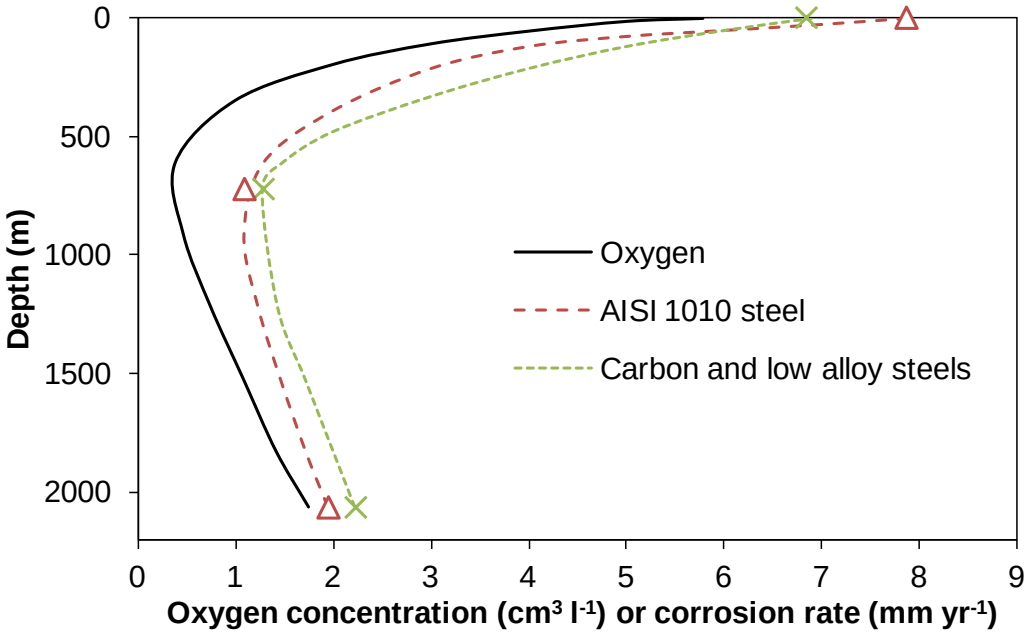

Figure 5: The corrosion of steels with depth in seawater (1 year of exposure) and its correlation with the dissolved oxygen concentration (redrawn from reference [94]).

(a)

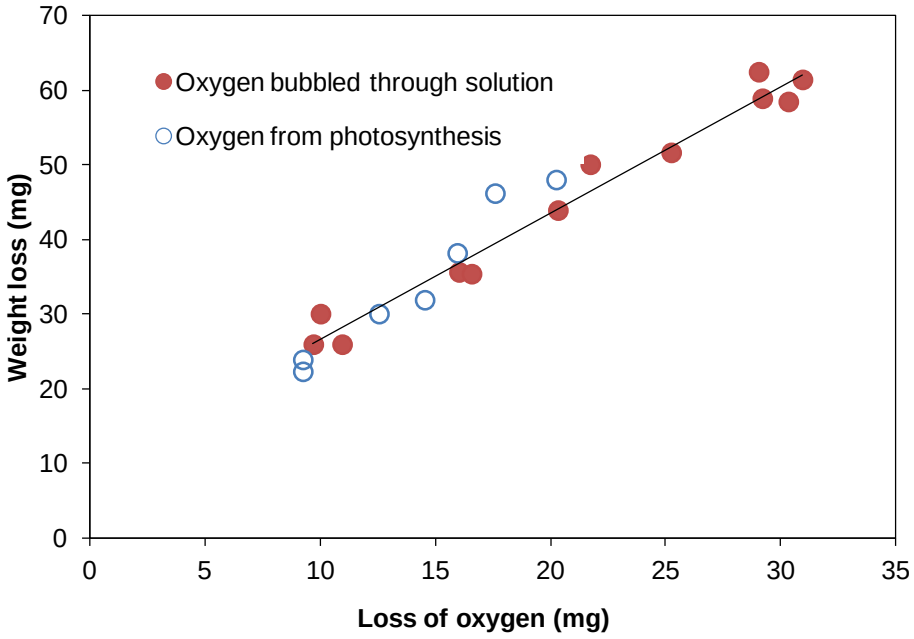

b)

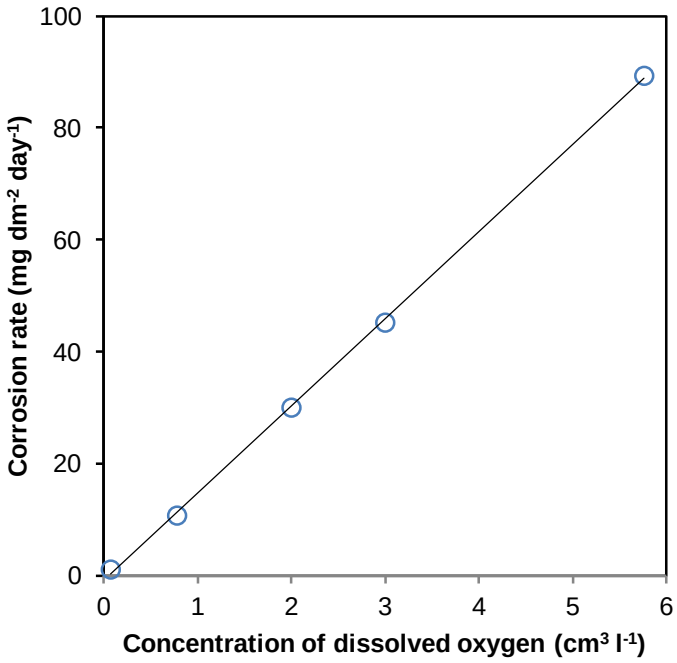

Figure 6: Effect of dissolved oxygen on corrosion rate of steel in (a) seawater (redrawn from reference [85]) and (b) slowly moving water containing 165 ppm $CaCl_2$ (redrawn from reference [24]).

It is important to distinguish between data from experiments in which the test solution is static and those where a rotating electrode is used to fix the mass transport rate of oxygen to the surface. In controlled mass transport rotating electrode experiments (*e.g.* [86-88]) the corrosion rate is under anodic control and is proportional to the oxygen and chloride concentrations, and temperature (see Figure 7 to Figure 9). At high oxygen concentrations, oxygen has a passivating effect [23]. However, in static experiments the corrosion rate is under cathodic control and is governed by the rate of diffusion of oxygen to the surface. In some experiments reported in the literature the test solution was actively sparged, which has the effect of stirring the solution and increasing the oxygen supply to the surface, so increasing the corrosion rate. The data from static immersion tests and real life exposure, are the most relevant to carbon steel in a GDF.

It is possible that hydrogen would be generated under aerobic conditions. For example, Hara *et al.* [89] measured the production of hydrogen from carbon steel as a function of the oxygen concentration in seawater at 80°C. The hydrogen production increased with increasing oxygen concentration, although the proportion of the corrosion associated with hydrogen production decreased with increasing oxygen concentration. The most likely explanation for this behaviour is that acidification had occurred within regions of localised corrosion, leading to hydrogen production.

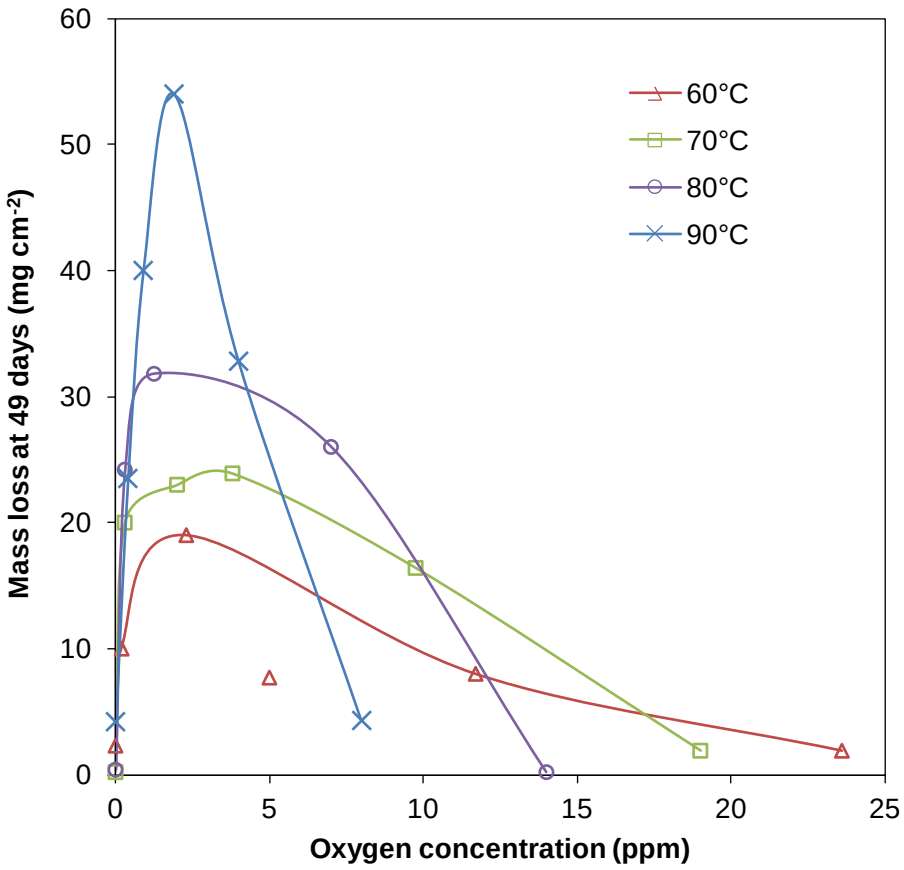

Figure 7: Mass loss of rotating disc mild steel specimens in distilled water at varying temperature and oxygen concentration (redrawn from reference [86]); the lines joining the points are included to aid the eye.

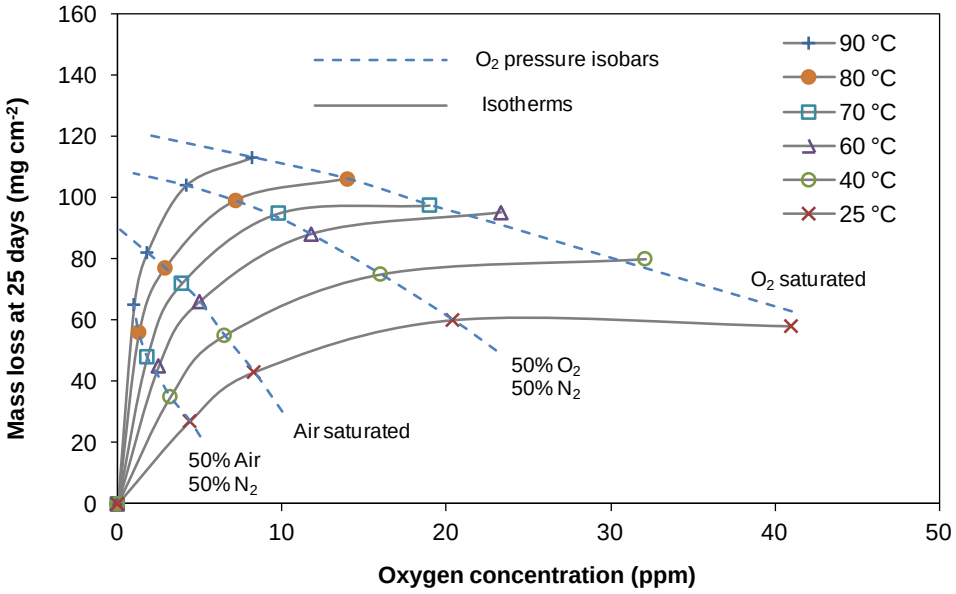

Figure 8: Mass loss of rotating disc mild steel specimens in sodium chloride solutions (35 ppm chloride) at varying temperature and oxygen concentration (redrawn from reference [86]).

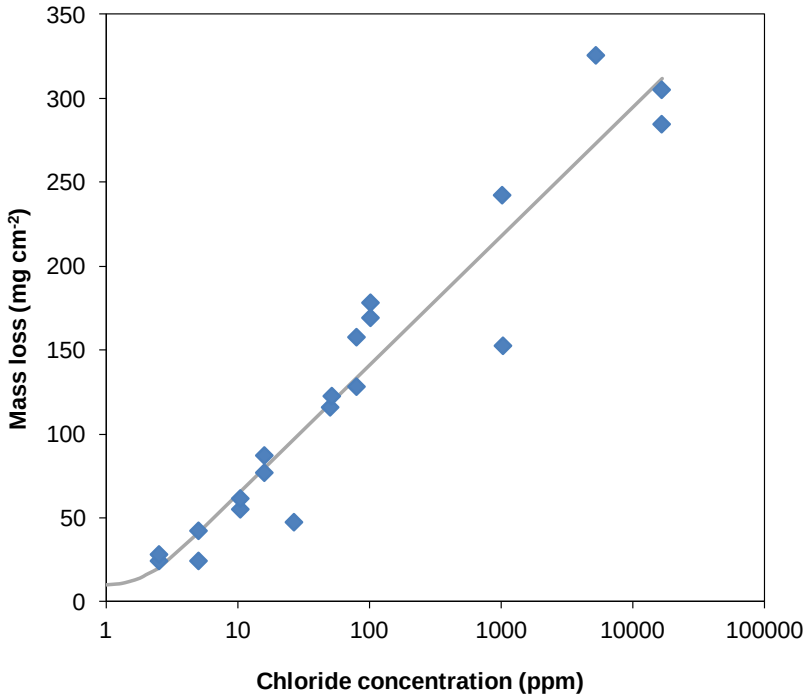

Figure 9: Mass loss of rotating disc mild steel specimens after 24 days in oxygenated sodium chloride solutions at varying chloride concentration (redrawn from reference [86]).

5.1.1.3 Effect of chloride concentration

In stagnant conditions the corrosion rate of steel in chloride solutions reaches a maximum at a chloride concentration of approximately 0.5M NaCl (Figure 10). At low chloride concentrations, the corrosion rate is increased by increasing the concentration of chloride, because the conductivity of the solution increases, but at higher concentrations the corrosion rate falls because the oxygen solubility is reduced. The corrosion rate is also different for different cations in chloride solutions (Figure 10).

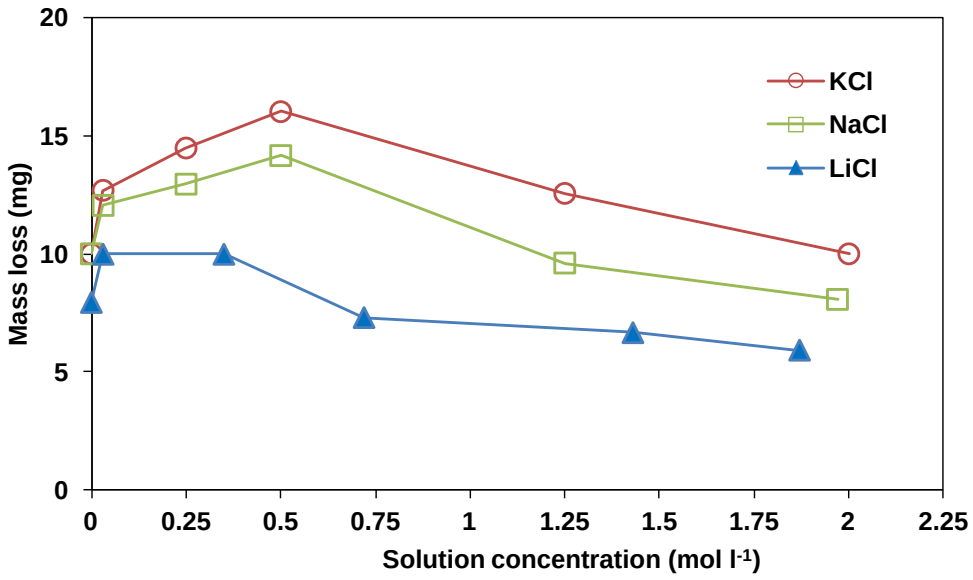

Figure 10: Corrosion rate of mild steel as a function of chloride concentration (redrawn from reference [90]); the lines joining the points are included to aid the eye.

5.1.1.4 Effect of dissolved gases

Dissolved carbon dioxide increases the corrosion rate of iron in water [22, 91, 92] by decreasing the pH of the water and hence increasing the current due to hydrogen ion reduction. Similarly, dissolved H_2S can increase the corrosion rate of metals by reducing the pH [22].

5.1.1.5 Effect of surface condition

The condition of the surface, *e.g.* whether the surface is freshly prepared, pre-corroded, or covered with mill scale, affects the subsequent corrosion rate. It is possible that the presence of some types of iron oxide would prevent the potential of the specimen becoming sufficiently negative to allow hydrogen generation by anaerobic corrosion.

5.1.1.6 Effect of radiation

Gamma radiation fields can cause an increase, and sometimes a decrease, in the corrosion rate. This is due to the production of oxidising agents in solution, such as free radicals and hydrogen peroxide. Some authors (*e.g.* [93]) have allowed for this by experimentally determining multiplier factors, which should be applied to the corrosion rate measured in the absence of a radiation field.

5.1.1.7 Effect of hydrodynamics

The corrosion rate of many materials is increased if the corrosive medium is flowing [28], because (i) diffusion restrictions on the supply of oxygen to the surface are reduced (see subsection 5.1.1(b) above), and (ii) the flow can exert a mechanical effect on the oxide surface, removing protective oxide films. In static solutions the corrosion rate is determined by the diffusion of oxygen to the surface, and is hence under cathodic control, whereas in flowing solutions the corrosion rate may be under mixed or anodic control [86, 87].

5.1.1.8 Effect of corrosion product build up and scaling

As corrosion proceeds, a layer of corrosion product forms on the surface. If it is tightly adherent and highly protective it is usually referred to as a passive film. A passive film forms a barrier layer on the metal surface and reduces the corrosion rate. A passive film usually forms very rapidly (*i.e.* within days). Similarly, the deposition of a mineral scale from the water can reduce the corrosion rate. Scale deposition can be caused by (i) a change in pressure, (ii) a change in temperature, or (iii) mixing waters of different composition. If this were to occur at the metal surface, a protective scale could develop. On the other hand, the formation of a scale can also lead to under-deposit corrosion, by producing a crevice at the metal surface [94].

5.1.2 Anaerobic neutral solutions

A summary of the data relating to the corrosion of carbon steel in anaerobic neutral solutions is given in Table 8.

Diercks *et al*. [95, 96] have published a compilation of literature corrosion rate data for anaerobic and aerobic acid chloride solutions, such as might occur in HLW repositories with concentrated brines at high temperatures. This compilation includes corrosion rates for mild steel in aerobic and anaerobic neutral solutions over a range of temperatures, which are illustrated in Figure 11. At temperatures below 100°C the corrosion rates fall in the range 1 to 100 µm yr^{-1}.

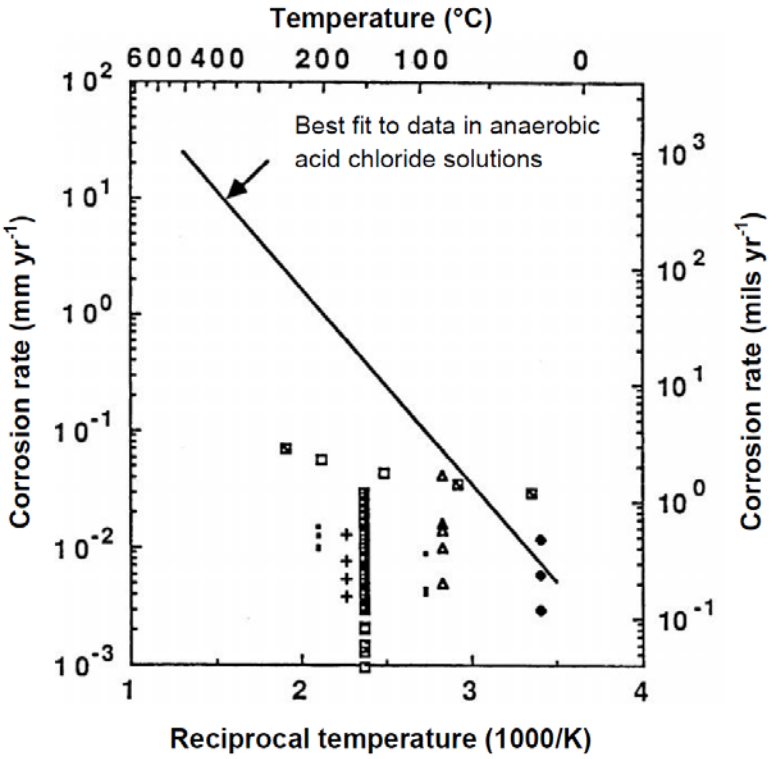

Figure 11: Comparison of corrosion rates for carbon steels in aerobic and anaerobic neutral and basic chloride solutions as a function of temperature (data points), and in anaerobic acid chloride solutions (best fit line) (redrawn from references [95, 96]); the unit mils yr^{-1} corresponds to thousandths of an inch per year.

Examination of the data in Table 8 shows that instantaneous electrochemical measurements give much higher corrosion rates than long-term weight loss and hydrogen evolution measurements. This is illustrated in Figure 12 and Figure 13, which show the corrosion rates measured using instantaneous and integrated techniques respectively, as a function of temperature, for all chloride concentrations. To increase confidence in the data used, it is preferable to use literature data from long-term exposure tests when assessing the potential long-term corrosion rates of waste containers. The corrosion rate in anaerobic neutral conditions is insensitive to temperature, in agreement with Jelinek and Neufeld [45]. Corrosion under neutral, anaerobic conditions has been reviewed by Platts *et al.* [97].

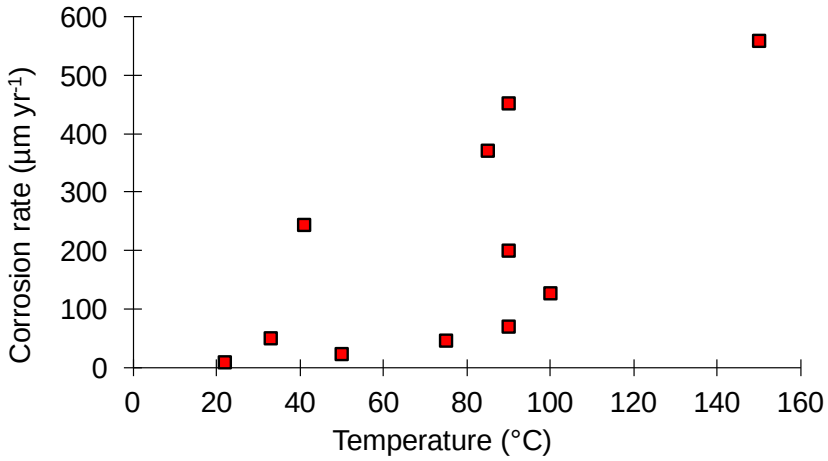

Figure 12: Instantaneous corrosion rate measurements for mild steel in anaerobic neutral solutions, as a function of temperature, based on data in Table 8.

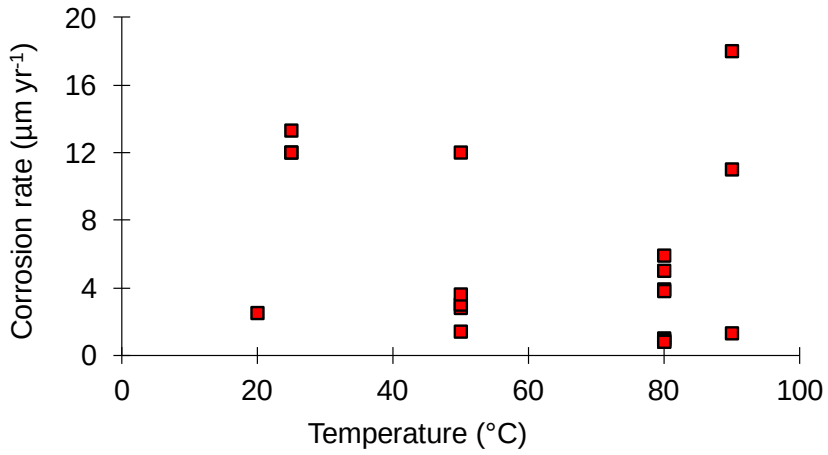

Figure 13: Integrated corrosion rate measurements for mild steel in anaerobic neutral solutions, as a function of temperature, based on data in Table 8.

5.2 Alkaline solutions

5.2.1 Aerobic alkaline solutions

A summary of the data relating to the corrosion of carbon steel in aerobic alkaline solutions is given in Table 9.

The results of Akolzin *et al*. [98] (Figure 14) show that the higher the concentration of $Ca(OH)_2$ the lower the corrosion rate. For passive mild steel, corrosion rates in the range 1-10 µm yr^{-1} have been reported for ambient temperatures. At high temperatures at pH above 14 the corrosion rate is very high, for example Yasuda *et al*. [99] (Figure 15) recorded 4,000 µm yr^{-1} at 117°C in 30% NaOH. There is a lack of information for intermediate temperatures. Grubitsch *et al*. [100] have shown that the rate of corrosion in $Ca(OH)_2$ increases with increasing chloride concentration.

a)

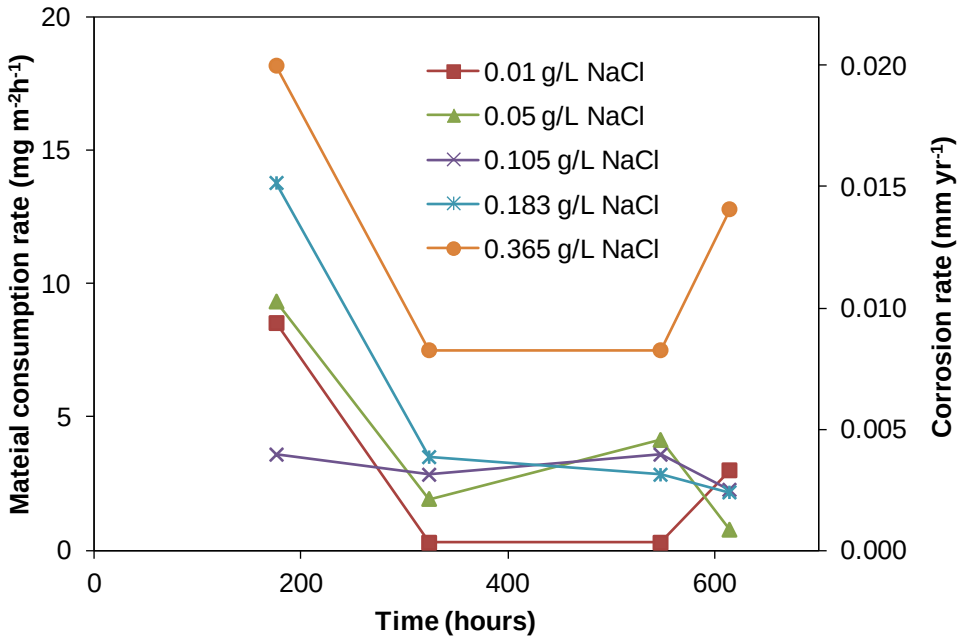

b)

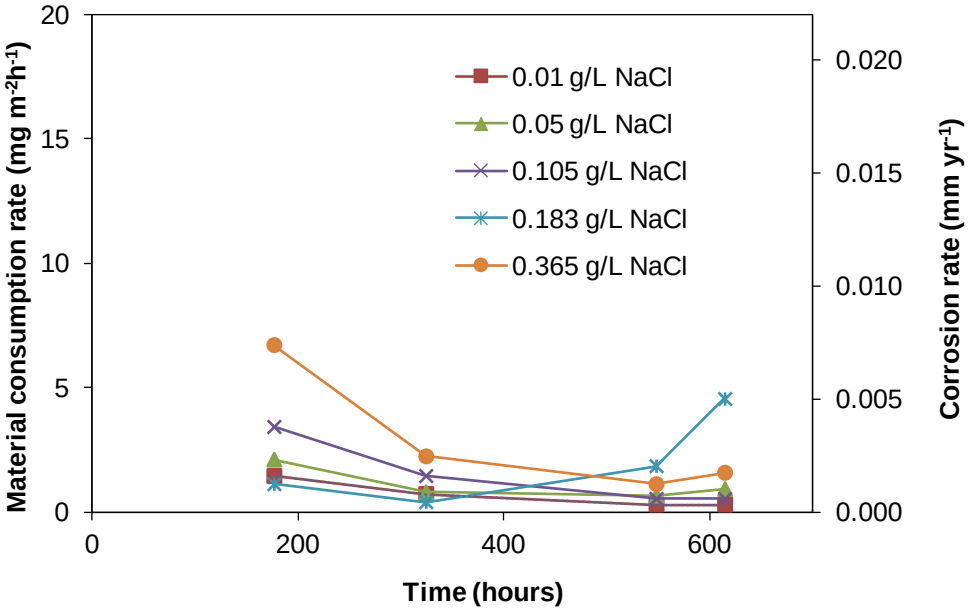

Figure 14: Change in the corrosion rates with time of carbon steel in: a) 0.43 g l^{-1} $Ca(OH)_2$ solution; and b) 0.76 g l^{-1} $Ca(OH)_2$ solution as a function of the sodium chloride content (redrawn from reference[98]); the lines joining the points are included to aid the eye.

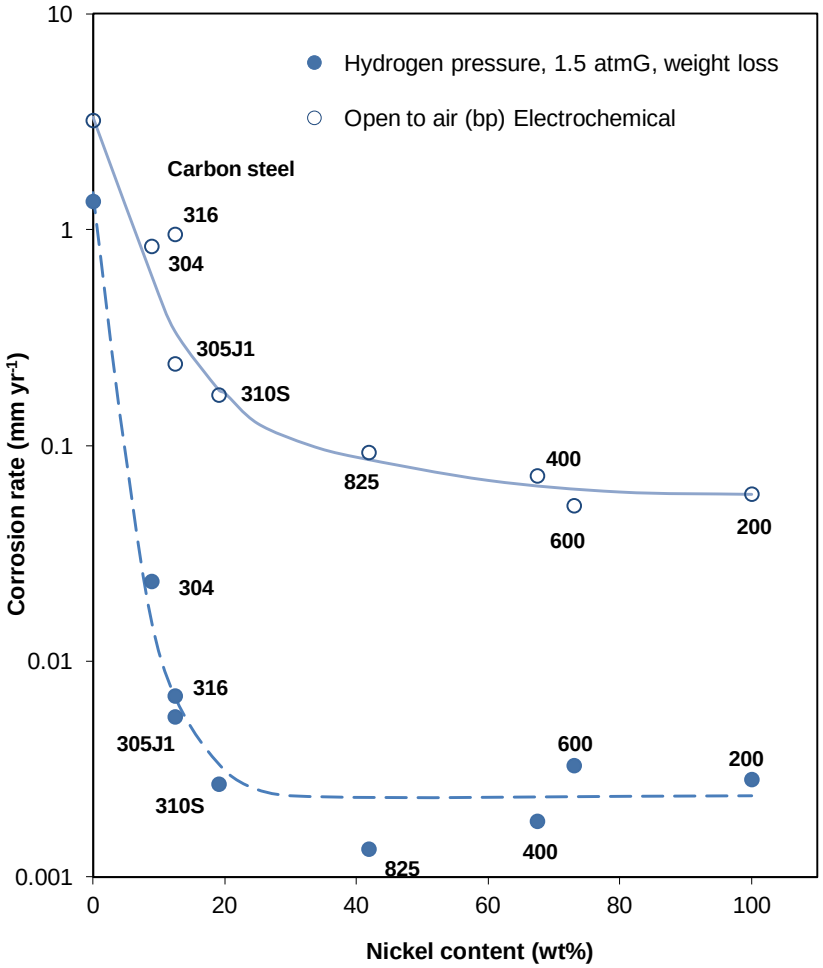

Figure 15: Corrosion rate of various materials in 30% NaOH solution as a function of the nickel content: solid line with open points - by the electrochemical technique in a solution open to the air; broken line with closed points - by weight loss measurements in a H_2 saturated solution (redrawn from reference [99]).

5.2.2 Anaerobic alkaline solutions

A summary of the data relating to the corrosion of carbon steel in anaerobic alkaline solutions is given in Table 10.

The most relevant data are those generated over very long periods by hydrogen evolution experiments [73, 74, 101]. These experiments show that the corrosion rate may fall as low as 0.07 nm yr^{-1} at 20°C. This is a reflection of the very low solubility of iron oxides at high pH and the low concentration of H^+ at high pH.

As part of the UK programme the hydrogen evolution rate for carbon steel and stainless steel was measured for a range of conditions; the data obtained have been summarised in reference [62]. The data for carbon steel are given in Table 13 and are shown graphically in Figure 16.

If the material is pickled to remove the air-formed film, there is an initial peak in corrosion rate, which then decreases with time to a low value as a layer of corrosion product builds up. This is predominantly magnetite in the tests carried out on the UK programme. This general form of the curve relating hydrogen evolution rate or corrosion to time has been observed both in strongly alkaline conditions [62], relevant to cement-based disposal concepts, and in weakly alkaline conditions studied on the Swedish programme (*i.e.* in bentonite or bentonite porewater simulant solutions) [102-104],which are more relevant to disposal concepts for spent fuel. In common with the work in strongly alkaline solutions, experiments within the Swedish programme found that the corrosion rates in aqueous conditions were higher initially at higher temperatures. However, the long-term corrosion rates were higher in the lower-pH bentonite solutions used in the Swedish programme than in the highly-alkaline solutions studied in the UK.

Japanese workers have reported the results from hydrogen generation rate corrosion measurements [105]; they obtained anaerobic corrosion rate data for carbon steel, stainless steel and Zircaloy in alkaline solutions under low oxygen conditions at 50°C. The corrosion rates for carbon steel, stainless steel and Zircaloy were given as 10^{-1} µm yr^{-1}, 10^{-2} µm yr^{-1} and 10^{-3} µm yr^{-1} respectively. In further work [106], the rate of hydrogen gas generation was measured in a solution of $Ca(OH)_2$ with 5,000 ppm chloride at pH 12.4. In these experiments the long-term instantaneous corrosion rates for carbon steel after 900 days and stainless steel after 650 days at 35°C were both ~2×10^{-2} µm yr^{-1}. The instantaneous corrosion rate for Zircaloy was ~1×10^{-2} µm yr^{-1} after 650 days at 35°C.

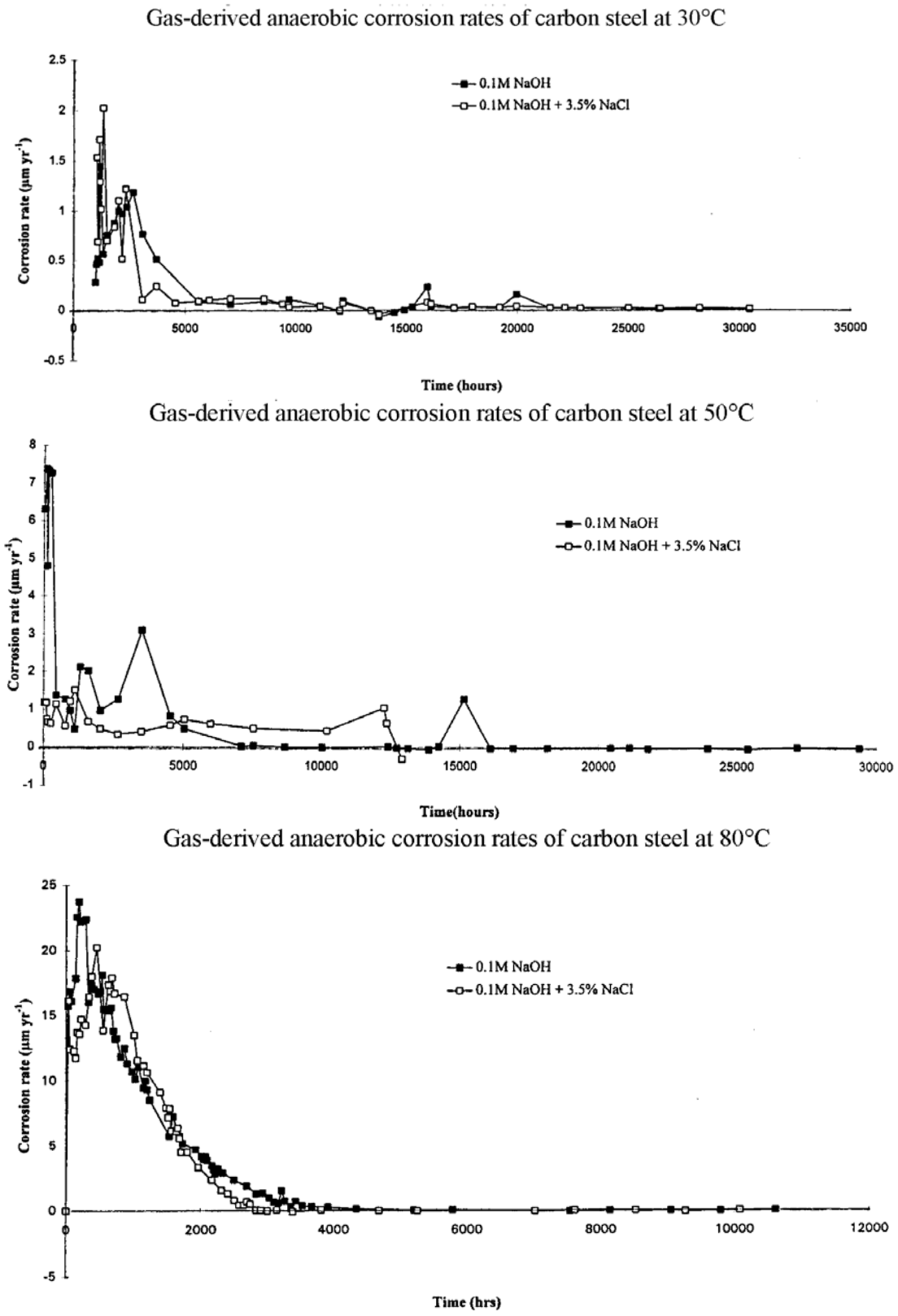

Figure 16: Gas-derived anaerobic corrosion rates for carbon steel in sodium hydroxide solution with and without 3.5% NaCl at 30, 50 and 80°C [107].

5.3 Corrosion in concrete

5.3.1 Aerobic

The corrosion of steel reinforcement bars in concrete is analogous to the corrosion of waste and containers in cementitious grout. The general features of corrosion in concrete have been described in a number of publications (*e.g.* [108-116]). The important parameters in determining the corrosion rate are the relative humidity [117, 118] of the surrounding atmosphere, the rate of movement of the carbonation front through the concrete (and whether it has resulted in a fall in pH at the steel-concrete interface), concrete porosity, cement type, chloride concentration, the OH^-/Cl^- concentration ratio at the metal interface and the rate of diffusion of oxygen through the concrete. The existence of cracks in the mortar can also affect the corrosion rate. Table 11 provides examples of corrosion rates for steel in concrete.

The work of Flis *et al*. [119] illustrates the range of corrosion rates that can occur in real structures. In constructions where chloride had not penetrated the concrete and the carbonation front had not reached the reinforcement bar, corrosion rates as low as 0.08 µm yr^{-1} were recorded. At the other extreme, reinforcement in concrete immersed in marine environments experienced corrosion rates up to 350 µm yr^{-1}. Tuuti [110] has also reported data from real structures; in the worst case the corrosion rate in a chloride-containing concrete reached 500 µm yr^{-1}. The likelihood of corrosion in concrete increases with temperature [120].

5.3.2 Anaerobic

In deaerated mortars without added chloride, corrosion rates in the range 0.23 to 1.44 µm yr^{-1} have been observed [121-125], although it was noted that these probably represented maximum values. Recently Newman *et al*. have reported very low corrosion rates (i.e. <0.01 µm yr^{-1}) for carbon steel in deaerated concrete [126, 127]. Work is currently in progress for the NIRAS-ONDRAF programme to measure the anaerobic corrosion rate of carbon steel under anaerobic conditions, mainly in alkaline solutions, but with a few experiments in a solid cementitious environment. A full report of recent data will be published later in 2014; selected data are available in published papers [128-132].

5.4 Atmospheric corrosion

During storage and subsequently during the operational phase of a GDF, carbon steel in the waste may be exposed to the ambient atmosphere, rather than be fully immersed in an aqueous phase. In this situation corrosion may arise as a result of the presence of a thin layer of moisture on the metal surface, which may contain chloride if the material is in a marine environment, and/or sulphur oxides in an industrial environment. The corrosion rate is therefore highly dependent on the exact atmospheric conditions. Typical atmospheric corrosion data in the literature are summarised in Table 12. In unpolluted, rural atmospheres the corrosion rates are typically in the range 10-50 µm yr^{-1}, but in humid marine atmospheres corrosion rates up to 1200 µm yr^{-1} may be experienced. A clear relationship exists between the deposition rate for chloride particulates and the corrosion rate, as shown by Figure 17. There is a lack of atmospheric corrosion rate data for temperatures greater than about 30°C.

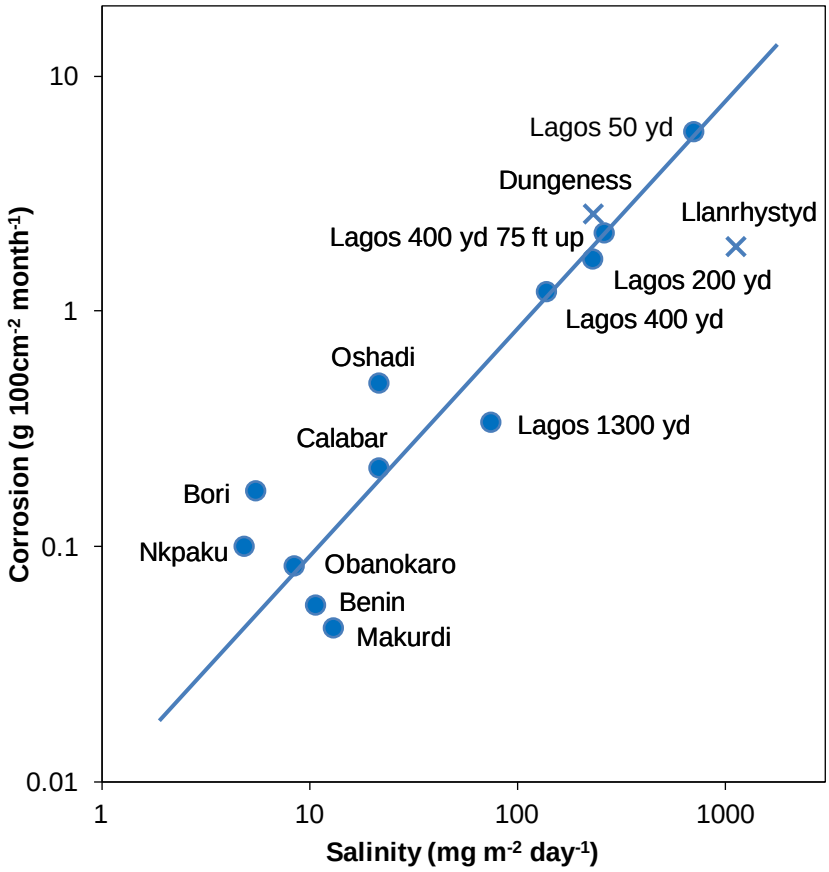

Figure 17: Relationship between corrosion of mild steel and salinity at exposure sites in Nigeria and the United Kingdom (redrawn from reference [133]).

5.5 Overview of carbon steel corrosion data

Having reviewed the available literature on the corrosion of carbon steel, the most relevant data have been considered by examining the corrosion rate summary tables (*i.e.* Table 7 to Table 12). In reality, it is likely that the carbon steel will experience a range of corrosion rates, depending on the exact nature of the chemical environment (e.g. that produced by the specific waste stream). The likely corrosion rates are discussed below.

5.5.1 Aerobic corrosion in grout, low chloride

There are not many data relating to the short-term corrosion rate of carbon steel; however Arya has reported electrochemical data as a function of time [134], showing an exponential

decrease with time for a number of different cement mixes containing 1% or 3% chloride. The initial peak corrosion rate was of the order of 200 µm yr^{-1}. The decay in corrosion rate probably reflects both the reduction in the availability of water during curing and the passivation of the steel surface. The passivation was more rapid in 1% chloride tests, where passivation was typically complete within 20 days, compared to 80 days with 3% chloride present. In the absence of chloride it is probable that passivation would be complete within a few hours. The precise corrosion rate will depend on the chemistry of the specific cement type and the wastestream.

In the absence of chloride and carbonation effects, the corrosion rate of carbon steel in cementitious environments is very low because of the protection offered by the passive film formed in alkaline conditions (Table 11).

There is a limited amount of data relating to the effect of temperature on the corrosion rate in concrete; most experimental work has been carried out at ambient temperature. However, Liu and Weyers [135] carried out a systematic 5-year study of the corrosion rate of steel in concrete as a function of temperature (0-35°C), concrete ohmic resistance and chloride content. They developed a model for predicting the corrosion rate in concrete and included the following relationship for the effect of temperature on the corrosion rate of steel in concrete:

$$i_2 = i_1 e^{2283\left(\frac{1}{T_1}-\frac{1}{T_2}\right)} \qquad (5)$$

where

T_1, T_2 are temperatures [K];

i_1 is the corrosion current[11] at temperature T_1 [A];

i_2 is the corrosion current at temperature T_2 [A].

[11] The corrosion current is directly proportional to the corrosion rate and can be converted to a corrosion rate by applying Faraday's laws of electrolysis.

It should be noted that changes in temperature will also affect other interacting factors which could influence corrosion rate, such as oxygen diffusion rate and the electrical resistance of the concrete.

5.5.2 Anaerobic corrosion, low chloride, alkaline conditions

For pre-corroded materials, there will probably be an incubation period before anaerobic corrosion initiates, as shown by Smart *et al*. [62] and Fujisawa *et al*. [136]. If any uncorroded carbon steel is present, the initial corrosion rate will depend on the temperature; there is an Arrhenius type relationship between the short-term corrosion rate and temperature [62]. For pre-corroded material it is reasonable to assume that eventually anaerobic corrosion will initiate at a low level, although it is likely that there will not be an initial peak in the corrosion rate.

Figure 18 shows the Arrhenius relationship for the initial corrosion rates. This plot gives a rate of approximately 0.5 µm yr^{-1} at a temperature of 30°C. The data in reference [62] show that although the initial anaerobic corrosion rates of carbon steel are higher at 50°C and 80°C, the corrosion rate falls more rapidly at higher temperatures.

The most relevant data for the long-term anaerobic corrosion rate of carbon steel is the gas evolution data obtained in the UK [62] (Table 13), in recent Japanese work [105,106,136] and in current work for the Belgium national programme on the anaerobic corrosion of the carbon steel overpack in the concrete buffer of their Supercontainer concept [128-132]. This programme has examined the corrosion behavior of carbon steel at pH 13.4 in concrete and aqueous environments as a function of temperature, chloride concentration, irradiation (25 Gy hr^{-1}) and the presence of sulphur species (specifically sulphide, thiosulphate), to reflect the operating conditions in the proposed Belgian repository concept. This programme has shown little effect of radiation, chloride or sulphur species on the anaerobic corrosion rate and the long-term corrosion rates have been found to be <0.1 µm yr^{-1}. Experiments are still in progress.

There does not appear to be any strong effect of temperature on the long-term anaerobic corrosion rate of carbon steel, due to the formation of a protective magnetite film, which leads to a slow decrease in the long-term corrosion rate. On the basis of the available data

(summarised in Table 13) and calibration calculations carried out using the SMOGG corrosion model, a long-term chronic anaerobic corrosion rate of 0.005 µm yr^{-1} was derived for alkaline conditions [13]. It was concluded that it was not possible to distinguish whether the corrosion rate would fall below a value of 0.005 µm yr^{-1} with time, owing to the sensitivity limits of the techniques used to measure the corrosion rates.

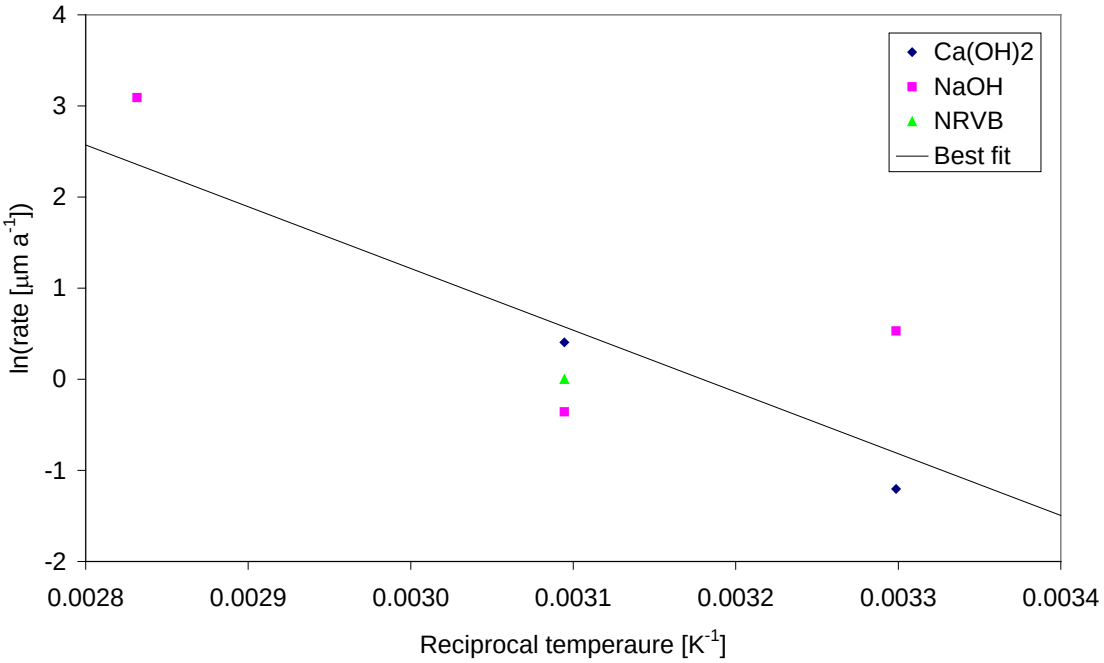

Figure 18: Examination of potential Arrhenius relationship between calibrated short-term anaerobic corrosion rates for carbon steel and temperature [13].

5.5.3 Anaerobic corrosion, high chloride, alkaline conditions

The anaerobic corrosion rate of carbon steel appears to be only weakly affected by the presence of chloride under alkaline conditions [62], as illustrated in Figure 16.

Table 7: Carbon steel corrosion rates in aerobic, neutral conditions.

Reference	Environment	Temp (°C)	Corr. rate (µm yr^{-1})	Times	Remarks
Borgmann [90]	0 to 2M NaCl, KCl, LiCl, aerated	ambient	40-120	2 days	Corrosion rates measured by weight loss as a function of chloride concentrations (Figure 10).
Braithwaite and Lichti [137]	Geothermal condensates	10-20	18	1 year	Corrosion rates measured by weight loss. Incomplete analysis of condensate composition, but ~2 mMol H_2S present, low Cl.
Breckheimer and D'Ans [138]	0.001 to 3M KCl	25-85	50-250		Corrosion rate increases with temperature but not appreciably with KCl concentration.
Canadillas *et al.* [139]	Q-brine Distilled water	35 55 90 35 55 90	25 25 62 67 62 41	75 & 148 days	Weight loss experiments carried out in a closed system, so the oxygen would have been exhausted after a short period. In Q-brine "acid corrosion" occurs at higher temperatures so the corrosion rate increases.
Elmorsi and Issa [140]	Groundwater	40	28-211	2-12 months	Corrosion rate was measured using a "corrosometer" in Egyptian well waters, with a wide range of compositions; TDS 150-731 ppm, ~2ppm H_2S present.
Francis and Mercer [86], Mercer and Lumbard [88]	Forcibly aerated distilled water	40 60 70 80 90	93 120 160 230 324	up to 100 days	Corrosion rate was measured by weight loss measurements in static solutions. Corrosion rates were higher when the air was passed through the solution rather than over the surface. In static experiments the corrosion rate was independent of chloride concentration, because oxygen diffusion is the controlling parameter. In experiments using a rotating electrode (1 Hz) corrosion rate was related to oxygen concentration, temperature and chloride concentrations (Figure 7-Figure 9). Oxygen has a passivating effect at high concentrations.

Table 7 (Cont.): Carbon steel corrosion rates in aerobic, neutral conditions.

Reference	Environment	Temp (°C)	Corr. rate (µm yr^{-1})	Times	Remarks
Gaonkar *et al.* [141]	Distilled water and drinking water	25 40 60 70 80	90 222 324 340 334	up to 5 days.	The corrosion rate was measured by weight loss measurements over the temperature range 25-100°C. The maximum corrosion rate occurred at about 70°C. The shape of the curve was very similar to Figure 4. Chloride concentration 6 ppm.
Hache [142]	3% NaCl	0-80	.	16 hours	Corrosion rate in air saturated solution (11.5 ppm O_2 at 0°C to 4.2 ppm O_2 at 80°C) increased with temperature from 22 to 67 mg Fe d^{-1}; and from 6 to 66 mg Fe d^{-1} in partially dearated solutions (2.5-3.0 ppm O_2)
Higginson [87]	Mintek minewater	25	200	14 days	The corrosion rate in static solutions (0.03M chloride, pH 6.5), measured by weight loss, became constant after an initial period of rapid corrosion. Corrosion rate was also measured as a function of temperature, oxygen concentration and chloride concentration using a rotating electrode to control mass transport of oxygen to surface.
Ho and Roy [143]	Tropical seawater	28	350-530	2, 12 months	Weight loss measurements after immersion in natural seawater. In laboratory tests corrosion rate increased with temperature. Corrosion rate also affected by surface preparation and carbon content.
Honda *et al.* [144]	Seawater and distilled water mixed with compacted bentonite slurry	50-150	10-20	up to 180 days	Specimens were mounted between layers of bentonite and immersed in test solution. The corrosion rate was determined from weight loss.
Kalashnikova *et al.* [49]	Cuban Caribbean seawater	23-29	50-280	24 months	Weight loss and electrochemical measurements. Corrosion decreased over test period and reached a plateau after ~18 months.

Table 7 (Cont.): Carbon steel corrosion rates in aerobic, neutral conditions.

Reference	Environment	Temp (°C)	Corr. rate (μm yr^{-1})	Times	Remarks
Kennedy and Wilson [145]	Harbour seawater	ambient	60-130	35 years	The thickness of sheet metal pilings in New York Harbour were measured using an ultrasonic thickness probe.
Kritsky *et al*. [146]	Spent nuclear fuel pond water	ambient	40-80	340 days	Corrosion rate measured by weight loss measurements in pond water containing ~2 ppm dissolved salts at pH 5 to 9.
Kuron *et al*. [147]	Tap water with 0.28-15.5M chloride added	ambient	~45	10000 hours	Corrosion rate was measured using rotating disks and pipe. The chloride concentration did not affect corrosion rate. The figures given refer to zero flow experiments.
Larrabee [148]	Seawater	ambient	39±6	23.6 years	Steel pilings on pier in California
McRight and Weiss [149]	Aerated J13 well water pH 7.1-7.5, 6 to 8 ppm chloride	50 70 80 90 100	401 505 531 414 320	1500 hours	Weight loss measurements were carried out on mild steel 1020. The well water was air sparged to produce the most corrosive conditions (5-6 ppm oxygen).
Merz [150]	Brine and seawater	ambient to 250	7-10000		Contains a compilation of data for carbon steel and cast iron in brine and seawater as a function of temperature and pH.
Nissing *et al*. [151]	Drinking water, pH 7.2 and 8.0, as f[O_2] and flow rate	ambient	14-70	3.5 years	Ring specimens were exposed to flowing tap water with oxygen concentrations in the range 0.01-4 mg l^{-1} and pH 7.2 and 8.0. The corrosion rate is constant initially then it follows a power law.
Peterson and Waldron [152]	Harbour seawater	ambient	120	18 months	
Reinhart [153, 154], Larrabee [155]	Seawater	ambient	50-200 average ~100	0-16 years	Corrosion rate decays with time. Corrosion rate reduces with depth.

Table 7 (Cont.): Carbon steel corrosion rates in aerobic, neutral conditions

Reference	Environment	Temp (°C)	Corr. rate (µm yr^{-1})	Times	Remarks
Schwarzkopf *et al.* [156]	Concentrated brine (26.9 wt% NaCl)	90	120	1.5 years	A cast steel tube was stored for 18 months in a heated borehole containing NaCl brine, with temperatures from 90°C to 200°C.
Shannon [157]	geothermal brines, seawater, various pHs	43	25 to 30 at pH7 ~130 at pH7	7 days	A compilation of literature results for 1 ft $second^{-1}$ flow, 60 ppb oxygen.
Simpson and Weber [158]	Aerated Böttstein groundwater 0.1 mg g^{-1} O_2	80	24 52 60	700 hours 2200 hours 6200 hours	Weight loss experiments were carried out in a refreshing autoclave, so that the oxygen concentration could be maintained.
Smailos *et al.* [159-162]	Q-brine	90	31-50 14 23 37 460	1 year	radiation levels of 0 1 10 100 1000 Gy hr^{-1}. Corrosion rates decreased with time.
Southwell and Alexander [163]	Freshwater Seawater	ambient	18 64	16 years	Coupons were suspended in seawater and freshwater and the corrosion rate was monitored by weight loss. The corrosion rate decreased with time initially to achieve a constant longer-term rate after about 4 years.
Uhlig [24]	Natural seawater	ambient	25-200, average 109	up to 31 years	The reference includes a tabulation of 34 weight loss measurements from continuous immersion tests at a range of world-wide locations.
White *et al.* [164]	Mediterranean seawater Dead Sea seawater	day: 40°C night: RT	73 14-20	103 days	Static immersion tests

Table 7 (Cont.): Carbon steel corrosion rates in aerobic, neutral conditions

Reference	Environment	Temp (°C)	Corr. rate (µm yr^{-1})	Times	Remarks
New Data[12]					
Atashin *et al*. [165]	Seawater, salinity 40g/L, without stirring pH 10.5 pH 7.5 pH 10.5 pH 7.5 pH 7.5 (stirred)	 23°C 23°C 65°C 65°C 65°C	 6.8 41 57 239 326	5 hours	Carbon steel CK 45 AISI 1045. Corrosion rate determined by potentio-dynamic polarisation scan (NB: short-term data).
Huet *et al*. [166]	Rebar immersed in saturated $CaCO_3$ solution, pH 8.3.	ambient	360 270	7 days 85 days	Mild steel FeE500, with a carbon content lower than 0.02%. Corrosion measured by mass loss. Corrosion rates estimated from plot in the paper.
	Rebar immersed in saturated $CaCO_3$, SiO_2, 0.025M $NaHCO_3$, pH 9.4.		160 ~10	7 days 85 days	

[12] This refers to data identified since the original literature review was carried out for preparing reference [13].

Table 7 (Cont.): Carbon steel corrosion rates in aerobic, neutral conditions

Reference	Environment	Temp (°C)	Corr. rate (μm yr^{-1})	Times	Remarks
Sherar *et al*. [167]	0.2 M $NaHCO_3$, 0.1 M NaCl, 0.1 M Na_2SO_4, pH 8.95, aerobic and anaerobic	ambient	4000 7800	28 days 35 days	X65 carbon steel. Calculated from R_p data
Tadros and Osman [168]	Natural seawater samples. pH 7.4 to 8.3	ambient	40-190	24 hours	Measurements by weight loss and polarisation technique. Results from the two methods were in good agreement.

Table 8: Carbon steel corrosion rates in anaerobic, neutral conditions.

Reference	Environment	Temp (°C)	Corr. rate (µm yr^{-1})	Times	Remarks
Blackwood *et al.* [169]	Granitic groundwater	50	initially ~2, long-term <0.1	5000 hours	The test specimens had pre-formed corrosion product films.
Diercks *et al.* [95, 96]	Anaerobic acid chloride solutions	20-400	10->1000		The reports contain compilations of literature results for anaerobic, acid, neutral and basic chlorides (e.g. Figure 11). There is an Arrhenius relationship with activation energy 32kJ mol^{-1} for the anaerobic, acid conditions.
Farvaque-Bera and Leistikow [170]	0.5M sulphate pH 0.4 to 6.0 and brines	25-90	80-154000 depending on pH and temp.	0	Instantaneous corrosion rates from polarisation curves.
Grassiani [171]	De-aerated 6% $MgCl_2$	33 41 85 90	50 244 371 452		Corrosion rates were measured using the linear polarisation technique.
Haberman *et al.* [172]	High-magnesium brine	90	~200	1 month	Corrosion rates were measured for ASTM 216 grade WCA mild steel using the linear polarisation technique. Arrhenius relationship for corrosion rate.
Helie *et al.* [173]	De-aerated 3 g l^{-1} NaCl	90		1000 hours	Polarisation resistance was used to measure corrosion rate as a function of time. It was found that the corroded thickness, e, was given by $e=kt^{½}$, where k = 5 mm $y^{-½}$ and t = time of exposure.
Kreis [174], Kreis and Simpson [175]	Groundwater, distilled water, 0.8% chloride	21	<0.08 to 0.7		Hydrogen evolution measurements were used to measure the corrosion rate of iron (0.91%C) in a range of media. Corrosion rate falls with time.

Table 8 (Cont.): Carbon steel corrosion rates in anaerobic, neutral conditions

Reference	Environment	Temp (°C)	Corr. rate (µm yr^{-1})	Times	Remarks
Jelinek and Neufeld [45]	De-aerated distilled water	90	1.3 (after 43 days)	0-43 days	Hydrogen evolution experiments. Corrosion rate derived from weight loss. Variables investigated: temperature; dissolved copper concentration and pH. The results were not temperature sensitive over the range 60-316°C.
Marsh *et al.* [72]	De-aerated synthetic seawater	20 50 90	2.1-3.1 5.3-14.6 10.6-21.6	up to 425 days	Corrosion rate was measured by weight loss. It decreases to ~6 µm yr^{-1} with time. The reference also includes data for effect of radiation and results for forged, cast and low carbon steel.
Posey and Palko [176]	4M NaCl, pH 2-7	25-200	7.6 to 12700	0	Electrochemical measurements of corrosion rate in a stirred autoclave. An Arrhenius relationship exists for corrosion rate for a range of pH values.
	pH 7	22 50 75 100 150 200	8.9 23 46 127 559 1270		
Reda *et al.* [177]	Dilute $MgCl_2$/NaCl solutions (up to 0.5M $MgCl_2$ and 0.85M NaCl)	25 distilled water 0.85M NaCl 0.5$MgCl_2$	9-17 12 12 13.3	up to 1100 hours	The pH of the solutions was in the range 4.6 to 6.6. The corrosion rate was measured by weight loss. The reference also includes data on the effect of radiation.
Simpson *et al.* [178,179], Schenck [180]	Groundwater and NaCl solutions pH 7 pH 8.5 pH 10	25-80	 2.8 1.4 0.3	6000 + hours (until gas evolution rate constant)	Hydrogen evolution experiments. Various types of hydrogen evolution behaviour were identified. The corrosion rates are average figures for all chloride concentrations and temperatures.
Simpson *et al.* [179]	Säckingen 0.1 µg g^{-1} O_2	80	86 34	500 hours 1440 hours	Integrated corrosion rates derived from weight loss measurements on cast mild steel.

Table 8 (Cont.): Carbon steel corrosion rates in anaerobic, neutral conditions.

Reference	Environment	Temp (°C)	Corr. rate (µm yr^{-1})	Times	Remarks
Simpson *et al.* [179] continued	Böttstein, Säckingen ground water, oxygen free (<0.01 µg g^{-1} O_2)	80	30-42 14-16 4-6	700 hours 2100 hours 6300 hours	Hydrogen evolution measurements. Steady state corrosion rates.
		25 50 80	1.1-1.5 3.2-6.5 1.5-2.5	2-3 days	
	$NaHCO_3/Na_2CO_3$ 0 mg g^{-1} Cl 80 mg g^{-1} Cl 800 mg g^{-1} Cl 8000 mg g^{-1} Cl	80	pH 7 8.5 10 0.9 0.3 0.5 3.8 1.5 2.5 5.0 0.5 1.0 0.8 2.5 0.5	2-3 days	
Simpson and Vallotton [181]	Böttstein, 0 O_2 0.1 mg/g O_2	80	5-10 60-68	6170 hours	Corrosion rates were derived from weight loss measurements; the corrosion rate decreases with time. Salinity and oxygen concentration had a greater effect than temperature.
	Säckingen, 0 O_2 0.1 mg/g O_2		5-6 7-18		
Simpson and Weber [158]	Anaerobic Böttstein groundwater	80	42 14 10	700 hours 2200 hours 6200 hours	Corrosion rates were determined from weight loss measurements.
Smith and Van der Schijff [182]	Domestic water, pH 9	25	3	<1 hour	Corrosion rates were derived from polarisation resistance measurements
Stahl and Miller [183]	Basalt groundwater	90	~70	<1 hour	Corrosion rates for 1018 steel were derived from electrochemical measurements.

Table 8 (Cont.): Carbon steel corrosion rates in anaerobic, neutral conditions

Reference	Environment	Temp (°C)	Corr. rate (µm yr^{-1})	Times	Remarks
Tas *et al*. [184]	interstitial claywater	90	10	9 months	Initial corrosion rates are high but decline significantly with time. The equivalent corrosion rate in aerated conditions was 25 µm yr^{-1}.
Westerman *et al*. [185]	$MgCl_2$ brine (6.7M Cl^-)	90	18	6 months	A216 steel weld metal.
New data[12]					
Felicione *et al*. [186]	In sealed vessels. In brine. Pressure 146 atm. Microbes added to simulate those in natural brine. Vessel purged with N_2 and pressurised to 146 atm.	30°C	Up to 2.3	6.5 years	Test samples were of mixed wastes, containing combinations of sludge, plastics, rubber and cellulose and well as carbon steel. Carbon steel wastes gave the highest H_2 production rates. Corrosion rates were calculated from H_2 generation assuming that all was due to corrosion. Note: experiments were carried out in the presence of microbes.
Lee *et al*. [187]	Groundwater simulants, pH 8.9, continuous purging with argon	ambient	1200 800 4600	400 hours	Steel type A516 Gr 70. From R_p data. ~0.8V. 0.2M $NaHCO_3$ / Na_2CO_3 + 0.1M Na_2SO_4 + 0.1M NaCl 0.2M $NaHCO_3$ / Na_2CO_3 + 0.1M Na_2SO_4 1.0M $NaHCO_3$ / Na_2CO_3
Sherar *et al*. [188]	0.2 M $NaHCO_3$, 0.1 M NaCl, 0.1 M Na_2SO_4, pH 8.95, aerobic and anaerobic	ambient	<1000	28 days	X65 carbon steel. Calculated from R_p data. Only aerobic shows measureable rate

Table 8 (Cont.): Carbon steel corrosion rates in anaerobic, neutral conditions

Reference	Environment	Temp (°C)	Corr. rate (μm yr^{-1})	Times	Remarks
Stoulil *et al*. [189]	Steel immersed in moist bentonite. Bentonite pore solution composition: pH 9.7 Cl^- 1 x 10^{-4} M SO_4^{2-} 5 x 10^{-5} M HCO_3^- 4 x 10^{-3} M	40°C and 90°C 40°C 90°C	200 11.8 7.9	24 hours 200 hours 200 hours	Carbon steel. Higher initial rate, was attributed to residual oxygen by the authors.
Wall and Wadsö [190]	Seawater. Salinity 0.2% to 0.8%	Ambient seawater temperature	10 - 70	36 to 51 years	From measurements on steel harbour structures, sited in Swedish coastal waters.
Martin *et al*. [191]	Iron immersed in Callovo Oxfordian claystone, anaerobic, pH 7.6	90	12 ~0.5	3000 hours 17000 hours	Pure Armco iron used to represent low alloyed steel. Measurements made by EIS

Table 9: Carbon steel corrosion rates in aerobic, alkaline conditions (there are no new data compared to reference [13]).

Reference	Environment	Temp (°C)	Corr. rate (µm yr^{-1})	Times	Remarks
Akolzin *et al.* [98]	0.43 and 0.76 g l^{-1} $Ca(OH)_2$ (pH12 and 12.3) + Cl^-	22	0.5 to 20	0	The corrosion rates were determined by polarisation resistance measurements. Figure 14 shows corrosion rates as a function of time, calcium hydroxide concentration and chloride concentration.
Blackwood *et al.* [192]	0.1M NaOH	30 50 80	0.1 0.4 2.3		Passive current measurements.
Byakova *et al.* [193]	30% KOH	ambient	6.1	"fairly long times"	
Drazic and Hao [194]	5M KOH	ambient	30	0	The corrosion rates of iron were derived from Tafel slope extrapolation.
Hubbe [195]	NaOH / NaCl, pH 9.5 at start NaOH / NaCl, pH 7.7 at end	ambient	200	48 hours	Corrosion rates of mild steel were determined by weight loss and polarisation resistance measurement.
Lesnikova and Frejd [196]	KOH pH 12 pH 13 pH 14	20	90-140 75-120 55-60	900 hours	
Schwenk [197]	0.5M $NaCO_3$ / 1M $NaHCO_3$	25	active 33 passive 3.5	up to 2500 hours	The corrosion rate of iron was measured by weight loss as function of potential.
Yasuda *et al.* [99]	30% NaOH	117	4000	0	The corrosion rates of mild steel and alloy steels were measured using the linear polarisation method (Figure 15).

Table 10: Carbon steel corrosion rates in anaerobic, alkaline conditions.

Reference	Environment	Temp (°C)	Corr. rate (μm yr^{-1})	Times	Remarks
Fujiwara *et al.* [198]	artificial cement porewater, pH 12.5-13.5	35	0.005-0.01	60 days	Corrosion rate was found to increase at pH 14, due to the formation of soluble $HFeO_2^-$ species. Hydrogen was also formed under aerobic conditions when localised corrosion and acidification occurred.
Fujisawa *et al.* [136]	mortar-equilibrated water pH 12 $Ca(OH)_2$ pH 12.8 synthetic groundwater + bentonite, pH 8	15 30 45 15	0.004 0.02 0.2 0.09	9,000 hours	Incubation period observed before gas generation started. The samples were not pickled initially. The incubation period was shorter at higher temperatures. Arrhenius relationship demonstrated at pH 12.6. There could have been an inhibition effect from dissolved glass. Black surface film observed. Activation energy 100 kJ mol^{-1}.
Grauer *et al.* [74], Grauer [101]	de-aerated groundwaters and porewaters, and KOH, $Ca(OH)_2$, and NaOH	21	0.00007-0.7	up to 12000 hours	The reference contains a literature survey which indicates that the corrosion rate in cement is in the range 0.08 to 1 μm yr^{-1}. Hydrogen evolution experiments were used to measure the corrosion rate of iron wire. The corrosion rate was lowest in porewaters. Different time dependencies were observed in NaOH, KOH, $CaOH_2$ and porewaters.
Grauer *et al.* [73]	sat. $Ca(OH)_2$ dilute alkali hydroxide, porewater	21	0.00015 to 0.0064	up to 13500 hours	Hydrogen evolution experiments were used to measure the corrosion rate of iron wire. The corrosion rate either decreased with time or remained constant.
Hansson [199]	$Ca(OH)_2$, pH 12.6 KOH, NaOH added in some experiments.	ambient	23-58	24 hours	Dynamic polarisation curve passive current densities were used to measure the corrosion rates. The results are probably an overestimate of the corrosion rate.

Table 10 (Cont.): Carbon steel corrosion rates in anaerobic, alkaline conditions.

Reference	Environment	Temp (°C)	Corr. rate (μm yr^{-1})	Times	Remarks
Kreis [174, 200]	porewater, NaOH, $Ca(OH)_2$, KOH, pH 12.5-13.2	21	<0.08		Hydrogen evolution measurements were used to measure the corrosion rate of iron (0.91%C) in a range of media. The corrosion rate depends on media. In some porewaters and groundwater corrosion rate <0.005 μm yr^{-1}.
Matsuda *et al.* [201]	artificial cement porewater	ambient	5	up to 30 days	Hydrogen analysed by gas chromatography. Corrosion rates also measured by weight loss. Short-term measurements.
Naish [107]	various mixtures of 0.1M KOH, 0.1M NaOH, $Ca(OH)_2$ NaCl up to 10,000 ppm chloride and with application of hydrogen overpressure.	ambient, 30, 50 and 80	10 initially to <0.001 long-term		Hydrogen evolution measurements used to measure the corrosion rate of carbon steel in a range of media. The corrosion rate at 30, 50 and 80°C decreased with time (Figure 16). The presence of an existing aerobically produced corrosion product film significantly reduced the rate of hydrogen gas production.
Yasuda *et al.* [99]	30% NaOH	117	1500	2 weeks	Weight loss measurements were made for a number of materials under hydrogen (Figure 15).
New data					
Smart *et al.* [128-132]	Young cement water, pH 13.4 and cement	25 80	<0.1	>5 years	Work carried out in support of Belgian Supercontainer concept on anaerobic corrosion of carbon steel. Corrosion rate measurements by hydrogen evolution and weight loss. Corrosion rate studied as a function of radiation, temperature, chloride, sulphide, thiosulphate at representative concentrations for repository concept.

Table 11: Carbon steel corrosion rates in concrete.

Reference	Environment	Temp (°C)	Corr. rate (μm yr^{-1})	Times	Remarks
Andrade and Alonso [202]	Concrete ranging from dry, uncarbonated, no chloride to highly contaminated with chloride	ambient	1-1100		Linear polarisation resistance.
Andrade *et al.* [203]	Laboratory experiments on reinforcing bars in carbonated mortar with chlorides	ambient	<1-100	45 days	Data showed strong effect of varying relative humidity and partial immersion on corrosion rate.
Arya and Xu [134]	Cement paste with various binders, with chloride content ranging from 0 to 3%. Samples exposed to salt solution at 95% humidity.	ambient	**1% chloride** 116-348 <1 **3% chloride** 116-812 20-116	 0-40 days 40-120 days 0-70 days 70-120 days	Chloride binding and its influence on the rate of reinforcement corrosion was investigated in a range of mixes by, respectively, pore solution analysis and measuring the galvanic current in macro corrosion cells formed by embedding mild steel bars in two layers of concrete. The corrosion rates increased with increasing chloride content for all mixes due to an increase in the amount of free chloride. Anodic current densities of corrosion cells were measured.
Baccay *et al.* [204]	Carbonated concrete samples. Various cement binders used containing air entraining agent and water reducing agent. 90% humidity	Varied 20-40	0.01-2.8	0-35 days	Rate of carbonation increases with temperature. Higher corrosion rate with higher temperature in OPC concrete.

Table 11 (Cont.): Carbon steel corrosion rates in concrete.

Reference	Environment	Temp (°C)	Corr. rate (μm yr^{-1})	Times	Remarks
Cao *et al*. [205]	Cement paste, containing different binders (35% BFS and 20% PFA). Cured in saturated lime, with cast in chloride and exposure to chloride solution.	ambient	2.6-41.6	3-28 days	Water to cement ratio 0.8; a high water/cement ratio. Corrosion rate measured using polarisation curves with scan rate of 17mV/sec.
Chitty *et al*. [206]	Ancient mortars	ambient	0.8 to 8		Examination of archaeological artefacts ranging from 80 to 1700 years old. Corrosion rate declined with age. Range of corrosion products found, including magnetite.
Flis *et al*. [119]	Concrete bridges	ambient	0.0812 to 350		Corrosion rates of steel rebars were measured in real structures using electrochemical techniques. The corrosion rate was found to be dependent on the potential, in a similar way to a normal polarisation curve. The corrosion rates are related to the concrete resistivity and chloride exposure (e.g. marine atmosphere, de-icing chemicals).
Gonzalez *et al*. [207]	Various mortars no additives with chloride and carbonation	ambient	<1 up to 100	8 days	The corrosion rate of steel rebar was measured in blocks of mortar, some of which contained added chloride, using polarisation resistance measurements. The corrosion rate depended on the chloride concentration, concrete resistivity and the percentage water saturation.

Table 11 (Cont.): Carbon steel corrosion rates in concrete.

Reference	Environment	Temp (°C)	Corr. rate (μm yr^{-1})	Times	Remarks
Hakkarainen [208]	Concrete samples with various binders. Tests carried out in synthetic sea water and tap water.	ambient	0.016-0.05	10 months to 2 years of exposure	Cyclic polarisation curves used to obtain corrosion rate with time. No corrosion observed in samples exposed to tap water.
Hansson [121-123]	De-aerated mortar	22-43	1-7	10 months	Electrochemical measurements (Tafel slope extrapolations and polarisation resistance measurements) were used to measure corrosion rates. There is some doubt about whether the concrete was completely de-aerated. The films on the surface of the steel were cathodically reduced before the experiment.
Hauser and Köster [209]	Cemented waste forms, pH 12, O_2 5 mg l^{-1}	25 50 90	< 1 2 18	12 months	Weight loss measurements were used to assess the corrosion rate of cast iron in cemented waste forms.
Lee [210]	Cement paste with varied binders (PFA, BFS) exposed to saturated air	ambient	0.34-6.07	2 to 84 days	Similar corrosion rate in all samples. Rate of corrosion falls to very low values within one to two weeks.
Lysogorski *et al.* [211]	Steel in simulated pore solution, wet dry cycles, short term exposure to chloride solution. Concrete samples long-term exposure, wet-dry cycle.	ambient	0-2.23 negligible	28-84 days 0-450 days	Polarisation resistance measurements were used to obtain corrosion rates.
Naish *et al.* [124, 125]	Various anaerobic concrete / cement mixes	ambient	0.23-1.44	up to 2.5 years	Weight loss measurements were used to measure the corrosion rates of carbon steel in cement. It was noted that the rates represented maximum values.

Table 11 (Cont.): Carbon steel corrosion rates in concrete.

Reference	Environment	Temp (°C)	Corr. rate (μm yr^{-1})	Times	Remarks
Saito *et al*. [212]	Carbonated and non carbonated concrete samples exposed to various conditions: outdoors, indoors, underground, tunnel	ambient	10-25	1 year	Measurements were obtained using the potential step method and converted to corrosion current and mass loss. The calculated mass loss was compared with actual mass loss of the sample after the bars were removed from the bar. Lower corrosion rate measured in carbonated concrete compared to bare steel in water. Corrosion rate controlled by water and oxygen availability.
Tuuti [110]	Balcony slabs	ambient	50	20 years	Corrosion rate data were reported for real concrete structures: Rebars, carbonated, but no chloride
	Concrete silo		200-400	25 years	Salted sand had been stored in silo, chloride high, carbonated
	Power line poles		50	50 years	Carbonated, but no chloride
	Concrete building		100-500	10 years	$CaCl_2$ added to concrete
New data					
Aligiziki [213]	Type 1 Portland cement with limestone and sand aggregate	ambient	90-730	28 days	Steel reinforcing bars, Grade 60. I_{corr} calculated from R_p data using Tafel plot method. Corrosion accelerated by applying 500 mA cm^{-2} current, until cracking of concrete occurred due to the corrosion.
Arrendondo-Rea *et al*. [214]	Portland cement with aggregates	ambient	1-2	20 weeks	Carbon steel bars UNS G10180. I_{corr} determined from R_p using Tafel constant of 0.052 V for passive corrosion and 0.026 V for active corrosion.

Table 11 (Cont.): Carbon steel corrosion rates in concrete.

Reference	Environment	Temp (°C)	Corr. rate (μm yr^{-1})	Times	Remarks
Boden and Pettersson [215]	Conventional concrete Low-pH concrete Conventional concrete in 10% chloride solution Conventional concrete, 2% chloride cast-in Low-pH concrete, 2% chloride cast-in	ambient	12.5 12.0 37.9 15.2 22.1	515 to 525 days	Steel bars embedded in conventional and low-pH concretes. Steel bars in low-pH concrete were also tested in 10% chloride solution, but the results were the same as without chloride because chloride did not penetrate though the denser concrete to the steel bars.
Geng *et al*. [216]	Concretes: 0.45 water/cement 0.65 water/cement	ambient	10-20 20-40	~42 days	Steel bars cast in concrete of varying water content. Concrete cover thickness 15mm. Current densities reported from linear polarisation measurements.
Hussain [217]	OPC: 5wt% chloride 10wt% chloride)	ambient	100 60 500 300	30 days 750 days 30 days 750 days	Mild steel encased in OPC of varying added chloride content. Corrosion rates derived from corrosion current density.

Table 11 (Cont.): Carbon steel corrosion rates in concrete.

Reference	Environment	Temp (°C)	Corr. rate (μm yr^{-1})	Times	Remarks
Xu *et al*. [218]	OPC with varying fly ash plus 6wt% NaCl: 0% fly ash 30% fly ash	ambient	 120 40	~300 days	Steel rebars cast in cement with 6wt% NaCl added to increase the corrosion rate. Rates derived from corrosion current density data
Yokota *et al*. [219]	Concrete with 10% NaCl solution permeating	ambient	115	Average over 1620 days	Steel bars in concrete. Corrosion rate measured by linear polarisation resistance.
Yuan *et al*. [220]	Concrete made from Portland cement and aggregate	ambient	70 80	14 days 192 days	Steel bars embedded in concrete. Corrosion rate measured by linear polarisation resistance.

Table 12: Atmospheric corrosion of carbon steel.

Reference	Environment	Temp (°C)	Corr. rate (μm yr^{-1})	Times	Remarks
Ambler and Bain [133]	Various marine atmospheres	ambient	~10-1000	up to 12 months	There is a linear relationship between corrosion rate and salt deposition rate (Figure 17).
Blackwood *et al.* [169]	Anaerobic, high humidity atmosphere	50	Initially ~20, but decreasing to <0.1 after 5000 hours	up to 5000 hours.	Hydrogen evolution experiments.
Bragard and Bronnarens [221]	Various sites	ambient	typically 40	up to 10 years	The following law was found to apply: $C = At^n$, where C = weight loss, *t* = exposure time, and A and n are constants that depend on exposure site and steel grade.
Copson [222]	Various marine atmospheres	ambient	16-1193	up to 18 years	The corrosion rate depends on the proximity to sea.
Feliu *et al.* [223, 224]	Various atmospheres	ambient	average 74.5, SD 113.7, min 3.2, max 743		Analyses of 324 reports in literature and fits equations to the data.
Knotkova *et al.* [225]	Intermittent distilled water spray Intermittent seawater spray	35	136 806	up to 30 days	Results of laboratory tests in environmental chambers.
Shastry *et al.* [226]	Various sites	ambient	2.5 - 10 typically	20 years	The data fit the law log C = log A + B log *t*, where C = corrosion loss in micrometers, *t* = time in years, and A and B are constants. Values of A and B are given for various sites.
Dechema Corrosion Handbook volume 7 [21]	Rural Industrial Sea coast	ambient	10-50 50-380 60-170	various	Typical data are given - much depends on the type of climate.

Table 12 (Cont.): Atmospheric corrosion of carbon steel.

Reference	Environment	Temp (°C)	Corr. rate (µm yr^{-1})	Times	Remarks
New data					
Fuentes *et al.* [227]	Rural	ambient	8 ~3	1 year 13 years	Mild steel. Composition (wt%) 0.44 C, 0.40 Mn, 0.018 S, <0.22 P, <0.05 Si, <0.1 Cr, <0.1 Ni, <0.1 Mo and <0.05 Cu. Corrosion rates marked ~, were estimated from plot in Figure 1 of paper.
	Urban	ambient	44 ~6	1 year 13 years	
	Industrial	ambient	70 ~45	1 year 13 years	
	Marine light	ambient	50 ~25	1 year 13 years	
	Marine severe	ambient	93 ~60	1 year 10 years	

Table 13: Anaerobic corrosion rates of carbon steel, derived from hydrogen generation experiments in the UK [62].

Cell number	Test solution	Temp (°C)	Test duration (days)	Maximum (µm yr^{-1})	Average (µm yr^{-1})	Time for LT mean (hrs)	Mean LT (µm yr^{-1})	Total H_2 (mmol m^{-2})
5	0.1M NaOH	30	3949	3.11	0.04	>10000	0.010	68
27	0.1M NaOH	30	3821	1.21	0.11	>10000	0.098	158
14	0.1M NaOH	50	3492	5.50	0.11	>10000	0.011	~150
47	0.1M NaOH, mercury cell, no liner	80	311	29.63	0.35	>4000	0.025	41.5
51	0.1M NaOH, mercury cell	80	2591	23.71	0.29	>10000	0.002	376
9	0.1M NaOH + 3.5%NaCl	30	3949	1.27	0.06	>10000	0.023	91.7
28	0.1M NaOH + 3.5%NaCl	30	3821	0.69	0.057	>10000	0.044	84
15	0.1M NaOH + 3.5 % NaCl	50	3932	0.88	0.08	>10000	0.03	118.8
53	0.1M NaOH + 3.5% NaCl, Hg cell	80	1520	20.24	0.41	>10000	0.0047	359
18	Sat. $Ca(OH)_2$	50	3494	5.07	0.037	>10000	0.003	50
24	Sat. $Ca(OH)_2$ + NaOH	30	3743	1.43	0.08	>30000	0.022	108.6
26	Sat. $Ca(OH)_2$ + NaOH	50	773	2.07	0.16	>10000	0.11	48.49
19	Sat. $Ca(OH)_2$ + 3.5%NaCl	50	1225	2.14	0.16	>10000	0.006	74.36
23	Sat. $Ca(OH)_2$ + NaOH + 3.5% NaCl	30	3743	0.87	0.08	>30000	0.027	110.2
25	Sat. $Ca(OH)_2$ + NaOH + 3.5% NaCl	50	773	1.96	0.28	>10000	0.009	84.06
37	NRVB water	50	3045	3.60	0.056	>10000	0.024	65.6

Table 13 (Cont.): Anaerobic corrosion rates of carbon steel, derived from hydrogen generation experiments in the UK [62].

Cell number	Test solution (pre-treatment)	Temp (°C)	Test duration (days)	Maximum (μm yr^{-1})	Average (μm yr^{-1})	Time for LT mean (hrs)	Mean LT (μm yr^{-1})	Total H_2 (mmol m^{-2})
39	NRVB water + 20,000 ppm Cl^-	50	2591	2.35	0.065	>10000	0.010	65.2
55	0.1M NaOH (as received)	50	1037	0.28	0.022	>10000	0.001	8.94
42	0.1M NaOH (degreased)	50	817	0.11	0.08	>10000	0	25.6
41	0.1M NaOH (pre-rusted in 3.5% NaCl)	50	2493	0.36	0	>10000	0	2.3
56	0.1M NaOH (pre-rusted in 3.5% NaCl)	50	2100	0.71	0.21	>10000	0.404	168 [1]
43	Groundwater pH 4, unbuffered	50	827	5.06	0.78	>5000	0.61	247
44	Groundwater pH 7, unbuffered	50	856	1.85	0.43	>5000	0.35	141
49	Groundwater pH 4, buffered	50	2609	9.21	1.31	>10000	2.17	432 [1]
50	Groundwater pH 7, buffered	50	2607	5.04	0.122	>5000	0.052	123

Notes

1. In these cases, the true values are in excess of this figure. The volume of gas generated was measured by fluid displacement. In these cases, the reservoir of displacement fluid emptied on a number of occasions due to rapid gas generation.

6 Corrosion rates of stainless steels during waste management

The data presented in this section include those originally presented in reference [13], and have been supplemented with data that were either identified from recent literature searches or provided by the partners in the CAST project. The data are summarised in a tabular manner (see Table 14 to Table 20) by corrosive environment. The additional data have been appended after the data from reference [13].

6.1 Neutral solutions

6.1.1 Aerobic neutral solutions

The general corrosion rate of stainless steels is very low, but localised corrosion can occur in stagnant solutions and therefore most literature has concentrated on the localised corrosion of stainless steel. A summary of the data relating to the aerobic corrosion of stainless steels in neutral solutions is given in Table 14; some of the data are shown in Figure 19 and Figure 20. Weight loss experiments give corrosion rates of 0.1 to 0.5 µm yr^{-1} at <30°C, but 130 µm yr^{-1} at 90°C [228]. The high rate at 90°C was probably due mainly to pitting attack rather than general corrosion. There is a lack of data for intermediate temperatures.

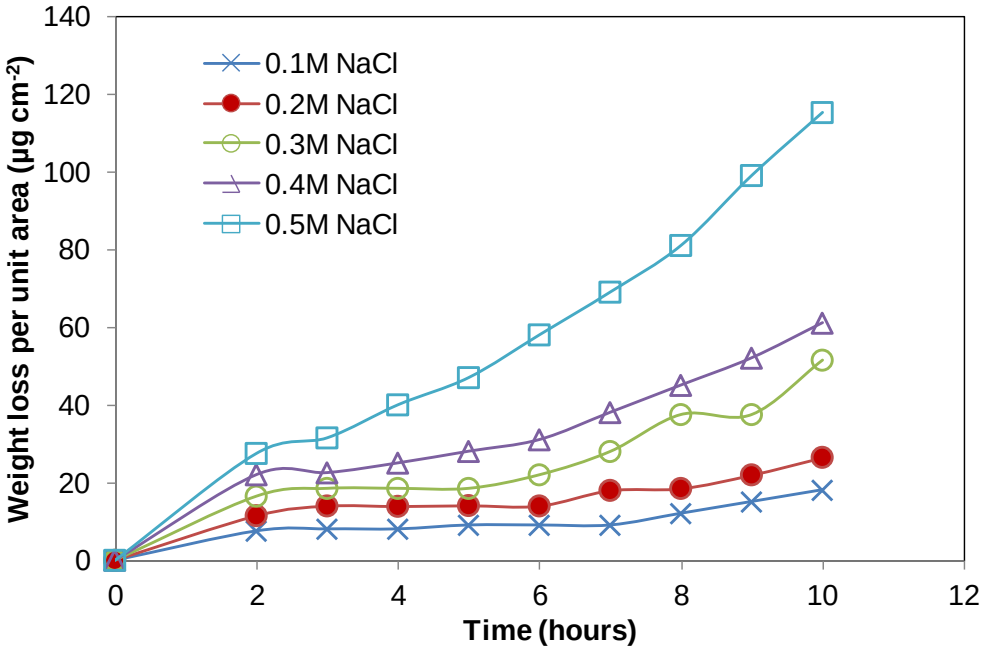

Figure 19: Effect of salt concentration on the corrosion of stainless steel at 90°C (redrawn from reference [228]); the lines joining the data are included to aid the eye.

a)

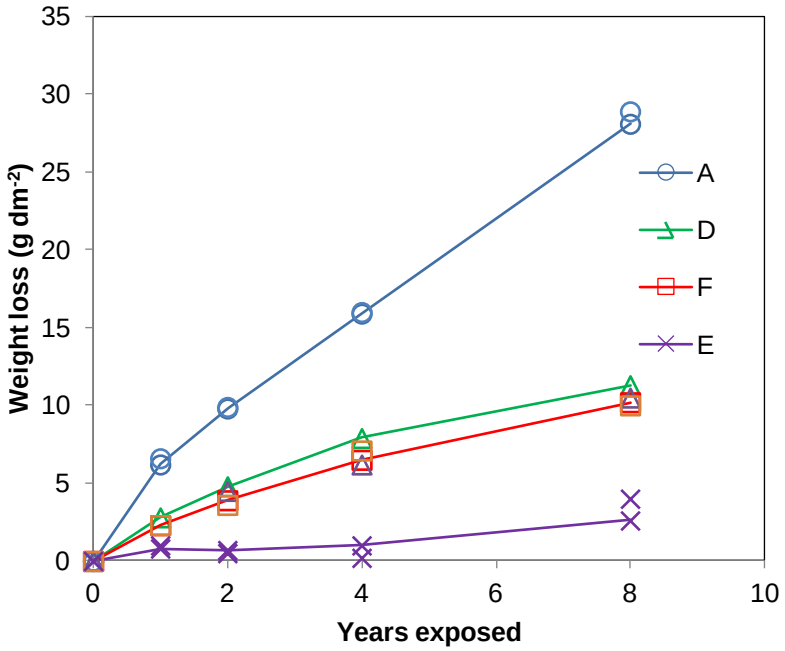

b)

Maximum penetration in mm (plates perforated)				
Alloy	A	D	E	F
1 year	6.60	6.63	6.22	6.86
8 years	6.60	5.99	6.22	6.86

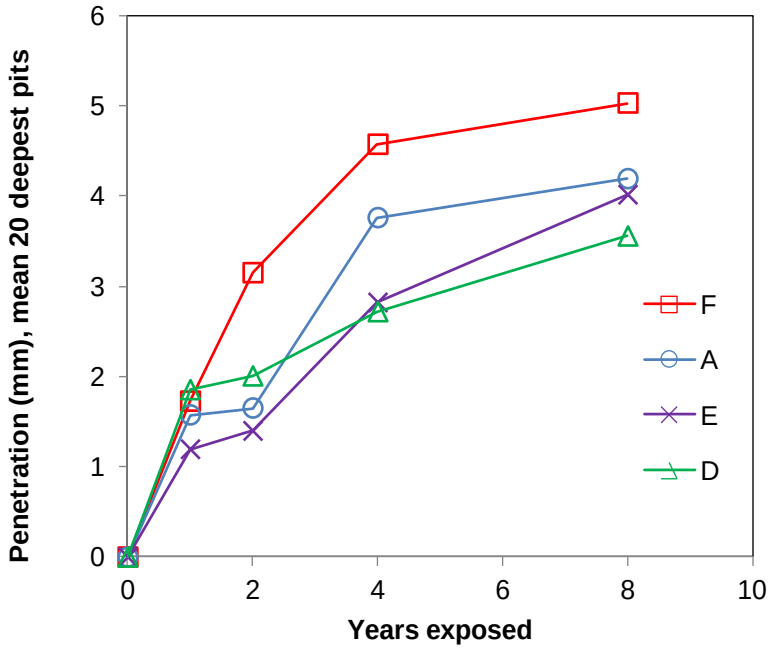

Figure 20: Comparative corrosion rates in terms of: a) weight loss; and b) mean depth of 20 deepest pits; for various stainless steel alloys continuously immersed in tropical seawater: A - type 410; D - type 302, E - type 316, F - type 321; (redrawn from reference [229]); the lines joining the points are included to aid the eye.

6.1.2 Anaerobic neutral solutions

Only one reference in the open literature has been found for corrosion of stainless steel in de-aerated neutral conditions (see Table 15) [164]. This lack of data is indicative of the fact that both the general corrosion and localised corrosion rates of stainless steels would be expected to be very low under these conditions and hence they do not pose a risk to the use of stainless steels in industrial engineering applications in these conditions.

Additional information has been supplied by KIT on corrosion studies of stainless steels and nickel alloys in brines and acidic (pH 4) magnesium chloride solutions at elevated temperatures (170°C) and this is reproduced in Appendix 2. Based on mass loss data, six of the materials studied had corrosion rates in the range 10 to 13 µm yr^{-1} in magnesium chloride solutions at 170°C, assuming uniform corrosion. The highest corrosion rates were measured for a material called ELA-Ferrit (steel grade 1.4591, X1 CrMoTi 182) for which the rate was 1 µm d^{-1} after 40 days decreasing to 0.34 µm d^{-1} after 135 days. The point is made, that these steels underwent localised corrosion under these conditions, resulting in much deeper, but localised, penetration into the materials than expected by assuming uniform corrosion.

6.2 Alkaline solutions

6.2.1 Aerobic alkaline solutions

A summary of the data relating to the corrosion of stainless steel in aerobic alkali solutions is given in Table 16. At ambient temperature in aerobic solutions, the corrosion rate is <0.3 µm yr^{-1}, but at high temperatures in concentrated alkali solutions the corrosion rate may exceed 760 µm yr^{-1}.

6.2.2 Anaerobic alkaline solutions

A summary of the data relating to the corrosion of stainless steel in anaerobic alkali solutions is given in Table 17. For anaerobic conditions, at ambient temperature, the corrosion rate determined by passive current measurements was found to be of the order of 0.4 µm yr^{-1} [230]. However, later passive current measurements on stainless steel in the UK [231] have yielded values as low as 0.05 µm yr^{-1}. At high temperatures and high

concentrations of alkali the corrosion rate increases (*e.g.* 30 µm yr^{-1} in 30% NaOH at 117°C) [99], but it is not as high as in aerobic conditions at the same temperature.

Attempts have been made in the UK research programme to measure the gas generated by the anaerobic corrosion of stainless steels in alkaline solutions, by monitoring gas cells over a period of over ten years [62]. During these measurements it was not possible to measure any hydrogen generation, indicating that the anaerobic corrosion rate of stainless steel was less than the detection limit for the gas cell technique, which was estimated to be less than 0.01 µm yr^{-1}. Japanese workers have also reported the anaerobic corrosion rate of stainless steel to be 0.01 µm yr^{-1} [105], based on gas evolution measurements using a mass spectroscopy technique to measure the amount of hydrogen evolved. Interestingly, this corrosion rate is similar to that measured in long-term aerobic corrosion experiments in concrete (Table 19), suggesting that the long-term corrosion rate in alkaline conditions is determined by the properties of the passive film (*e.g.* very low solubility of chromium oxyhydroxides), rather than the nature of the cathodic reactant (*i.e.* oxygen in aerated conditions and water in de-aerated conditions). Other work has suggested that the passive film is able to reform if it is disrupted by reaction with the surrounding water [232], even in the absence of oxygen. It is worth noting that a corrosion rate as low as 0.01 µm yr^{-1} corresponds to only a few unit cells of an oxide film thickness per year.

Recently, RWMC in Japan have reported some experimental measurements [233, 234] on the corrosion rate of 18Cr-8Ni stainless steel under anoxic conditions in pH 12.5 solution at 30 to 80°C over test periods up to 720 days (Figure 21), in support of assessments of the release rate of carbon-14 from stainless steels under geological disposal conditions. The corrosion rate was measured using the hydrogen generation technique (the amount of gas released was measured using gas chromatography (GC)). The measured corrosion rates for 720 days exposure at 30, 50, 80°C were 0.00077 µm yr^{-1}, 0.0026 µm yr^{-1}, and 0.0075 µm yr^{-1} respectively (i.e. the corrosion rate increases with temperature).

a)

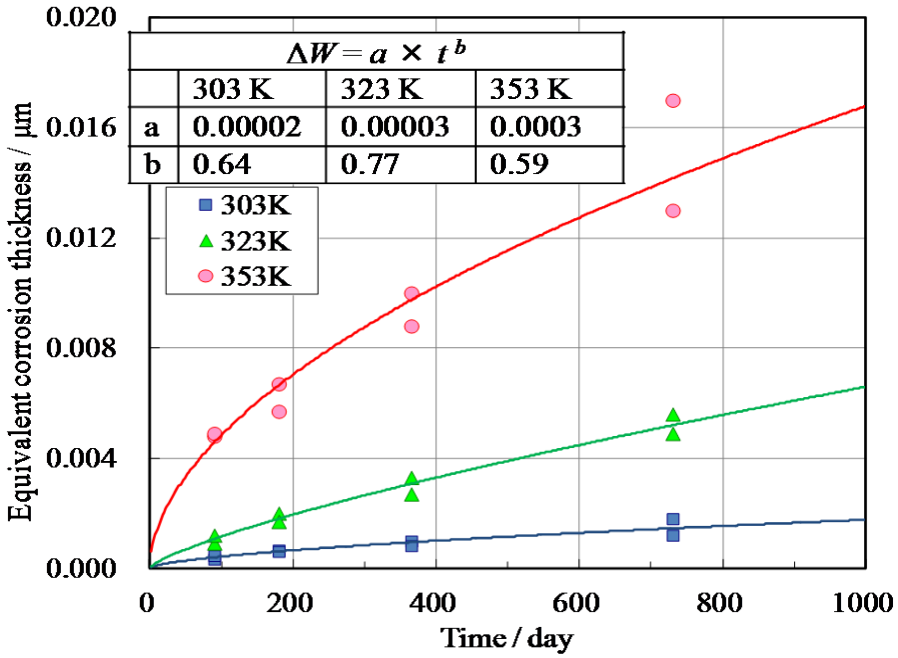

b)

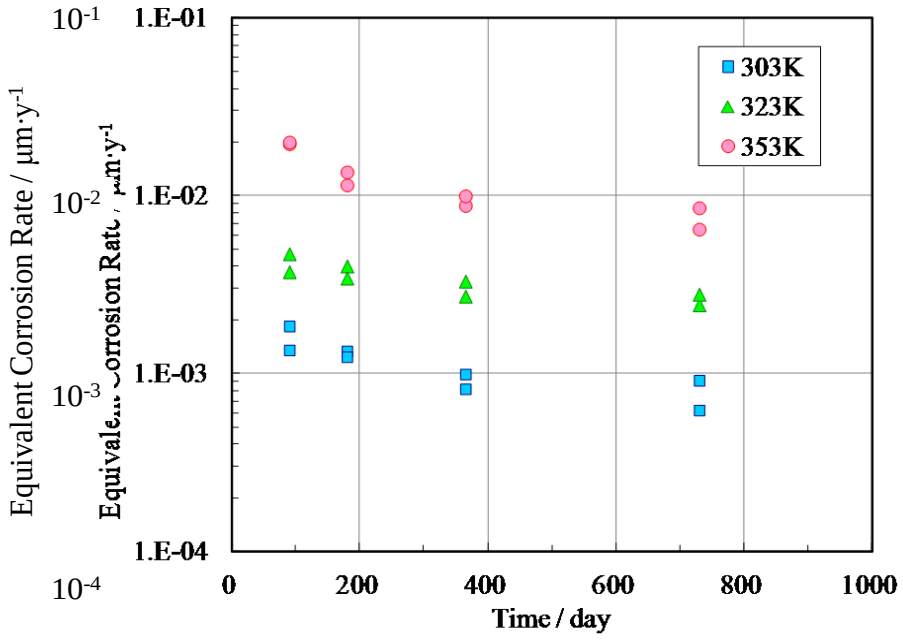

Figure 21: Anaerobic corrosion of 304 (18-8) stainless steel in pH 12.5 solution under at 30 to 80°C: a) equivalent corrosion thickness; and b) average corrosion rate with time (from reference [233] with permission from RWMC).

6.3 Corrosion in concrete

Stainless steel is becoming more common as a material for use as reinforcing bar in concrete structures; indeed there is practical experience of its use for over 75 years (*e.g.* [235, 236]). In general, the corrosion rates of stainless steel in cements and concrete are very low, with a high resistance to chloride (Table 18 and Table 19). In fact the threshold chloride concentrations probably exceed the solubility limit for chloride in cementitious porewater [237].

Bertolini *et al.* [238] investigated the corrosion resistance of a range of stainless steels in chloride contaminated and carbonated concrete. In the absence of chloride the corrosion rates of 304L and 316L, measured by linear polarisation resistance (LPR), were both of the order of 0.05 µm yr^{-1} for the test duration of ~28 months. This applied to tests both at ambient temperature when exposed outdoors and at 40°C at 95-98% RH. Both stainless steels exhibited similar corrosion rates in carbonated concrete and concrete containing up to 6% chloride by mass of cement, under ambient / external exposure conditions, at 40°C and 95-98% RH. In carbonated concrete containing up to 4% chloride by mass of cement, the corrosion rate of 304L and 316L was ~0.06 µm yr^{-1} under ambient / external exposure conditions and 0.1 µm yr^{-1} at 40°C at 95-98% RH. The presence of a high temperature scale (*e.g.* from welding) on the surface of the 304L increased the corrosion rate in high chloride conditions (*e.g.* 1 µm yr^{-1} in 4 wt% chloride) but 316L was unaffected by a heat tint surface film.

Treadaway *et al.* [239] measured weight loss from a range of steels including 302, 315 and 316L stainless steel in concrete containing chloride at a range of concentrations, with two different cement : aggregate ratios (8:1 and 6:1) and cover thicknesses (10 mm and 20 mm) for periods up to 9.5 years. Corrosion rates were measured by weight loss. The results for the 302 and 315 austenitic stainless steels, together with their compositions, are summarised in Table 19; the data for 316L were only expressed as percentage annual weight loss, which was fairly constant at ~0.008% yr^{-1}, irrespective of chloride content (it was not possible to convert this value to a corrosion rate because the initial specimen dimensions are not given in the paper). Table 19 shows the range of the mean corrosion rates for the two different cement : aggregate ratios and cover thicknesses; there was no clear effect of either of these

two parameters on the corrosion rate. No visible corrosion attack was visible on any of the austenitic stainless steels, apart from slight micro-pitting on the 302 stainless steel. It is possible that some of the weight loss measured was due to the cleaning process when the specimens were removed from the test for examination, although the authors claim to have taken this effect into account.

Smart has reviewed the effect of chloride on the risk of corrosion of stainless steel [14] in concrete for the UK NDA. Generally speaking, localised corrosion of stainless steel will only occur under aerated conditions if the chloride concentration in the grout exceeds a threshold value.

Most of the corrosion studies for steel in concrete have examined corrosion in aerated conditions and there are few studies of steel embedded in deaerated cementitious environments. Some work on stainless steel has been reported in the UK programme [62] (steel in NRVB) and the Belgian programme (steel in Supercontainer buffer material, e.g. [131]).

6.4 Atmospheric corrosion

Atmospheric corrosion data for stainless steels are summarised in Table 20. Atmospheric attack is minimal; 2.8 µm yr^{-1} was reported for marine atmosphere exposure, but it may be as low as 0.03 µm yr^{-1}. No data were found for atmospheric corrosion at elevated temperatures or in anoxic conditions.

There are few data for the uniform atmospheric corrosion rate of stainless steels, because the corrosion rates are so low that most authors have concentrated on the depths of pits that are formed. However, Wallinder *et al.* [240] have measured the actual release rates of chromium and nickel from stainless steels exposed to rainwater during atmospheric exposure; this work was carried out because of environmental concerns about the release of chromium and nickel, rather than to determine the corrosion rate for engineering reasons. The annual release rates during atmospheric exposure in Stockholm, Sweden for 304 were 0.25-0.3 mg Cr m^{-2} and 0.3-0.4 mg Ni m^{-2}; for 316 they were 0.35-0.4 mg Cr m^{-2} and 0.7-0.8 mg Ni m^{-2}. The iron release rates were not measured. For comparison, a value of

1 mg Ni $m^{-2}yr^{-1}$ corresponds to a corrosion rate of 1.1 10^{-4} µm yr^{-1}. Other work has shown that the iron dissolution rate is 2-3 orders of magnitude higher [241], giving an overall corrosion rate, which is predominantly due to the loss of iron, of the order of 0.01-0.1 µm yr^{-1}. It is possible that the depth of pitting may be important when considering the rate of release of carbon-14 from corroding stainless steels because the total mass of material lost may be greater than that from the main surface area which is protected by the passive film. Pit propagation rates are important in determining the point of first penetration of a stainless steel waste container [242]. There are few data available regarding the propagation rates for pitting and it is difficult to generalise the rates for the range of conditions that could arise during waste disposal.

6.5 Overview of stainless steel corrosion data

Since stainless steel repassivates rapidly if the passive film is disrupted [232], it is anticipated that there will not be a distinct period of rapid corrosion and that the long-term general corrosion rate will be low, as shown by the data in Table 14 to Table 18 for the various environmental conditions identified earlier (Section 4.2).

6.5.1 Atmospheric corrosion

One of the main concerns of work in the literature has been the rate of toxic metal loss rather than the risk of localised corrosion. In general, there is a lack of atmospheric corrosion data for stainless steel indoors because the corrosion rate is so low. On the basis of the data in Table 20, the data reported by Wallinder *et al*. [240] and the fact that the stainless steel will experience an indoor environment where the time of wetness will be short, a uniform corrosion rate of 0.03 µm yr^{-1} was selected as being representative in a previous review [13]. This is probably conservatively high.

There are no relevant data relating to the effect of temperature on the atmospheric corrosion rate of stainless steel, but there is unlikely to be any significant effect of temperature on the atmospheric corrosion rate within the range expected during ILW storage or GDF operation (*e.g.* 0-50°C).

6.5.2 Aerobic corrosion in grout, low chloride

The aerobic corrosion rate of stainless steel in concrete will be very low, even if the chloride content increases, for example if a high chloride waste is grouted. On the basis of long-term weight loss data reported by Treadaway *et al*. [239] a corrosion rate for stainless steel in aerated grout of 0.02 µm yr^{-1} was selected as being representative in a previous review [13]. Bertolini *et al*.'s data [238] gave slightly higher values, but the measurements were made electrochemically and these types of measurements are likely to over-estimate the measured corrosion rates. The corrosion rate is likely to remain constant with time.

In relation to the effect of temperature on corrosion rate, passive current densities measured for stainless steel in alkaline simulated porewater [231] gave the following data for 30, 50 and 80°C respectively: 0.05, 0.15 and 0.8 µm yr^{-1}. Figure 22 shows that these data follow an Arrhenius relationship. Based on the line of best fit, the activation energy is 50 kJ mol^{-1}. The data of Treadaway *et al*. are preferred to the passive current measurements for a general measure of long-term corrosion rate, as they are based on measurement of weight loss and hence require fewer assumptions to be made in calculating corrosion rate.

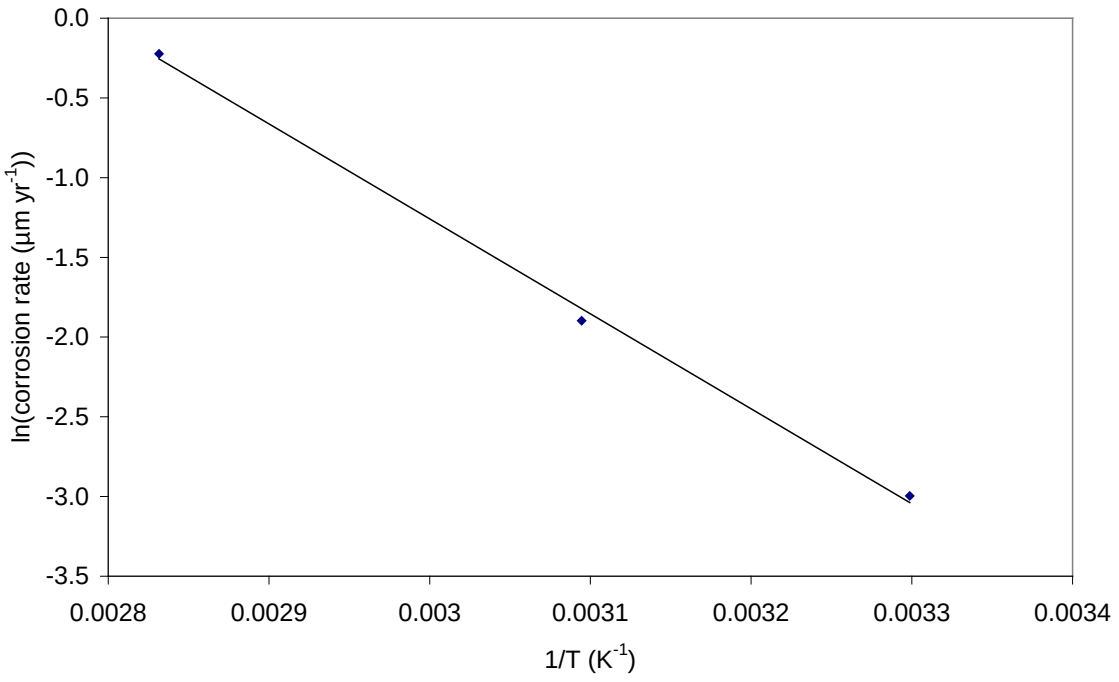

Figure 22: Fit of passive current measurements for stainless steel in simulated porewater [231] to an Arrhenius relationship.

6.5.3 Anaerobic corrosion, low chloride

Anaerobic corrosion rates of stainless steel in alkaline solutions are very low and have proved difficult to measure in the past. On the basis of UK measurements in anaerobic alkaline conditions [62] (which provided only an upper limit for the corrosion rate) and comparable, independent Japanese work [105], a corrosion rate of 0.01 µm yr^{-1} was selected as being representative in a previous review [13]. It was also concluded that there is no initial high corrosion-rate phase and that the corrosion rate is likely to remain constant in the long term.

Recent Japanese work, using a more sensitive GC method to monitor the release of hydrogen gas, has successfully measured the very low corrosion rates of stainless steel under these conditions and confirmed that they are below 0.01 µmyr^{-1} [233]. The new data indicate a mean anaerobic corrosion rate of 0.0008 µm yr^{-1} for 18/8 stainless steel at 30°C after two years exposure, about one order of magnitude lower than the current value used in gas generation calculations in the UK [243]. The Japanese data also show a decrease of the anaerobic corrosion rate under alkaline conditions with time, and a temperature dependence (with corrosion rate increasing with temperature), neither of which could be discriminated previously.

6.5.4 Anaerobic corrosion, high chloride

Chloride is unlikely to affect the corrosion rate under anaerobic conditions, and so the same rates are expected as for the low chloride situation.

Table 14: Stainless steel corrosion rates in aerobic, neutral conditions.

Reference	Environment	Temp (°C)	Corr. rate (µm yr^{-1})	Times	Remarks
Alexander *et al.* [229]	Pacific seawater	ambient	302 stainless: 18 316 stainless: 4	8 years	Weight loss experiments were carried out in tropical Pacific seawater. Most of the weight loss was due to pitting, rather than general corrosion (see Figure 20).
Little and Mansfield [244]	Seawater	ambient	~4		The corrosion rates were measured using electrochemical techniques. The corrosion current, I_{corr} was not limited by mass transport; the corrosion rate depends on the passive current.
Juhas *et al.* [245]	J-13 water	28	0.24-0.28	9000 hours	The reference gives results for weight loss measurements for 304 stainless steel in Tuff repository water. Corrosion rates decreased in the presence of radiation.
Kritsky *et al.* [146]	Spent nuclear fuel pond water	ambient	0.1-0.5	340 days	Corrosion rates were derived from weight loss measurements in pond water containing 2 ppm dissolved salts, pH 5-9. Up to 8 µm yr^{-1} was recorded with 12000 Gy/hr in aerated distilled water.
Morsy *et al.* [228]	0.1M - 0.5M NaCl with 0.1 to 0.7M KCl additions	90	10-130	up to 10 hours	Weight loss corrosion rate measurements of a steel similar to AISI 304 increased with NaCl concentration. KCl additions were inhibitive at low concentrations but increased the corrosion rate at >0.4M KCl (Figure 20).
White *et al.* [164]	Mediterranean seawater	day: 40 night: ambient	0.55	120 days	Static immersion tests. Solubility of oxygen in Dead Sea water is only 1-1.5 ml l^{-1} compared to 5.4 ml l^{-1} for normal seawater.
	Dead Sea seawater		4.8		

Table 14 (Cont.): Stainless steel corrosion rates in aerobic, neutral conditions.

Reference	Environment	Temp (°C)	Corr. rate (µm yr^{-1})	Times	Remarks
New Data[13]					
Adler Flitton and Yodler [246]	Buried underground at depth 4ft and 10 ft	Ambient at 4ft and 10 ft depth	6 - 7 6 - 8 8 - 12 5 - 6	3 years	Duplex SS 304L SS 316L SS 316L SS welded Rates measured by mass loss.
Adler Flitton *et al.* [247]	Buried in underground trenches. Groundwater pH 4.8. Soil pH 6.2	Ambient at 2.5 feet depth	annealed none detected sensitised 0.3 to 1.3	33.5 years	Type 301. Measured by mass loss. Initial masses were estimated from volume because they were not recorded at the start. This is a continuation of work reported in reference [246].
			annealed 0.06 to 0.48 sensitised 0.3 to 1.1		Type 304. Measured by mass loss. Initial masses were estimated from volume because they were not recorded at the start. This is a continuation of work reported in reference [246].
			None detected		Type 316. Measured by mass loss. Initial masses were estimated from volume because they were not recorded at the start. This is a continuation of work reported in reference [246].

[13] This refers to data identified since the original literature review was carried out for preparing reference [13].

Table 14 (Cont.): Stainless steel corrosion rates in aerobic, neutral conditions

Reference	Environment	Temp (°C)	Corr. rate (µm yr^{-1})	Times	Remarks
Atashin *et al.* [248]	Seawater, salinity 40g/L, without stirring pH 10.5 pH 7.5 pH 10.5 pH 7.5 pH 7.5 (solution stirred)	23°C 23°C 65°C 65°C 65°C	0.4 0.8 1 3 56	5 hours	Stainless steel grade AISI 316. Corrosion rate determined by potentiodynamic polarisation scan.
Bechtel SAIC [249]	Freshwater, ambient pH	25 to 100	0.21		304L
	Saltwater, ambient pH	27 90	11.4 5.82		304L
	Freshwater, ambient pH	30 50-100	0.01 0.25		316L
	Saltwater, ambient pH	27	1.94		316L
Casteels *et al.* [250]	Interstitial clay water, ambient pH	25 50 75	0.2-0.96 0.22-0.23 0.3-0.35		304
	Interstitial clay water, ambient pH	25 50 75	0.1-0.24 0.1-0.34 0.1-0.17		316

Table 14 (Cont.): Stainless steel corrosion rates in aerobic, neutral conditions

Reference	Environment	Temp (°C)	Corr. rate (µm yr^{-1})	Times	Remarks
Cuevas-Arteaga and Porcayo-Calderón [251]	Lithium bromide in distilled water (50 % wt/wt)	25 50 60 70 80	0.04 7.8 9.0 6.2 9.3	15 days	SS304. Average rate from weight loss measurements.
Pakshir *et al*. [252]	Seawater, salinity 40g l^{-1}, without stirring pH 10.5 pH 7.5 pH 10.5 pH 7.5 pH 7.5 (solution stirred)	 23°C 23°C 65°C 65°C 65°C	 0.01 0.5 1.7 3.3 1.4	5 hours	SS304. Corrosion rate determined by potentiodynamic polarisation scan.

Table 15: Stainless steel corrosion rates in anaerobic, neutral conditions (no new data since reference [13]).

Reference	Environment	Temp (°C)	Corr. rate (µm yr^{-1})	Times	Remarks
White *et al*. [164]	Mediterranean seawater	Day: 40 and night: ambient	0.9	120 days	Static immersion tests under nitrogen atmosphere.
	Dead Sea water		0.8		

Table 16: Stainless steel corrosion rates in aerobic, alkaline conditions (no new data since reference [13]).

Reference	Environment	Temp (°C)	Corr. rate ($\mu m\ yr^{-1}$)	Times	Remarks
Blackwood *et al.* [192]	0.1M NaOH	30 50 80	0.06 0.18 0.82		Passive current measurements above the oxygen reduction potential. Electrochemical measurements tend to overestimate the corrosion rate.
Kearns *et al* [253]	20%-70% NaOH	93	3-9	96 hours	Weight loss measurements.
MacDonald *et al.* [254]	0.3N KOH, 0.05N NaOH, 3% NaCl, pH 13.3	ambient	304: 0.3 316: 0.6	28 days	Linear polarisation resistance measurements after 28 days of cyclic wet-dry testing.
Rabald [255]	$Ca(OH)_2$ + $CaCO_3$, NaOH, NaS	50	<0.3		
Rubinshtejn *et al.* [256]	1% NaOH	ambient	1-6		CrNi(Mo) steels; exact composition of steels not checked because Russian alloys used.
Scarberry *et al.* [257]	50% NaOH	Boiling	~1500		Weight loss experiments on 304/316 stainless steel.
Sedriks *et al.* [258]	50% NaOH	Boiling	~6000	10 days	Weight loss experiments.
Swandby [259]	0 - 100 wt% NaOH	0 to 400	< 25 to > 760		The corrosion rate data are shown as an iso-corrosion chart (Figure 37 in reference [13]).
Yasuda *et al.* [99]	30% NaOH	117	900	0	Electrochemical measurements of the corrosion rate for 304 and 316 are shown in Figure 15.

Table 17: Stainless steel corrosion rates in anaerobic, alkaline conditions.

Reference	Environment	Temp (°C)	Corr. rate (µm yr^{-1})	Times	Remarks
Blackwood *et al.* [192]	0.1M NaOH	30 50 80	0.06 0.18 0.82	A few weeks	Passive current measurements above the oxygen reduction potential.
Mihara *et al.* [105]	pH 10 - pH 13.5	50	0.01	Up to 12 months	SUS304; hydrogen evolution experiments.
Naish *et al.* [260]	(a) 0.1M NaOH (b) $Ca(OH)_2$/NaOH pH 12.9 (a) or (b)+ 3.5wt% Cl^-	30, 50	No gas detected	Up to 11,000 hours	AISI 316L; hydrogen evolution experiments.
	0.1M KOH + 10000 ppm, Cl^- under H_2 of 100 kPa, 1 MPa and 10 MPa	ambient	<0.1	372 and 624 days	AISI 316L; weight loss; autoclave experiments. Hydrogen overpressure in the range 100 kPa to 10 MPa was found to have no discernible effect on anaerobic corrosion rate.
Sedriks *et al.* [258]	50% NaOH	316	1655	14 days	Weight loss experiments.
Sharland and Newton [230]	0.1M KOH agar gel	ambient	0.4-1.6	1200 hours	Corrosion rates were derived from passive current density measurements.
Wanklyn and Jones [261]	anaerobic KOH, pH 10.7 to 11.2	270-280	surface roughening - stress corrosion main failure mode	440 hours	18/8 stainless steels
Yasuda *et al.* [99]	30% NaOH	117	10-30	2 weeks	304/316. Weight loss measurement under hydrogen.

Table 17 (Cont.): Stainless steel corrosion rates in anaerobic, alkaline conditions.

Reference	Environment	Temp (°C)	Corr. rate (µm yr^{-1})	Times	Remarks
New data					
Fujisawa *et al.* [262]	pH 12.8 pH 10.5	30, 45	0.0003 0.01	200 days 60 days	Type 304
Wada and Nishimura [263]	pH 10 pH 12.5 pH 13.5	50	0.009 0.0055 0.0063	230 days	Type 304
Yoshida *et al.* [233]	pH 12.5 NaOH, anoxic (N_2 atmosphere glovebox)	30 50 80	7.7×10^{-4} 2.6×10^{-3} 7.5×10^{-3}	720 days	18Cr-8Ni steel. Measured by hydrogen evolution (GC detection). Mean of duplicate measurements.
		30 50 80	9.1×10^{-4} 3.0×10^{-3} 9.4×10^{-3}	360 days	
		30 50 80	1.7×10^{-3} 4.2×10^{-3} 2.0×10^{-2}	90 days	

Table 18: Stainless steel corrosion rates in cementitious conditions.

Reference	Environment	Temp (°C)	Corr. rate ($\mu m\ yr^{-1}$)	Times	Remarks
Sorensen *et al.* [264]	Mortar prisms	ambient	no Cl^-: 0.01 to 0.1 + Cl^-: 1 to 100		Passive current measurements for 304 and 316 stainless steel reinforcement.
New data					
Medina *et al.* [265]	Portland cement (OPC) with between 0% and 4% $CaCl_2$ added to the cement mortar.	ambient	0.14 (0.0% $CaCl_2$) 0.08 (0.4% $CaCl_2$) 0.12 (2.0% $CaCl_2$) 0.05 (4.0% $CaCl_2$) 0.05 (0.0% $CaCl_2$) 0.08 (0.4% $CaCl_2$) 0.12 (2.0% $CaCl_2$) 0.05 (4.0% $CaCl_2$)	1 year	Steels encased in OPC. Linear polarisation resistance data Steel AISI 304 Steel AISI 304 Steel AISI 304 Steel AISI 304 Steel AISI 2304 Steel AISI 2304 Steel AISI 2304 Steel AISI 2304

Table 19: Results of 9.5 year exposure tests for 302 and 315 stainless steels in concrete containing chloride (wt% cement); the chloride was added as $CaCl_2$ to the mix water [239], showing corrosion rates in µm yr^{-1}.

% Cl in concrete	302 [1]	315 [1]
0	0.017-0.033	0.010-0.038
0.32	0.018-0.037	0.025-0.075
0.96	0.015-0.033	0.022-0.032
1.9	0.013-0.026	0.028-0.034
3.2	0.027-0.041	0.030-0.067

Notes

1. 302 composition (wt%): Cr 17.8; Ni 8.8; Mn 0.78; Mo 0.18; C 0.096; Si 0.047; N 0.02;P 0.021; S 0.023

   315 composition (wt%): Cr 17.0; Ni 10.1; Mn 1.64; Mo 1.42; C 0.056; Si 0.29; N 0.03; P 0.03; S 0.009

   cf. 316L composition (wt%): Cr 17.3; Ni 12.35; Mn 1.87; Mo 2.14; C 0.041; Si 0.46; N 0.22; P 0.03; S 0.007

Table 20: Atmospheric corrosion of stainless steel (no new data since reference [13]).

Reference	Environment	Temp (°C)	Corr. rate (μm yr^{-1})	Times	Remarks
Alexander *et al.* [229]	Marine seashore	ambient	2.8 0	8 years	Tests were carried out in the Panama canal zone. Type 302 Type 313
Baker and Lee [266]	Marine	ambient		26 years	No general corrosion. Test specimens were assessed for degree of rust, staining and pitting.
Johnson and Pavlik [267]	Range of atmospheres, including New York atmosphere, marine, industrial, urban	ambient	0.022 <0.03 0.05-2 0.01	5-15 years	Type 304 Type 304/316 Type 304 Type 316 Examples of corrosion rates measured in the range of atmospheres on the left. Type 316 more resistant than 304.
Kearns *et al.* [268]	Various industrial/urban	ambient	~0.03-3	4-15 years	Type 304 steel. Corrosion rate investigated as function of alloying in a range of environments. Attack leads to surface tarnishing, corrosion rate negligible.
Dechema corrosion handbook volume 7 [21]	Various	ambient	0.05		Stainless steel hardly corroded in urban and marine atmospheres, may be some pitting. Undersides more heavily rusted than topsides.

7 Carbon and carbon-14 release from steels

In Section 2.3, the possible forms of carbon-14 in steels and the resulting chemical forms in which they may be released were reviewed. Based on chemical arguments concerning the reactions of metal carbides and carbonitrides, a number of predictions of the chemical forms of carbon-14 release on leaching irradiated steel were made[14].

In this section, the currently available information on the speciation of both stable carbon (carbon-12 and carbon-13) releases from unirradiated irons, steels and carbides, and carbon-14 from irradiated steels by corrosion is reviewed in some detail. Only limited information is available on the three studies of carbon-14 release from irradiated stainless steel that have been conducted to date, all in Japan. Unfortunately, a proper evaluation of these experiments is hindered by a lack of detailed reports available in English[15]. Studies of stable carbon releases, outlined in the following section, provide information on the range of carbon-14 species that could be generated from the corrosion of irradiated steels and provide a basis for developing and testing experimental methods for species discrimination.

7.1 Studies of stable carbon release

Much of the available information on the release of stable carbon from iron and steels has come as a by-product from studies of environmental clean-up of chlorinated hydrocarbons using zero-valent iron [273, 274, 275]. The formation of background hydrocarbons from the iron-water system in the absence of chlorinated solvents had been observed on a number

[14] This approach is consistent with the conclusions of Wieland and Hummel [19], who have considered the thermodynamics of the C-H-O system with regard to predicting the chemical forms of carbon-14 in the near field of a GDF. They concluded that at complete thermodynamic equilibrium, the aqueous C-H-O system would be dominated by carbonate ion and methane, depending on the pH and redox conditions, with insignificant amounts of carboxylate species at the predominance boundary between the two major species. However, they note this does not reflect the complex speciation of organic chemistry, which is dominated by metastable states and partial equilibria. They conclude that limited understanding of metastable states means that there is as yet no predictive capability for carbon speciation in real systems that are not at thermodynamic equilibrium. However, they note that the distribution of products in some field observations [e.g. 269] and experimental studies [e.g. 270] has been interpreted by considering both possible reaction mechanisms and kinetic arguments rather than thermodynamic considerations.

[15] In fact, there is relatively more information on carbon-14 release from zirconium alloys, which has also been studied in the framework of the Japanese programme [e.g. 271,272].

of occasions; Hardy and Gillham [273] investigated these unexpected findings. They used a combination of batch- and column-type experiments to study the formation of hydrocarbons in an iron-water system using commercial iron filings (~90% iron and containing 2.4% carbon). The experiments were carried out in a simulated groundwater solution (Na-Mg-Ca-Cl-SO_4-HCO_3 composition) at pH = 6 containing about 2 x 10^{-4} mol dm^{-3} bicarbonate ion. For some batch experiments, the iron samples were pre-treated with hydrogen before use. In the batch experiments, 10g iron was placed in contact with the solution in 40 cm^3 glass vials, which were sealed without headspace. After equilibration for 6 days, the samples were centrifuged to remove suspended iron and then aliquots of the liquid phase were transferred into 2 cm^3 vials with a 0.5 cm^3 headspace. The vials were shaken for 15 minutes to allow volatile species to equilibrate between gas and liquid phases. Headspace samples were then collected and analysed by gas chromatography (GC) using flame ionization detection (FID). The carbon compounds in the liquid phase were not determined, however. In all batch experiments, volatile hydrocarbons were detected in the headspace. The hydrocarbons reported include methane, ethane, ethene, propane, propene and butene isomers. The concentrations ranged between about 2 μg L^{-1} and 10 μg L^{-1}, significantly less than the bicarbonate concentration in solution. It was noted that the pre-treatment of the samples with hydrogen gave an increase in the total amount of hydrocarbons formed in the system. However, significant amounts of hydrocarbons were also formed from untreated iron and the addition of further carbonate to the system did not increase hydrocarbon production.

The authors considered three possible explanations for the generation of the hydrocarbons observed:

1. release by corrosion of the commercial iron;
2. transformation products of unidentified organics in the source water; and
3. synthesis from the reduction of aqueous CO_2.

On the basis that the majority of the carbon in the iron filings was expected to be in graphitic form, and so unreactive, and the observation of a detectable hydrocarbon release, though at lower concentrations, in parallel tests carried out on a low-carbon content

electrolytic iron (>99% iron but carbon content not specified), the first explanation was discounted. The second possibility was also excluded on the basis that:

1. no organic species were identifiable in the source waters; and
2. batch tests in which the water was first treated by filtration through activated carbon and exposure to UV light to remove organic species gave similar levels of hydrocarbons to tests with untreated water.

Drawing analogies with previous reports of electro-reduction of dissolved CO_2 by metal electrodes to produce alkanes and alcohols [e.g. 276], Hardy and Gillham hypothesised that the hydrocarbons observed in their experiments were formed by the reduction of aqueous CO_2. A mechanism was proposed in which the CO_2 was reduced on the iron surface and converted to hydrocarbons with a distribution of chain lengths by a process analogous to Fischer-Tropsch (F-T) synthesis. In the F-T process, CO and hydrogen in the gas phase are passed over a metal catalyst, such as iron, nickel or cobalt, at elevated temperature, to form hydrocarbons [277]. F-T synthesis is known to result in the production of a distribution of hydrocarbon species of differing chain length, known as the Anderson-Schultz-Flory distribution (ASF, defined by a parameter called the chain growth probability). Hardy and Gillham noted that the the range and relative ratios of the hydrocarbon products observed were consistent with an ASF distribution.

Subsequent studies by Campbell *et al*. [274] confirmed that hydrocarbons were formed in an iron-water system under conditions similar to those used by Hardy and Gillham [273]. However, Campbell *et al*. found that hydrocarbons were generated in argon-purged (CO_2-free) water as well as in what was described as CO_2-amended water[16]. On the basis of these findings, Campbell *et al*. proposed an alternative interpretation of both their and Hardy and Gillham's results: that it was the carbon impurities bound in the iron samples used that were the likely source of carbon for hydrocarbon production rather than CO_2 dissolved in water.

[16] The meaning of this term is unclear, but the context suggests that it refers to a solution containing dissolved CO_2.

The findings of Campbell were followed up by a more detailed study by the same group [275]. Deng *et al*. studied the generation of hydrocarbons in iron-water systems using iron from a variety of sources and with a wide range of carbon contents (from 3% in iron filings to <0.002% in an electrolytic iron). Iron corrosion experiments with low and high dissolved CO_2 concentrations were conducted in zero-headspace systems in a manner similar to that used by Hardy and Gillham [273]. The solutions comprised Milli-Q (demineralised) water with a low CO_2 concentration (acidified, boiled and Ar-purged) and Milli-Q water in equilibrium with 1 atm CO_2. Equilibration times ranged from 15 hours to 16 days. The iron samples were not pre-contacted with hydrogen except in one experiment where sample preparation and equilibration were carried out in a glovebox with a 5% hydrogen in nitrogen atmosphere.

After the required duration, the iron-water experiments were sampled by displacing 5 cm^3 of supernatant solution from the reaction bottle into a 10 cm^3 assay bottle via a stainless steel cannula by injecting a small volumes of air in the reaction bottle. The assay bottle was then vortexed to facilitate the distribution of volatile organics between liquid and gaseous phases. A small volume of the assay-bottle headspace was sampled and analysed by GC-FID or GC-MS (mass spectrometry). Note that Deng and co-workers did not analyse the liquid phase for dissolved organic species.

The results of the headspace analysis showed the formation of volatile hydrocarbons in the systems at both low and high aqueous CO_2 concentrations. The species identified included methane, ethene, ethane, propene, propane, butene, and pentene, i.e., C1 – C5 hydrocarbons. The concentrations ranged in value between about 1 μg L^{-1} and 100 μg L^{-1}, depending on the iron materials used and the reaction time.

The results in terms of the total carbon releases with time from three of the iron samples, are presented in Figure 23. Deng *et al*. considered that there was no significant dependence on the CO_2 concentration as the hydrocarbon production rate at low and high CO_2 concentrations differed by less than a factor of 2. Importantly, for two high-carbon irons, the total amounts of carbon present in the hydrocarbons formed exceeded the initial carbonate concentrations in solution, implying that sources of carbon other than carbonate were

a)

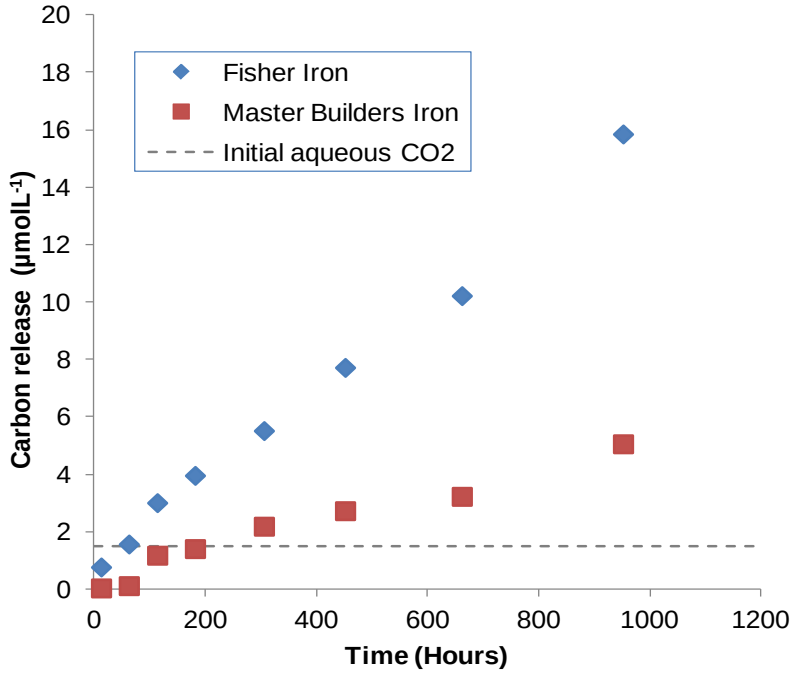

b)

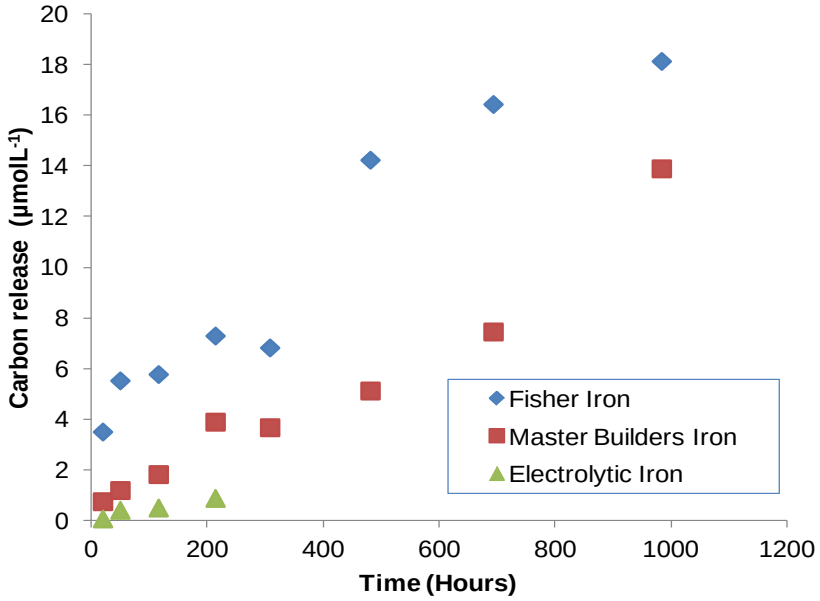

Figure 23: Release of total carbon with time from iron samples on leaching in: a) low CO_2 and b) high-CO_2 water (based on data presented by Deng *et al.* [275]); no carbon releases were detectable from the electrolytic iron in low-CO_2 solution.

present. One experiment was also conducted using ^{13}C-labelled CO_2 to investigate whether the carbon from CO_2 was incorporated into the hydrocarbon products. The result of this test was negative. No hydrocarbons were detected in control experiments without iron.

It was also reported that when the iron samples were dissolved in 6 mol dm^{-3} hydrochloric acid, the same hydrocarbons were produced as in the iron-water corrosion experiments. They noted that in experiments in which a high proportion of the carbon was present in the iron as graphite (so-called grey cast irons), acid dissolution yielded both hydrocarbons and residual graphite. The dissolution of metallic irons containing only carbide carbon yielded total carbon conversion to hydrocarbons. They concluded that graphite was not converted to hydrocarbons and that carbide carbon was the likely source of carbon for hydrocarbon production.

In common with Hardy and Gillham [273], Deng *et al*. suggested that the mechanism of hydrocarbon production in iron-water systems was connected to Fischer-Tropsch synthesis [275]. However, rather than the connection arising from the reduction of aqueous CO_2, they suggested that the connection was through the reactions of the carbides exposed at the metal surface. They suggested that the carbide was indistinguishable from the intermediates that have been shown to form by the chemisorption and decomposition of CO and hydrogen on the surface of a metal catalyst; these intermediates include methylidyne (carbide), methylene and methyl species [278]. Thus hydrogenation of the carbide, hydrocarbon chain growth and subsequent hydrocarbon desorption may occur by the same processes that occur in F-T synthesis. In the case of iron corrosion in water, hydrogen is generated at the metal surface under anaerobic conditions as a result of the corrosion reactions.

In the above studies, hydrocarbon releases from corroding iron were detected in the gas phase, but no measurements were made of dissolved organic concentrations in the liquid phase. In early work carried out on the Japanese programme, Kaneko *et al*. [30] measured dissolved carbon releases on leaching of [low-]carbon steel powder (containing 0.12 wt% carbon), and iron carbide (Fe_3C) in NaOH solutions at pH 8 and pH 12.5 under a reducing atmosphere, but without measuring gas phase releases. Kaneko *et al*. [30] report that both

inorganic and organic carbon compounds were released into solution over 16 months with slightly higher concentrations of organic compounds. Total organic carbon (TOC) concentrations measured in the steel leachates were somewhat variable across the timescale of the experiments and there are no clear trends of increasing concentration with time[17]; TOC concentrations appear to be about 20 ppm at pH 12.5 and 10 ppm at pH 8. Inorganic carbon concentrations appear to average about 15 ppm at pH 12.5 and ~3 ppm at pH 8.

Low molecular-weight organic species were tentatively identified in the carbon steel leachate by high performance liquid chromatography (HPLC) including formic and acetic acids, smaller amounts of formaldehyde and low levels of methanol and ethanol. In the case of the iron carbide, the organic species comprised nearly 100% carboxylic acids. No attempt was made to estimate the rates of release in terms of the available surface area, however[18].

Further information on what appears to be the same set of experiments was presented by Sasoh [279] and later was provided to the NDA Carbon-14 Project by RWMC and Toshiba [1, 280] and has been reported in a recent paper on the development of the analytical methods used on the Japanese programme [281]. Sasoh [279] reports that a headspace analysis by GC was carried out on the experiments with carbon steel, and that low molecular weight alkanes and alkenes were "slightly detected". Unfortunately, no further details are available.

The reported distribution of the carbon released between organic and inorganic species is summarised in Table 21.

Sasoh [279] has also provided further information on the distribution of carbon releases between the different organic species identified by HPLC as shown in Table 22; although it is stressed by Takahashi *et al*. [281], that these identifications are tentative. In addition to

[17] The basis of the trend curves plotted with the data is not explained; given the variability of the data, a constant, average line would appear equally applicable.

[18] A liquid to solid ratio of 1 $cm^3 g^{-1}$ was used for the tests but the particle size or the surface areas of the powders used is not given.

the experiments described by Kaneko *et al*. [30], Sasoh also presents the results of organic species' distributions for pearlite and martensite (referred to as parlite and martainsite in the publication) leached at pH 10[19], although no further experimental details are provided.

Unfortunately, a lack of experimental details make a full evaluation of these results difficult.

Table 21: The fractions of organic and inorganic carbon in liquid and gas phases after leaching carbon steel and iron carbide.

Phase	Chemical form	Carbon steel	Fe_3C
Gas	Organic	~0.01%	nm
Liquid	Organic	70-85%	55-65%
	Inorganic	15-30%	35-45%

nm = not measured

Table 22: The fraction of each organic species (%) detected in the liquid phases after leaching in near-neutral or alkaline solution [279].

Solid	pH	Formic acid	Acetic acid	Form-aldehyde	Acet-aldehyde	Methanol	Ethanol	Propanol
Carbon steel	8	36	45	12	nd	nd	7	nd
	12.5	20	71	6	nd	nd	3	nd
Fe_3C	8	51	49	nd	nd	nd	nd	nd
	12.5	52	48	nd	nd	nd	nd	nd
Pearlite	10	23	77	D	D	D	D	nd
Martensite	10	14	26	nd	nd	12	33	6

D = detected at trace levels; nd = not detected

[19] The leaching solution is likely to be a calcium silicate hydrate gel solution with Ca/Si = 0.65 which is mentioned as leachant in a parallel paper [283] and which is known to equilibrate at pH 10 [282].

The measurement of 40% of the carbon release from iron carbide as inorganic carbon, seems at odds with the findings of Deng *et al*. [275] and Hardy and Gillham [273]. As the focus of the iron-water studies was on gaseous hydrocarbon releases and that of the Japanese programme on dissolved oxygenated organic releases, the results may not be exclusive but potentially complementary [19]. However, this remains to be demonstrated.

In experiments carried out by AMEC (formerly Serco) for NDA RWMD in the UK programme [31], an attempt was made to measure releases of carbon species to both the gas and liquid phases on leaching a high carbon steel (0.9 wt% C), a 316L stainless steel and a variety of metal carbides in solutions at acid, near-neutral and alkaline pH conditions. Only very small amounts of methane were detected in the gas phase from either a carbon steel wire or stainless steel powder leached in saturated calcium hydroxide solutions at ambient temperature and 50°C for 125 to 142 days. Methane, ethane, ethene and some C_3 species as well as hydrogen were detected in the gas phase above the carbon steel after leaching in 1.0 mol dm^{-3} hydrochloric acid for 141 days; only methane, hydrogen and a small amount of ethane were detectable above the stainless steel under similar conditions. These findings were broadly consistent with expectations of gas phase releases based on the findings of Hardy and Gillham [273] and Deng *et al*. [275]. Measured concentrations of organic acids and alcohols in solution were comparable to background levels. As a result, organic releases to the solution phase could not be unambiguously distinguished and the findings of Kaneko *et al*. [30] could not be confirmed. This highlights the sensitivities of carbon release experiments to potential contamination with background levels of carbon that are ominipresent and difficult to exclude rigorously from experimental systems.

7.2 Studies of carbon-14 release from irradiated steels

Published information on carbon-14 release from irradiated stainless steel and nickel alloys is currently very limited and arises entirely from research undertaken in Japan, mostly by Toshiba on behalf of RWMC. Currently published information consists of three short papers [279, 283, 284] in the proceedings of the Nagra/RWMC workshop held in 2003 [2] and a recent extended abstract in Japanese in conference proceedings [285]. This information is insufficient to allow a full review of the studies. A recent paper presented at the MRS meeting in 2013, provides more details on the analytical methods used by Toshiba

for carbon-14 speciation analysis [281]. Some further information on the Toshiba experiments has also been provided in handouts of oral presentations made at conferences and to the NDA RWMD's Carbon-14 Project [1]. In combination, these sources provide the information that is presented here. There are no reported studies of the release of carbon-14 from irradiated carbon (mild) steels to date.

In two parallel papers [279, 283], Sasoh provides limited details and results of what appear to be the same or similar experiments in which a sample of irradiated reactor stainless steel (from a BWR upper grid [281]), cut into pieces, was leached in a cement-equilibated water with a pH of 10. The solution was prepared by equilibration with a CSH gel with a ratio of calcium to silicon of 0.65. The focus of these papers is on the speciation of carbon-14 release rather than on its rate of release. In the first paper [279], the speciation results of organic carbon-14 releases to solution are presented. In the second paper [283], the stability of these released organic species in solution over time was reported; the activated metal was leached for one month under a reducing atmosphere before separation of the solution from the steel and removal of the cobalt-60 by cation exchange prior to analysis and the subsequent stability study. For quantification, the inorganic and organic fractions of carbon-14 were separated by a sequential acidification and wet oxidation method using the equipment shown in Figure 24 [280].

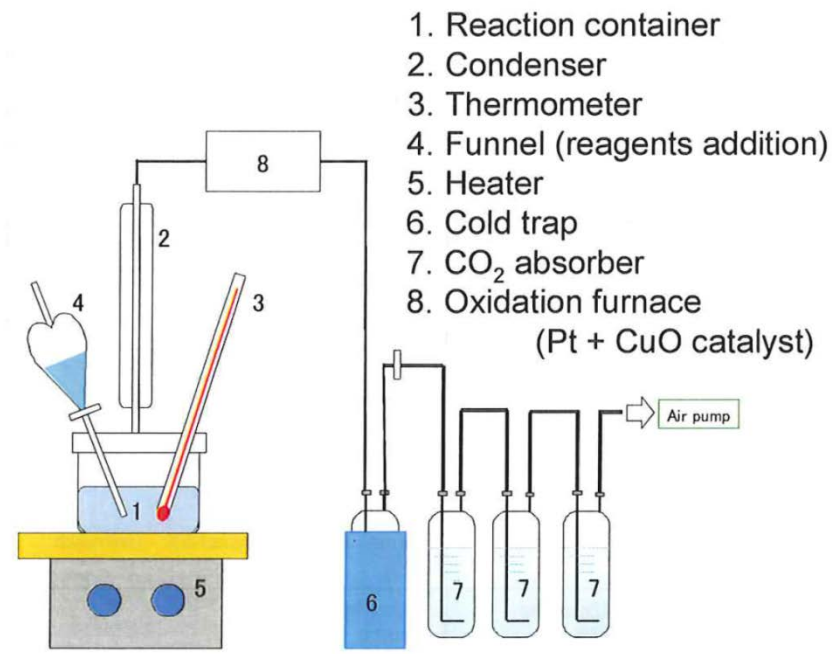

Figure 24: Apparatus used for separation and collection of inorganic and organic fractions of carbon-14 in leachates from irradiated materials by Toshiba (from reference [280] with permission from RWMC).

The speciation of organic carbon-14 was studied by HPLC. Based on handouts provided by RWMC and Toshiba, the HPLC measurement conditions for the irradiated stainless steel leachates were the same as those used by Kaneko *et al*. [30] for inactive studies. The eluate from the HPLC column was collected in a fraction collector and the fractions were individually counted for carbon-14 by LSC to give a carbon-14 chromatogram. The carbon-14 peak retention times were then compared with those of standard organic compounds determined either by UV detection (210 nm) or changes in refractive index. However, it is acknowledged by Takahashi *et al*. [281] that this does not provide a definitive identification of the organic species and that improvements can potentially be made by further analysing eluate fractions by mass spectrometry.

It is reported that 23-34% of the carbon-14 was released from the irradiated stainless steel as inorganic carbon-14 and 66-75% as organic species [281]. The organic carbon-14 species potentially identified were formic acid (~10%), acetic acid (~43%), formaldehyde (~9%),

methanol (~10%) and ethanol (~6%) with over 20% of the organic release unattributed [279]. A slow decrease in the amount of organic carbon-14 in solution was noted over about one year [283]. No gas phase results are reported for this experiment.

In a separate study, Kogawa [284] reports measurements of carbon-14 releases to solution from two samples of activated stainless steel, a nickel alloy and a zirconium alloy under anaerobic alkaline conditions. The steel and nickel alloy reactor samples were cut into plates and were polished "*to eliminate the oxide film*". Leaching experiments were conducted for 1, 3 and 6 months for steels and for 11 months for the nickel alloy. A similar procedure is outlined for discriminating the inorganic and organic fractions of the carbon-14 releases as used by Toshiba; it is reported that most of the carbon-14 was released in organic form. The carbon-14 leach rate was reported to coincide approximately with the corrosion rate (based on measurements on unirradiated speciments) of the metal. The leaching rate of carbon-14 from a "high" irradiated stainless steel was found to be less than that from a "low" irradiated stainless steel but this was attributed to the rapid reformation of the oxide film on the steel surface after polishing and a resultant lowering of the corrosion rate. However, due to the lack of supporting details, this study provides limited data concerning carbon-14 releases from irradiated steels.

The most recent study by Toshiba on the leaching of an irradiated stainless steel sample has included measurements of gas phase releases [285]. This appears to be a single test in which a sample of activated stainless steel plate (from a BWR shroud [281]) was leached in NaOH solution at pH 12.5 for 42 months. A release of 4.76 Bq of carbon-14 was reported from a total carbon-14 inventory of 2.93 MBq (a release fraction of 1.6×10^{-6}). Despite the very small activity of carbon-14 released, it is reported that 25% of this release was to the gas phase, with a ratio of organic to inorganic carbon-14 of nearly one in both gas and solution phases. The organic fraction of carbon-14 was separated into neutral and anionic forms by passing the leachate through an anion exchange resin. Organic carbon-14 species in solution are reported to be predominantly in anionic forms (e.g. carboxylates, 82%) rather than neutral species (e.g. alcohols, 18%). However, no information is available on the size and surface area of the sample or whether it was subjected to any surface treatment which may affect the initial corrosion rate or how the gas phase was sampled. Further information

concerning uncertainties in the analytical data and background levels of carbon-14 that may have been measured would be beneficial given the small activities of carbon-14 released.

The results of the speciation studies relevant to carbon-14 releases from irradiated steels undertaken in Japan are summarised in Table 23.

7.3 Summary of current understanding

The speciation of carbon releases from steels on corrosion is likely to be determined both by the chemical form of the carbon in the steel and the corrosion conditions, in particular the availability of oxygen. In the low carbon-content steel wastes of interest in CAST WP2 (generally <0.3wt% carbon), carbon may be present in steels in the form of interstitial carbides, dissolved in the principal iron phase of the steel (ferrite in carbon steel or austenite in 300–series stainless steel), as a distinct carbide phase (ionic or intermediate carbides) with other alloying components (e.g. niobium, manganese) and/or as carbonitride phases. The distribution of carbon between different species will depend on the steel composition and its production process.

There is considerable uncertainty concerning whether carbon-14 produced by activation of nitrogen-14 will be present in the same chemical forms in irradiated steels as the carbon present in the steels at the time of their production; radiation-induced segregation of alloying components of steel may also contribute to a redistribution of the carbon species.

As an irradiated steel slowly corrodes, the carbon-14 in its different chemical forms will be exposed to the waste disposal environment; different forms of carbon-14 may be expected to be released in different ways. On the basis of the known information on the reactions of metal carbides and carbonitrides with water, the following carbon-14 release behaviour might be expected on leaching an irradiated steel:

- Ionic and intermediate carbides and interstitial carbon present in the iron phase may be hydrolysed over relatively short time periods to form methane, and other hydrocarbons.
- Intermediate carbonitrides may be hydrolysed at a much slower rate than the equivalent carbides to yield a range of products that may include hydrocarbons and compounds containing C-N bonds such as amines and cyanides.

- Stable carbides and carbonitrides may react only very slowly (if at all) and may be released in particulate form.

There is relatively little published information on the release of carbon from irons and steels and the processes involved and the possible range of carbon species released are not well understood. Current understanding can be summarised as follows:

- Experiments on inactive iron-water systems have shown clear evidence for the release of carbon as hydrocarbon species as a result of the hydrolysis of carbide species in the iron. A variety of species ranging from C1 to C5 hydrocarbons have been identified in the gas phase in separate studies [273, 275], and quantitative conversion of carbide carbon to hydrocarbons has been reported [275]. The mechanism of hydrocarbon formation is proposed to occur through processes similar to those that occur in Fischer-Tropsch synthesis [273, 275]; it is suggested by Deng *et al*. [275] that the carbide species exposed at the iron surface may be similar to the intermediates formed on the surfaces of metal catalysts in the Fischer-Tropsch synthesis.
- The measurement of small amounts of hydrocarbons in corrosion experiments with a carbon steel and 316L stainless steel under both acid and alkaline conditions [31] is consistent with the above findings.
- In contrast, in Japanese experiments on inactive carbon steel and iron carbide, which focused on releases to the solution phase, carbon releases were presented as arising primarily as water soluble organic species, although some of the carbon in solution was found to be inorganic [279]. A range of low-molecular weight organic species were identified on the basis of HPLC, although these identifications must be treated as tentative. Carbon-14 releases from iron carbide were identified as both inorganic and organic, which appears to be at odds with the results of iron-water studies. These findings remain to be corroborated.

The information on carbon-14 release from irradiated steels is sparse; only three experimental studies have been performed to date, all in Japan. Unfortunately, insufficient information is available to allow a full evaluation of these studies. The findings are outlined below, but again require corroboration:

- In an experiment in which a sample of irradiated stainless steel from the upper grid of a BWR was leached in a pH 10 cement-equilibrated water, carbon-14 was reported to be released to the solution phase as a mixture of inorganic (25-34%) and organic (66-75%) species. No measurements were made of gas phase releases, and no information is available concerning the amount of carbon-14 released.
- In experiments with irradiated metals where the sample was first acid-cleaned to remove the passivating oxide film, carbon-14 is reported to be released from irradiated stainless steel, nickel alloy and zirconium alloy into solution at rates that are consistent with metal corrosion rates [284].
- In the most recent experiment reported [285], a small amount of carbon-14 was reported to be released to the gas phase on leaching irradiated stainless steel in alkaline solution for 42 months; the distribution of the 4.76 Bq released was reported to be 25% to the gas phase with a ratio of organic to inorganic carbon-14 of nearly one in the solution phase. Organic species in solution were reported to be predominantly in anionic forms (i.e. carboxylates) rather than neutral species (e.g. alcohols). Again, these findings require corroboration.

Table 23: Summary of the speciation studies of carbon-14 releases from irradiated steels and carbides undertaken in Japan [280]; results are presented in terms of the fraction of carbon-14 released as gas phase species and as dissolved inorganic and organic species.

Material		Analysis method	Gas phase	Liquid phase	
				Inorganic C-14	Organic C-14
Activated stainless steel	BWR Upper grid	Wet oxidation, HPLC+LSC	Not measured	23 ~ 34%	66~75% Formate 10%; acetate 43%; formaldehyde 9%; methanol 10%;ethanol 6%; unknown 22%
	BWR Shroud	Ion exchange + LSC	42 months : 25%	42 months : 37%	42 months: 38% comprising: neutral 18%; anion 82%
Non-activated	Fe_3C	HPLC	Not measured	35~45%	55~65%
	Carbon steel	HPLC	~0.01%	15~30%	70~85%

8 Discussion and conclusions

8.1 Steel corrosion rates

During the course of preparing the current document, a number of additional references, published since reference [13] was prepared, were identified and summarised. In general, they have not changed the view of the likely corrosion rates for carbon steel in the conditions expected during waste storage and disposal or for stainless steel under aerobic (storage) conditions. However, the paper by Yoshida *et al.* [233] has provided data for the very low corrosion rates experienced by stainless steels under anoxic alkaline conditions, and these results are important in relation to the issue of carbon-14 release from stainless steels during waste disposal in alkaline conditions. The data are all below 0.01 μm yr^{-1} (Table 17 and Figure 21), which was the upper value recommended previously [13] and which has been used in recent assessments of gas generation and carbon-14 release from steels in the UK [e.g. 243]. The Japanese data also show a decrease of the anaerobic corrosion rate under alkaline conditions with time (the significance of which is not yet clear), and a temperature dependence, neither of which could be discriminated previously.

In the previous review [13], parameters for use in RWM's SMOGG corrosion model were obtained for the anaerobic alkaline corrosion of carbon steel by calibration against experimental data (the data sets used are summarised in Table 13). However, it was not possible to calibrate the model for stainless steel owing to the scarcity of suitable data. It would now be possible to investigate the calibration of the SMOGG model using the new Japanese data.

The key findings of the review concerning the corrosion rates of carbon and stainless steel under conditions relevant to waste storage and disposal are summarised in the following sub-sections.

8.1.1 Carbon steel

8.1.1.1 Aerobic corrosion in grout

For carbon steels that have been treated to remove the passivating layer before encapsulation in cement, the corrosion rate is very high initially, typically of the order of

~200 µm yr^{-1} at ambient temperature. The corrosion rate increases at higher temperatures. However, the acute phase is short-lived and the corrosion rate typically decays to <1 µm yr^{-1} over a matter of days (if not hours). The rate of passivation is reduced in the presence of higher concentrations of chloride (up to 80 days in cement with 3% chloride addition).

In general, in the absence of chloride and carbonation effects, the long-term corrosion rate of carbon steel in cementitious environments is very low because of the protection offered by the passive film formed under alkaline conditions. Corrosion rates as low as 0.08 µm yr^{-1} have been measured. For rebars taken from some concrete structures, where carbonation may be important, higher values in the range 10-50 µm yr^{-1} over 1-50 years have been reported. The actual corrosion rates of cemented carbon steel wastes, prior to closure of a disposal facility, are likely to depend on the specific cement types and waste stream and the environmental conditions (in particular the relative humidity).

8.1.1.2 Anaerobic corrosion, alkaline conditions

The acute corrosion rate of carbon steel is reduced under anaerobic, alkaline conditions and, in general, measured values are <5 µm yr^{-1} at near-ambient temperatures (≤30°C). However, the duration of the acute phase is correspondingly longer than under aerobic conditions, and may last for up to 5 years before longer-term rates are achieved. The acute corrosion rate increases with temperature following an Arrhenius relationship but the rate of passivation is also increased.

For pre-corroded materials, an incubation period is likely before anaerobic corrosion starts; and when it does it may initiate at a low level. In experiments over 10 years, long-term anaerobic corrosion rates in the range 0.04-0.11 µm yr^{-1} have been measured at 30°C in alkaline solutions on the UK programme. Recent work on the Belgian programme is in agreement with these findings with long term rates after 5 years <0.1 µm yr^{-1}. These studies have found little effect of γ-irradiation, chloride or sulphur species on anaerobic corrosion under alkaline conditions and little effect of temperature on the long-term rates due to the formation of a protective magnetite film.

8.1.2 Stainless steel

8.1.2.1 Aerobic corrosion in grout

In contrast to carbon steels, stainless steels undergo very rapid passivation if the oxide layer is disrupted and, in general, there is not expected to be a distinct period of acute corrosion. Under alkaline conditions, the corrosion rate of stainless steel is very low and, in general, long-term rates measured for grout-encapsulated stainless steels have fallen in the range 0.01 to 0.04 µm yr^{-1} with the presence of chloride having only a small, if any, effect.

The corrosion rate measured in a cement-equilibrated water by passive current densities (which are somewhat higher than those discussed above) increases with temperature and shows an Arrhenius relationship.

8.1.2.2 Anaerobic corrosion, alkaline conditions

Anaerobic corrosion rates of stainless steel in alkaline solutions are very low and have proved difficult to measure in the past. Recent Japanese work has successfully measured these very low corrosion rates and confirmed that they are below 0.01 µmyr^{-1} [233] which was the value recommended as an upper limit in the previous review for the UK programme [13]. The new data indicate a mean anaerobic corrosion rate of 0.0008 µm yr^{-1} for 18/8 stainless steel at 30°C after two years exposure, about one order of magnitude lower than the value used in recent assessments of gas generation and carbon-14 release from steels in the UK [243]. The Japanese data also show a decrease of the anaerobic corrosion rate under alkaline conditions with time (the significance of which is not yet clear), and a temperature dependence (with corrosion rate increasing with temperature), neither of which could be discriminated previously.

8.1.3 Effects of irradiation

It should be borne in mind that all of the corrosion data considered in this review were obtained on unirradiated steels. However, it is known that radiation-induced segregation of alloying components in steels occurs under neutron irradiation and this may have an impact on the corrosion rate of waste stainless steels, due to the depletion of chromium at grain boundaries [67]. As stated by Was, there are currently no data concerning the effect

of irradiation on the corrosion of stainless steel [68]. However, data do exist concerning the impact of irradiation on the in-service corrosion of zirconium alloys in nuclear reactors. In general, irradiated zirconium alloys showed an increase in thickness of the oxide film formed on the metal surface compared to unirradiated materials by between 5- and 40-fold dependent on the irradiation conditions and neutron flux. The impact of the irradiation history on the corrosion rate of the steel samples that will be used in CAST WP2 is not known. Although it is not a key objective of WP2, it is possible that the experiments performed under WP2 may provide some insight on the relative corrosion rates of irradiated compared to unirradiated steels.

8.2 Carbon and carbon-14 release from irradiated steels

The current understanding of carbon releases from steels and carbon-14 releases from irradiated steels on corrosion in aqueous solutions was outlined in section 7.3. This review has highlighted the current lack of well-documented inactive studies of the release of carbon from low-carbon and stainless steels that include measurements of carbon releases to both the gas phase and to the solution phase under aerobic and anaerobic conditions. The inactive studies planned by VTT and RWMC in WP2 could potentially throw light on the apparent discrepancy in the observed speciation of carbon releases between studies of zero-valent iron and those performed on the Japanese programme. The formation of hydrocarbons from the hydrolysis of certain metal carbides has been recognised for over a century (see for example [286]), whereas the formation of more oxidised water-soluble species requires confirmation.

A clearer understanding of the speciation of carbon releases from steels on corrosion will aid the development of advanced methods for determining the speciation of the much smaller quantities of carbon-14 released from irradiated steels in corrosion experiments that are planned under WP2. However, there remains significant uncertainty concerning the speciation of carbon-14 derived from neutron activation of nitrogen-14 in irradiated steels and whether it is the same as carbon in unirradiated materials. This review has noted the potential for carbon-14 to be present in irradiated steels as carbonitride phases as well as carbides. In general, carbonitrides are expected to be more resistant to hydrolysis

than the equivalent metal carbides and may give rise to hydrolysis products containing carbon-nitrogen bonds such as cyanides or amines, in addition to hydrocarbons.

The distribution of carbon between different phases (metal carbide phases, cementite, *etc*.) in steels has not been included within the scope of this review. However, work has been undertaken recently at Loughborough University for RWM on the distribution of carbon and nitrogen in unirradiated samples of steels used in the UK nuclear programme [287]. In particular, it was found that the carbon and nitrogen content of two titanium-stabilised steels (including the 20/25 Cr/Ni steel used in AGR fuel assemblies) contained carbon and nitrogen predominantly in the form of titanium carbonitride particles.

9 Acknowledgements

The following representatives of partner organisations in CAST WP2: Bernhard Kienzler (KIT), Nikitas Diomidis (Nagra), Erich Wieland (PSI), and Hiromi Tanabe (RWMC) are thanked for providing published or draft reports and/or draft text for inclusion in this review. RWMC are thanked for permission to reproduce Figure 21 and Figure 24. The authors thank Brinsley Myatt (AMEC) for assistance with preparation of some of the tables and redrawing of a number of figures presented in this report.

This work was funded by Radioactive Waste Management Limited, as a contribution to the EU FP7 CAST Project.

10 References

1 Nuclear Decommissioning Authority, *Geological Disposal. Carbon-14 Project – Phase 1 Report*, NDA/RWMD/092, December 2012.

2 L. Johnson and B. Schwyn (eds.), *Proceedings of a Nagra/RWMC Workshop on the release and transport of C-14 in repository environments*, Nagra report NAB 08-22, 2008.

3 The Nuclear Safety Commission of Japan, *Basic guide for safety review of Category 2 radioactive waste disposal*, NSCRG Report F-Rw-I.02, 2010.

4 Japan Atomic Energy Agency and the Federation of Electric Power Companies, *Progress report on disposal concept for TRU wastes in Japan*, JAEA-Review 2007-010, 2007.

5 Nagra, *Project Opalinus Clay – safety report. Demonstration of disposal feasibility for spent fuel, vitrified high-level waste and long-lived intermediate-level waste (Entsorgungsnachweis)*, Nagra Technical Report NTB 02-05, 2002.

6 Nirex, *The viability of a phased geological repository concept, for the long-term management of the UK's radioactive waste*, Nirex Report N/122, 2005.

7 http://www.nda.gov.uk/aboutus/geological-disposal/rwmd-work/dssc/index.cfm

8 A.C. Adeogun, *Carbon-14 Project Phase 2: Inventory (Tasks 1& 2)*, AMEC Report AMEC/200047/003 (Pőyry/390936/Phase 2), to be published.

9 Nagra, *The Nagra research, development and demonstration (RD&D) plan for the disposal of radioactive waste in Switzerland*, Nagra Technical Report 09-06, 2009.

10 United Kingdom Nirex Limited, *Generic repository studies: The Nirex phased geological repository concept*, Nirex Report N/074, 2003.

11 ONDRAF/NIRAS, *Research, development and demonstration (RD&D) plan for the geological disposal of high-level and/or long-lived radioactive waste including irradiated fuel if considered as waste, State-of-the-art report as of December 2012*, ONDRAF/NIRAS Report NIROND-TR 2013-12E, 2013.

12 JAEA and FEPC, *Second progress report on research and development for TRU waste disposal in Japan*, JAEA and FEPC Report TRU-2, 2007.

13 N.R. Smart and A.R. Hoch, *A survey of steel and Zircaloy corrosion data for use in the SMOGG gas generation model*, Serco Report SA/ENV-0841, Issue 3, 2010.

14 N.R. Smart, *Review of effect of chloride on corrosion of stainless steels in cementitious environments*, Serco Report SA/SIS/14921/R001 Issue 3, 2010.

15 F. King, *Corrosion resistance of austenitic and duplex stainless steels in environments related to UK geological disposal*, Quintessa Report QRS-1384C-R1 version 1.2, 2009.

16 F. King and S. Watson, *Review of the corrosion performance of selected metals as canister materials for UK spent fuel and/or HLW*, Quintessa Report QRS-1384J-1, version 2.1, 2010.

17 N.R. Smart, *Corrosion behaviour of carbon steel radioactive waste packages: A summary review of Swedish and U.K. research*, Corrosion **65**, 195-212, 2009.

18 F. King, *Corrosion of carbon steel under anaerobic conditions in a repository for SF and HLW in Opalinus Clay*, Nagra Technical Report NTB 08-12, 2008.

19 E. Wieland and W. Hummel, *The speciation of ^{14}C in the cementitious near field of a repository for radioactive waste*, PSI Report TM 44-10-01, 2010.

20 T. Heikola, *Leaching of ^{14}C in repository conditions*, VTT Technology Report 157, 2014.

21 *DECHEMA Corrosion Handbook: corrosive agents and their interaction with materials*, Volume 1: Potassium hydroxide (1987), Volume 2: Sodium hydroxide (1988), Volume 3: Lithium hydroxide (1988), Volume 5: Alkaline earth hydroxides (1989), Volume 7: Atmosphere (1990), Volume 10: Drinking water (1991), Volume 11: Seawater (1992), eds: D.Behrens (Volumes 1-9): G.Kreysa and R. Eckerman (Volumes 10 and 11).

22 F.N. Speller, *Corrosion: causes and prevention*, McGraw-Hill, 1951.

23 H.H. Uhlig, *Corrosion and corrosion control*, J. Wiley, 1971.

24 H.H. Uhlig, *The corrosion handbook*, J. Wiley, 1948.

25 M. Schumaker (ed.), *Seawater corrosion handbook*, Noyes Data Corporation, 1979.

26 D. Feron (editor), *Nuclear corrosion science and engineering*, Woodhead Publishing, Cambridge, 2012.

27 N. Sridhar, G.A. Cragnolino, D.S. Dunn and H.K. Manaktala, *Review of degradation modes of alternate container designs and materials*, SWI Report CNWRA 94-010, 1994.

28 A.J. Sedriks, *Corrosion of stainless steels*, John Wiley, second edition, 1996.

29 T.W.Hicks, M.B. Crawford and D.G. Bennett, *Carbon-14 in radioactive wastes and mechanisms for its release from a repository as gas*, Galson Sciences Ltd Report 0142-1, 2003.

30 S. Kaneko, H. Tanabe, M. Sasoh, R. Takahashi, T. Shibano and S. Tateyama, *A study on the chemical forms and migration behaviour of carbon-14 leached from the simulated hull waste in the underground condition*, MRS Symposium Proc. **757**, paper II.3.8, 2003.

31 P. Fennell, *Experimental study of the reactions of carbides with aqueous solutions*, AMEC Report AMEC/TAS/MCRL/19436/C001, to be published.

32 B.S. Mitchell, *An introduction to materials engineering and science*, pp. 165, Wiley-Interscience, Hoboken, New Jersey, 2004.

33 C. Jones, *The results of a search for information on the release of gaseous carbon-14 from activated metals*, Nuclear Technologies Report NT/P322/R101, 2005.

34 L.E. Toth, *Transition metal carbides and nitrides*, Academic Press, London, 1971.

35 F. Cataldo, *Organic matter formed from hydrolysis of metal carbides of the iron peak of cosmic elemental abundance*, Int. J. Astrobiol. **2**(1), 51-63, 2003.

36 H.O. Pierson, *Handbook of refactory carbides and nitrides, properties, characteristics, prossing and applications*, Noyes Publications, Westwood, New Jersey, USA, 1996.

37 K.K. Kelley, F.S. Boericke, G.F. Moore, F.H. Huffman and W.M. Bangert, *Thermodynamic properties of the carbides of chromium*, US Bureau of Mines Technical Paper 662, 1-43, 1944, quoted by B. Häjek, P. Karen and V. Brozek, *Hydrolyzable carbides: relationships between their structure and the composition of their hydrolysis products*, Reviews in Inorganic Chemistry **8**, 117-160, 1986.

38 *Metallic carbides*, Nature **54**, 357, 1896, doi:10.1038/054357a0.

39 F.A. Cotton and G. Wilkinson, *Advanced inorganic chemistry*, 4th Edition, Wiley-Interscience, New York, 1980 and 6th Edition, 1999.

40 R.W.K. Honeycombe, *Steels: microstructure and properties*, Edward Arnold, 1982.

41 K. Kurosawa, H.-L. Li, Y. Ujihira, and K. Nomura, *Characterization of carbonitrided and oxidized layers on low-carbon steel by conversion electron mössbauer spectrometry, X-ray diffractometry, and X-ray photoelectron spectrometry*, Corrosion **55**(3), 238-247, 1999.

42 S. Sugihara and S. Imoto, *Hydrolysis of thorium nitrides and carbonitirdes*, J. Nucl. Sci. Technol. **8**, 630-636, 1971.

43 See http://www.nda.gov.uk/ukinventory/, accessed on 23 May 2014.

44 F. King, P. Humphreys and R. Metcalfe, *A review of the information available to assess the risk of microbiologically influenced corrosion in waste packages*, Quintessa Report QRS-1384L-1, v. 3.0, 2011.

45 J. Jelinek and P. Neufeld, *Kinetics of hydrogen formation from mild steel in water under anaerobic conditions*, Corrosion **38**(2), 99, 1982.

46 U.R. Evans and J.N. Wanklyn, *Evolution of hydrogen from ferrous hydroxide*, Nature **162**, 27, 1948.

47 A. Vértes and I. Czako-Nagy, *Mössbauer spectroscopy and its application to corrosion studies*, Electrochimica Acta **34**(6), 721, 1989.

48 R.P. Frankenthal and J. Kruger, *Passivity of Metals*, The Electrochemical Society, 1978.

49 I. Kalashnikova, L. Nunez and F. Corvo, *Corrosion behaviour of metallic materials in the Cuban Caribbean Sea*, Corrosion Reviews **13**(2-4), 261, 1995.

50 T. Peev, M.K. Georgieva, S. Nagy and A. Vértes, *Mössbauer study of corrosion products formed on α-iron in sea water*, Radiochem. Radioanal. Lett. **33**, 265, 1978.

51 J. Chen, Z. Cai, Z. Wang and H. Zhang, *A study of the barrier layer rust formed on low alloy steels in sea water by conversion electron Mössbauer spectroscopy*, Proceedings of ICAME, Jaipur, India, 264, 1981.

52 K.K. Sagoe-Crentsil and F.P. Glasser, *Constitution of green rust and its significance to the corrosion of steel in portland cement*, Corrosion **49**(6), 457, 1993.

53 P. Refait and J.-M.R. Genin, *The oxidation of ferrous hydroxide in chloride-containing aqueous media and Pourbaix diagrams of green rust one*, Corrosion Science **34**(5), 797, 1993.

54 S. Haupt and H.H. Strehblow, *Corrosion, layer formation, and oxide reduction of passive iron in alkaline solution: a combined electrochemical and surface analytical study*, Langmuir **3**, 873, 1987.

55 D.D. Macdonald, M. Urquidi-Macdonald, G.R. Engelhardt, O. Azizi, A. Saleh, A. Almazooqi and O. Rosas-Camacho, *Some important issues in electrochemistry of carbon steel in simulated concrete porewater Part 1 – theoretical issues*, Corrosion Engineering, Science and Technology, **46**(2), 98, 2011.

56 A. Saleh, O. Azizi, O. Rosas-Camacho, A. Almazooqi and D.D. Macdonald, *Some important issues in electrochemistry of carbon steel in simulated concrete porewater Part 2 – experimental*, Corrosion Engineering, Science and Technology, **46**(2), 104, 2011.

57 A.M. Riley and J.M. Sykes, *The cathodic reduction of passive films on low-alloy steel in carbonate solutions*, Corrosion Science **28**(8), 799, 1988.

58 E.R. Vago and E.J. Calvo, *Electrocatalysis of oxygen reduction at Fe_3O_4 oxide electrodes in alkaline solutions*, J. Electroanal. Chem. **339**, 41, 1992.

59 S. Nasrazadani and A. Raman, *Formation and transformation of magnetite (Fe_3O_4) on steel surfaces under continuous and cyclic water fog testing*, Corrosion **49**(4), 294, 1993.

60 H. Konno, M. Kawai and M. Nagayama, *The mechanism of spontaneous dissolution of the air-formed oxide film on iron in a deaerated neutral phosphate solution*, Surface Technology **24**, 259, 1985.

61 D. Gilroy and J.E.O. Mayne, *The breakdown of the air-formed oxide film on iron upon immersion in solutions of pH 6-13*, British Corrosion Journal **1**, 102, 1965.

62 N.R. Smart, D.J. Blackwood, G.P. Marsh, C.C. Naish, T.M. O'Brien, A.P. Rance and M.I. Thomas, *The anaerobic corrosion of carbon and stainless steels in simulated cementitious repository environments: a summary review of Nirex research*, AEAT/ERRA-0313, 2004.

63 Z. Szklarska-Smialowska, *Pitting corrosion of metals*, National Association of Corrosion Engineers, 1986.

64 C.R. Clayton and I. Olefjord, *Passivity of stainless steels*, chapter 7 in P. Marcus (ed.), Corrosion Mechanisms in Theory and Practice, Dekker, 2002.

65 W.Z. Friend, *Corrosion of nickel and nickel-base alloys*, John Wiley, 1980.

66 F. King, *Review of the Performance of selected metals as canister materials for UK spent fuel and/or HLW - Appendix E corrosion of nickel alloys*, Quintessa Report QRS-1384J-1, v2.1, 2010.

67 G. Was, *Fundamentals of radiation materials science*, Springer-Verlag, 2007.

68 G. Was, *Irradiation assisted corrosion and stress corrosion cracking (IAC/IASCC) in nuclear reactor systems and components*, Chapter 6 in: D. Feron (ed.), Nuclear corrosion science and engineering, Woodhead Publishing, Cambridge, 2012.

69 G. Knowles, *Corrosion of sensitized advanced gas reactor fuel cladding in moist air: Evidence for incubation periods before onset of intergranular cracking*, in: Effects of radiation and environmental factors on the durability of materials in spent fuel storage and disposal, IAEA-TECHDOC-1316, 2002.

70 G.C. Moran and P. Labine (eds.), *Corrosion monitoring in industrial plants*, ASTM STP 908, 1986.

71 G.S. Haynes and R. Baboian, *Laboratory corrosion tests and standards*, ASTM STP 866, 1983.

72 G.P. Marsh, A.H. Harker and K.J. Taylor, *Corrosion of carbon steel nuclear waste containers in marine sediment*, Corrosion **45**(7), 579, 1989.

73 R. Grauer, B. Knecht, P. Kreis and J.P. Simpson, *The long term corrosion rate of passive iron in anaerobic alkaline solutions*, Werkstoffe und Korrosion **42**, 637, 1991.

74 R. Grauer, B. Knecht, P. Kreis and J.P. Simpson, *Hydrogen evolution from corrosion of iron and steel in intermediate level waste repositories*, p. 295 in Scientific Basis for Nuclear Waste Management **XIV**, T.A.Abrajano and L.H.Johnson (eds.), 1991.

75 Andra, *Dossier 2005 Argile – Tome - Phenomenological evolution of a geological repository*, Andra Report, 2005.

76 SKB, *Deep repository for long-lived low- and intermediate-level waste. Preliminary safety assessment*, SKB Report TR-99-28, 1999.

77 Nuclear Decommissioning Authority, *Geological Disposal. Near-field evolution status report*, NDA Report NDA/RWMD/033, 2010.

78 P.B. Bamforth, G.M.N. Baston, J.A. Berry, F.P. Glasser, T.G. Heath, C.P. Jackson, D. Savage and S.W. Swanton, *Cement materials for use as backfill, sealing and structural materials in geological disposal concepts. A review of current status*, Serco Report SERCO/005125/001 Issue 3, 2012.

79 H.F.W. Taylor, *Cement chemistry*, 2nd Edition, Thomas Telford, London, 1997.

80 L. Wang, E. Martens, D. Jacques, P. de Cannière, J. Berry and D. Mallants, *Review of sorption values for the cementitious near field of a near surface radioactive waste disposal facility. Project near-surface disposal of category A waste at Dessel*, ONDRAF/NIRAS Report NIROND-TR 2008-23E, 2009.

81 F. Neall, *Modelling of the near-field chemistry of the SMA repository at the Wellenberg site: application of the extended cement degradation model*, Nagra Technical Report NTB 94-03, 1995.

82 Nagra, *Project Opalinus Clay: model, codes and data for safety assessment. Demonstration of disposal feasibility for spent fuel, vitrified high-level waste and long-lived intermediate-level waste*, Nagra Technical Report NTB 02-06, 2002.

83 R.J. Winsley, N.R. Smart, B. Reddy, A.P. Rance and P.A.H. Fennell, *4 Metre box monitoring programme – Final report*, Serco Report SERCO/TCS/000730.01, 2010.

84 P.A.H. Fennell, N.R. Smart, M. Izzo, N.A. Turner, *Characterisation of environmental conditions in an ILW store*, AMEC Report D.005265/001, 2012.

85 A. Hache, L. Barriety, J. Debyser, *Effect of photosynthesis on the corrosion of steel in seawater*, Werkstoffe und Korrosion **10**, 145, 1959.

86 P.E. Francis and A.D. Mercer, *Corrosion of a mild steel in distilled water and chloride solutions: development of a test method*, in: G.S.Haynes and R.Baboian (eds.), Laboratory corrosion tests and standards, ASTM STP 866, p. 184 1985.

87 A. Higginson, *The effect of physical and chemical factors on the corrosivity of a synthetic minewater*, MINTEK Report M140, 1984.

88 A.D. Mercer and E.A. Lumbard, *Corrosion of mild steel in water*, British Corrosion Journal **30**(1), 43, 1995.

89 K. Hara, H. Ishikawa, A. Honda and N. Sasaki, *Influence of dissolved oxygen on the generation rate of hydrogen gas with corrosion of carbon steel*, Proc. Workshop on Gas Generation and Release from Radioactive Waste Repositories, Aix-en-Provence, September 1991, p. 121, OECD, 1992.

90 C.W. Borgmann, *Initial Corrosion Rate of Mild Steel - Influence of the Cation*, Ind. Eng. Chem. **29**(7), 814, 1937.

91 K. Videm and A. Dugstad, *Corrosion of carbon steel in an aqueous carbon dioxide environment Part 1: solution effects*, Materials Performance p. 63, March 1989.

92 K. Videm and A. Dugstad, *Corrosion of carbon steel in an aqueous carbon dioxide environment Part 2: film formation*, Materials Performance, p. 46, April 1989.

93 D.H. Lester, R.T. Stula and B.E. Kirstein, *Waste package performance evaluation*, ONWI-302, 1983.

94 F.L. Laque, *Marine Corrosion. Causes and prevention*, J. Wiley, 1975.

95 D.R. Diercks, A.B. Hull and T.F. Kassner, *Analysis of corrosion data for carbon steels in simulated salt repository brines and acid chloride solutions at high temperatures*, Conf-880377-3, DE88-012030, Joint US/FRG Technical Exchange Workshop, Albuquerque, March 1988.

96 D.R. Diercks and T.F. Kassner, *Analysis of the corrosion of carbon steels in simulated salt repository brines and acid chloride solutions at high temperatures*, ANL/PPRNT-90-207, DE90 009164, 1988.

97 N. Platts, D.J. Blackwood and C.C. Naish, *Anaerobic oxidation of carbon steel in granitic groundwaters: a review of the relevant literature*, AEA-InTec-1413, 1994.

98 A.P. Akolzin, P. Ghosh and Y.Y. Kharitonov, *Application and peculiarity of $Ca(OH)_2$ as inhibitor in presence of corrosion activators*, British Corrosion Journal **20**(1), 32, 1985.

99 M. Yasuda, K. Fukumoto, H. Koizumi, Y. Ogata and F. Hine, *On the active dissolution of metals and alloys in hot concentrated caustic soda*, Corrosion **43**(8), 492, 1987.

100 H. Grubitsch, L. Binder and F. Hilbert, *The Influence of various concentrations of chloride ions on the active-passive corrosion susceptibility of steel in saturated calcium hydroxide solution*, Werkstoffe und Korrosion **30**(4), 241, 1979.

101 R. Grauer, The corrosion behaviour of carbon steel in Portland cement, NAGRA Technical Report 88-02E, 1988.

102 N.R. Smart, D.J. Blackwood and L. Werme, *The anaerobic corrosion of carbon steel and cast iron in artificial groundwaters*, SKB Report TR-01-22, 2001.

103 N.R. Smart, D.J. Blackwood and L. Werme, *Anaerobic corrosion of carbon steel and cast iron in artificial groundwaters: Part 1 – Electrochemical aspects*, Corrosion **58**(7), 547, 2002.

104 N.R. Smart, D.J. Blackwood and L. Werme, *Anaerobic corrosion of carbon steel and cast iron in artificial groundwaters: Part 2 – Gas generation*, Corrosion **58**(8), 627, 2002.

105 M. Mihara, T. Nishimura, R. Wada and A. Honda, *Estimation on gas generation and corrosion rates of carbon steel, stainless steel and Zircaloy in alkaline solutions under low oxygen condition* (in Japanese), Saikuru Kiko Giho **15**, 91-101, Jun 2002.

106 T. Nishimura, R. Wada and K. Fujiwara, *Evaluation of gas generation rates caused by metal corrosion under the geological repository conditions* (in Japanese), R and D Kobe Seiko Giho **53**(3), 78-83, Dec 2003.

107 C.C. Naish, *Corrosion aspects of the proposed Sellafield waste repository*, U.K. Corrosion '93, 1993.

108 N. Kudo, *Corrosion and its prevention of reinforcement in concrete*, Corrosion Engineering **42**(7), 565, 1993.

109 A.P. Crane (ed.), *Corrosion of reinforcement in concrete construction*, Ellis Horwood, 1983.

110 K. Tuuti, *Corrosion of steel in concrete*, Swedish Cement and Concrete Research Institute, 1982.

111 J.E. Slater, *Corrosion of metals in association with concrete*, ASTM STP 818, 1983.

112 A. Alonso and C. Andrade, *Life time of rebars in carbonated concrete*, in: J.M.Costa and A.D.Mercer (eds.), Progress in the Understanding and Prevention of Corrosion, p. 634, Institute of Materials, 1993.

113 H. Arup, *The mechanisms of the protection of steel by concrete*, p. 151 in 'Corrosion of Reinforcement in Concrete Construction', A.P.Crane (ed.), Ellis Horwood, 1983.

114 E. Escalante, T. Oka and U. Bertocci, *Effect of oxygen transport and resistivity of the environment on the corrosion of steel*, p. 287 in Scientific Basis for Nuclear Waste Management **XIV**, Materials Research Society Symposium proceedings Volume 212, T.A.Abrajano, L.H.Johnson (eds.) 1991.

115 C.M. Preece, F.O. Grønwold and T. Frølund, *The influence of cement type on the electrochemical behaviour of steel in concrete*, p. 393 in Corrosion of Reinforcement in Concrete Construction, London, SCI, 1983.

116 A. Seghal, Y.T. Kho, K. Osseo-Asare and H.W. Pickering, *Comparison of corrosion rate-measuring devices for determining corrosion rate of steel-in-concrete systems*, Corrosion, **48**(10), 871, 1992.

117 J.A. Gonzalez, W. Lopez and P. Rodriguez, *Effects of moisture availability on corrosion kinetics of steel embedded in concrete*, Corrosion **49**(12), 1004-1010, 1993.

118 J.N. Enevoldsen, C.M. Hansson and B.B. Hope, *The influence of internal relative humidity on the rate of corrosion of steel embedded in concrete and mortar*, Cement and Concrete Research, **24**(7), 1373-1382, 1994.

119 J. Flis, S. Sabol, H.W. Pickering, A. Seghal, K. Osseo-Asare and P.D. Cady, *Electrochemical measurements on concrete bridges for evaluation of reinforcement corrosion rates*, Corrosion **49**(7), 601, 1993.

120 S.E. Benjamin and J.M. Sykes, Chloride induced pitting corrosion of swedish iron in ordinary Portland cement mortars and alkaline solutions: the effect of temperature, p. 59 in 'Corrosion of Reinforcement in Concrete', C.L. Page, K.W.J. Treadaway, P.B. Bamforth (eds.), Elsevier, 1990.

121 C.M. Hansson, *Hydrogen evolution in anaerobic concrete resulting from corrosion of steel reinforcement*, SKB-1984-11-28, 1984.

122 C.M. Hansson, *The corrosion of steel and zirconium in anaerobic concrete*, pg. 475 in Scientific Basis for Nuclear Waste Management IX, L. Werme (ed.), **50**, 475, 1985.

123 C.M. Hansson, *The corrosion of steel in anaerobic concrete and the associated evolution of hydrogen*, SKB report SFR 87-02, 1987.

124 C.C. Naish, P.H. Balkwill, T.M. O'Brien, K.J. Taylor and G.P. Marsh, *The anaerobic corrosion of carbon steel in concrete*, Nirex Report NSS/R273, 1990.

125 C.C. Naish, P.H. Balkwill, T.M. O'Brien, K.J. Taylor and G.P. Marsh, *The anaerobic corrosion of carbon steel in concrete*, EUR 13663, 1991.

126 R.C. Newman and S. Wang, *Feasibility study of hydrogen monitoring during anaerobic corrosion of carbon steel in grouts*, Nagra Report NAB 10-17, 2010.

127 R.C. Newman and S. Wang, *Understanding and quantifying the corrosion of carbon steel in grouts relevant to the Swiss L/ILW repository – status reports 2011 and 2012*, Nagra Report NAB 13-08, 2013.

128 N.R. Smart, A.P. Rance, R.J. Winsley, P.A.H. Fennell, B. Reddy and B. Kursten, *The effect of irradiation on the corrosion of carbon steel in alkaline media*, presented at the NUCPERF 2009 conference on Long-Term Performance of Cementitious Barriers and Reinforced Concrete in Nuclear Power Plants and Waste Management (EFC event 317), Cadarache, France, 30 March-2 April, 2009, published in RILEM proceedings PRO 64, 2009.

129 R.J. Winsley, N.R. Smart, A.P. Rance, P.A.H. Fennell, B. Reddy and B. Kursten, *Further studies on the effect of irradiation on the corrosion of carbon steel in alkaline media*, presented at The 4th International Workshop on Long-Term Prediction of Corrosion Damage in Nuclear Waste Systems, Bruges, Belgium, June 2010, published in Corrosion Engineering, Science and Technology **46**(2), 111-116, 2011.

130 N.R. Smart, P.A.H. Fennell, A.P. Rance, R.J. Winsley, B. Reddy and B. Kursten, *Experimental studies of the effect of irradiation on the anaerobic corrosion of carbon steel in relation to the Belgian Supercontainer Concept*, presented at the AMP 2010 International Workshop on Ageing Management of Nuclear Power Plants and Waste Disposal Structures (EFC Event 334), Toronto, Canada,

November 2010, published in The European Physical Journal (EPJ) Web of Conferences (eds V. L'Hostis, K. Phillipose, R. Gens and C. Galle), Volume 12, Paper 02003, 2011.

131 N.R. Smart, A.P. Rance, P.A.H. Fennell and B. Kursten, *The anaerobic corrosion of carbon steel in alkaline media – Phase 2 results*, International Workshop NUCPERF 2012: Long-Term Performance of Cementitious Barriers and Reinforced Concrete in Nuclear Power Plant and Radioactive Waste Storage and Disposal (RILEM Event TC 226-CNM and EFC Event 351) Cadarache, France, November 12-15, 2012 V. L'Hostis and R. Gens (Eds.) EPJ Web of Conferences Vol. 56, 2013.

132 N.R. Smart, A.P. Rance, P.A.H. Fennell and B. Kursten, *The effect of sulphur species on the anaerobic corrosion of carbon steel in alkaline media*, presented at the 5th. International Workshop on Long-Term Prediction of Corrosion Damage in Nuclear Waste Systems, Asahikawa, Japan, Corrosion Engineering Science and Technology, in press, 2014.

133 H.R. Ambler and A.A.J. Bain, *Corrosion of metals in the tropics*, J. Appl. Chem. **5**, 437, 1955.

134 C. Arya and Y. Xu, *Effect of cement type on chloride binding and corrosion of steel in concrete*, Cement and Concrete Research **25**(4), 893-902, 1995.

135 T. Liu and R.W. Weyers, *Modeling the dynamic corrosion process in chloride contaminated concrete structures*, Cement and Concrete Research **28**(3), 365-379, 1998.

136 R. Fujisawa, T. Cho, K. Sugahara, Y. Takizawa, Y. Horikawa, T. Shiomi and M. Hironaga, *The Corrosion Behaviour of iron and aluminum under waste disposal conditions*, Mat. Res. Soc. Symp. Proc. **465**, 675, 1997.

137 W.R. Braithwaite and K.A. Lichti, *Surface corrosion of metals in geothermal fluids at Broadlands, New Zealand*, in 'Geothermal scaling and corrosion' ASTM STP 717 L.A. Casper and T.R. Pinchback (eds.), 1980.

138 W. Breckheimer and J. D'Ans, *Corrosion of iron influenced by temperature differences of the attacking electrolyte*, Werkst. Korros. **5**(2), 43, 1954.

139 F. Canadillas, E. Smailos and R. Koster, *Corrosion studies on the suitability of a mild steel for the disposal of high level waste products*, Kernforschunszentrum Karlsruhe, KfK 3549, 1983.

140 M.A. Elmorsi and R.M. Issa, *Corrosion of metal pipes in ground water*, Bulletin of Electrochemistry **4**(9), 785, 1988.

141 K.B. Gaonkar, P.K. Chauhan and H.S. Gadiyar, *Corrosion behaviour of mild steel in natural and distilled waters: effect of temperature and addition of various chemicals*, Corrosion and Maintenance, July, 1983.

142 A. Hache, Rev. Métall. **1**, 76, 1956, taken from *DECHEMA Corrosion Handbook: corrosive agents and their interaction with materials*, Volume 11 'Seawater', G.Kreysa and R.Eckerman (eds.), 1992.

143 K.H. Ho and S.K. Roy, *Corrosion of steel in tropical sea water*, British Corrosion Journal **29**(3), 233, 1994.

144 A. Honda, T. Teshima, K. Tsurudome, H. Ishikawa, Y. Yusa and N. Sasaki, *Effect of compacted bentonite on the corrosion behaviour of carbon steel as geological isolation overpack material*, p. 287 in Scientific Basis for Nuclear Waste Management **XIV**, T.A. Abrajano and L.H. Johnson (eds.) 1991.

145 E.R. Kennedy and J.S. Wilson, *New York Harbour corrosion - Port of New York Authority conducts pile survey*, Mater. Protection **6**, 53, 1967.

146 V.G. Kritsky, V.V. Morozov, A.F. Nechaev, Y.A. Khitrov, N.G. Petrik, N.N. Kalyazin and T.F. Makarchuk, *Material corrosion under spent nuclear fuel storage conditions*, in Materials reliability in the backend of the nuclear cycle, IAEA-TECDOC-421, 1987.

147 D. Kuron, H. Grafen, H-P. Batroff, K. Fassler and R. Munster, *Influence of chloride content in tap water on the corrosion of unalloyed steel*, Werkstoffe und Korrosion **36**, 68, 1985.

148 C.P. Larrabee, *Steel has low corrosion rate during long sea water exposure*, Materials Protection 95, Dec 1962.

149 R.D. McRight and H. Weiss, *Corrosion behaviour of carbon steels under tuff repository environmental conditions*, p. 287 in Scientific Basis for Nuclear Waste Management **VIII**, C.M. Jantzen, J.A. Stone and R.C. Ewing (eds.), 1985.

150 M.D. Merz, *State-of-the-Art Report on corrosion data pertaining to metallic barriers for nuclear waste repositories*, Pacific Northwest Laboratory report, PNL-4474, 1982.

151 W. Nissing, W. Friehe and W. Schwenk, *Influence of oxygen content, pH and flow velocity under corrosion of hot-dip galvanised and bare piping of unalloyed steel in potable water*, Werkstoffe und Korrosion **33**(6), 346, 1982.

152 M.H. Peterson and L.J. Waldron, *Investigation of mild steel corrosion rate in San Diego Harbor*, Corrosion **17**, 114, 1961.

153 F.M. Reinhart, *Corrosion of materials in hydrospace*, U.S. Naval Civil Engineering Lab. Port Hueneme, California, Technical Report R504, 1966.

154 F.M. Reinhart, *Corrosion of materials in hydrospace - Part I. Irons, steels, cast irons and steel products*, U.S.Naval Civil Engineering Lab. Port Hueneme, California, Technical Note N-900, 1967.

155 C.P. Larrabee, *Corrosion of steels in marine atmospheres and in sea water*, Trans. Electrochem. Soc. **87**, 161, 1945.

156 W. Schwarzkopf, E. Smailos and R. Köster, *In-situ corrosion studies on cast steel for high-level waste packaging in a rock salt repository*, in: W. Lutze and R.C. Ewing (eds.), Scientific Basis for Nuclear Waste Management **XII**, p. 411, 1989.

157 D.W. Shannon, *Economic impact of corrosion and scaling problems in geothermal energy systems*, Battelle report, BNWL-1866, 1975.

158 J.P. Simpson and J. Weber, *Steel as a container material for nuclear waste disposal*, in 'Corrosion Problems Related to Nuclear Waste Disposal', European Federation of Corrosion Publication number 7, p. 43, Institute of Materials, 1992.

159 E. Smailos and R. Koster, *Corrosion studies on selected packaging materials for disposal of high level wastes*, in: Materials Reliability in the Backend of the Nuclear Cycle, IAEA-TECDOC-421, 1987.

160 E. Smailos, W. Schwarzkopf and R. Koster, *Corrosion Under Gamma Irradiation and Stress Corrosion Cracking Behaviour of Unalloyed Steels in a $MgCl_2$ Rich Brine*, Conf-880377-3, DE88-012030, Joint US/FRG Technical Exchange Workshop, Albuquerque, March, 1988.

161 E. Smailos, W. Schwarzkopf, R. Köster and B. Fiehn, *Gamma Irradiation and In-situ Studies On Unalloyed Steels for a High Level Waste Packaging in a Rock Salt Repository*, KfK 4529, 1989.

162 E. Smailos, W. Schwarzkopf, R. Köster and K.H. Gruenthaler, *Advanced corrosion studies on selected packaging materials for disposal of hlw canisters in rock salt*, in 'Corrosion problems related to nuclear waste disposal', European Federation of Corrosion Publication number 7, p. 23, Institute of Materials, 1992.

163 C.R. Southwell and A.L. Alexander, *Corrosion of metals in tropical waters. Structural ferrous materials*, Materials Protection **9**(1), 14, 1970.

164 J.H. White, A.E. Yaniv and H. Schick, *The corrosion of metals in the water of the Dead Sea*, Corrosion Science **6**, 447, 1966.

165 S. Atashin, M. Pakshir and A. Yazdani, *Synergistic effect of seawater environmental factors on carbon steel corrosion rate*, Proceedings of the ASME 2010 29th International Conference on Ocean, Offshore and Arctic Engineering, June 6-11, 2010, Shanghai, China. OMAE2010-20224, 2010.

166 B. Huet, V. L'Hostis, L. Tricheux and H. Idrissi, *Influence of alkali, silicate, and sulfate content of carbonated concrete pore solution on mild steel corrosion behaviour*, Materials and Corrosion 61, No. 2, 2010.

167 B.W.A. Sherar, P.G. Keech, D.W. Shoesmith, *The effect of sulfide on the aerobic corrosion of carbon steel in near-neutral pH saline solutions*, Corrosion Science **66**, 256–262, 2013.

168 H.R.Z. Tadros and M.G.M.Osman, *Relation between some physical and chemical papameters affecting on corrosion rate of steel from Abu Qir Till Al-Arish, Egypt during winter 2008*, World Applied Sciences Journal **18**(3) 385-395, 2012.

169 D.J. Blackwood, A.R. Hoch, C.C. Naish, A.P. Rance and S.M. Sharland, *Research on corrosion aspects of the advanced cold process canister*, SKB Technical report 94-12, 1994.

170 A.M. Farvaque-Bera and S. Leistikow, *Electrochemical studies of the corrosion behaviour of a low-carbon steel in aqueous chloride solutions simulating accident conditions of radioactive waste disposal*, Journal of Nuclear Materials **185**, 1, 1991.

171 M. Grassiani, *Corrosion of carbon steels in hot deaerated seawater*, p. 260 in Materials Engineering Conference, Haifa, Israel, 1981.

172 J.H. Haberman, D.J. Frydrych and R.E. Westerman, *Corrosion and hydrogen permeation of A216 grade WCA steel in hydrothermal magnesium containing brines*, PNL/SRP-SA-15684, Conf-880377-1, DE88-012030, presented at the Joint US/FRG Technical Exchange Workshop, Albuquerque, March 1988.

173 M. Helie and G. Plante, *HLW Container corrosion in geological disposal conditions*, in L. Werme (ed.), Scientific Basis for Nuclear Waste Management **IX**, p. 445, 1985.

174 P. Kreis, *Hydrogen Evolution from corrosion of iron and steel in low/intermediate level waste repositories*, NAGRA Technical Report 91-21, 1991.

175 P. Kreis and J.P. Simpson, *Hydrogen gas generation from the corrosion of iron in cementitious environments*, in Corrosion problems related to nuclear waste disposal, European Federation of Corrosion Publication number 7, Institute of Materials, 1992.

176 F.A. Posey and A.A. Palko, *Corrosivity of carbon steel in concentrated chloride solution*, Corrosion **35**(1), 38, 1979.

177 R.J. Reda, S.L.A. Hana and J.L. Kelly, *Intergranular attack observed in radiation enhanced corrosion of mild steel*, Corrosion **44**(9), 632, 1988.

178 J.P. Simpson and J. Weber, *Hydrogen evolution from corrosion in nuclear waste repositories*, UK Corrosion '88, p. 33, 1988.

179 J.P. Simpson, R. Schenk and B. Knecht, *Corrosion rate of unalloyed steels and cast irons in reducing granitic groundwaters and chloride solutions*, p. 429 in Scientific Basis for Nuclear Waste Management **IX**, L.Werme (ed.), 1985.

180 R. Schenk, *Untersuchungen uber die wasserstoffbildung durch eisen korrosion unter endlagerbdingungen*, NAGRA Technical Report 86-24, 1988.

181 J.P. Simpson and P.H. Vallotton, *Experiments on container materials for swiss high-level waste disposal projects Part III*, NAGRA Technical report 86-25, 1986.

182 D.J. Smith and O.J. Van Der Schijff, *Corrosion of galvanised steel and carbon steel in deaerated aqueous solutions of industrial fertiliser chemicals*, British Corrosion Journal **24**(3), 189, 1989.

183 D. Stahl and N.E. Miller, *Long-term performance of materials used for high-level waste packaging*, NUREG/CR-3427, 1984.

184 H.W. Tas, W. Debruyn and J. Dresselaers, *Compatibility of candidate overpack materials with deep argillaceous HLW disposal environments*, IAEA-TECDOC-421, 1987.

185 R.E. Westerman, J.H. Haberman, S.G. Pitman, K.H. Pool, K.C. Rhoads and M.R. Telander, *Annual report - FY 1986, Corrosion behaviour of A216 grade WCA mild steel and Ti grade 12 alloy in hydrothermal brines*, Battelle report PNL/SRP-6221, 1988.

186 F.S. Felicione, S.M. Frank and D.D. Keiser, *WIPP gas-generation. Experiments*, INL/EXT-07-12631, 2007.

187 C.T. Lee, Z. Quin, J.J Noel and D.W. Shoesmith, *Corrosion of stainless steel liners within failed nuclear waste containers*, in J. Luo *et al*. (eds), Environmental degradation in materials and corrosion controls of metals, Proceedings of the International Symposium, Vancouver, August 24-27, 2003, pp. 433-444, Canadian Institute of Mining, Metallurgy and Petroleum, 2003, http://publish.uwo.ca/~zqin/Publications/COM2003-433.pdf accessed on 14 August 2014.

188 B.W.A. Sherar, P.G. Keech, D.W. Shoesmith, *The effect of sulfide on the aerobic corrosion of carbon steel in near-neutral pH saline solutions*, Corrosion Science **66**, 256–262, 2013.

189 J. Stoulil, J. Kanˇok, M. Kourˇil, H. Parschová, P. Novák, *Influence of temperature on corrosion rate and porosity of corrosion products of carbon steel in anoxic bentonite environment*, Journal of Nuclear Materials **443**, 20–25, 2013.

190 H. Wall and L. Wadsö, *Corrosion rate measurements in steel sheet pile walls in a marine environment*, Marine Structures **33** 21–32, 2013.

191 F.A. Martin, S. Perrin and C. Bataillon, *Evaluating the corrosion rate of low alloyed steel in Callovo-Oxfordian clay: towards a complementary EIS, gravimetric and structural study*, Mater. Res. Soc. Symp. Proc. Vol. 1475, 2012.

192 D.J. Blackwood, L.J. Gould, C.C. Naish, F.M.Porter, A.P. Rance, S.M. Sharland N.R. Smart, M.I. Thomas and T. Yates, *The localised corrosion of carbon steel and stainless steel in simulated repository environments*, AEA Technology Report AEAT/ERRA-0318, 2002.

193 S.A. Byakova, V.F. Loskutov and I.S. Pogrebova, *Influence of vanadising on the corrosion rate of steels*, Zaschita Metallov **12**, 552, 1976.

194 D.M. Drazic and C.S. Hao, *Inhibition of anodic dissolution of iron in alkaline solutions*, Corrosion Science **23**, 683, 1983.

195 M.A. Hubbe, *Polarisation Resistance corrosivity test with a correction for resistivity*, British Corrosion Journal **15**, 193, 1980.

196 P.K. Lesnikova and M.K. Frejd, *The effect of boriding on the corrosion resistance of steels*, Zaschita Metallov **16**, 312, 1980.

197 W. Schwenk, *Some aspects of the corrosion of iron in alkaline solutions and associated fundamental questions*, Werkstoffe und Korrosion **34**, 287, 1983.

198 R. Fujiwara, I. Yasutomi, K. Fukudome, T. Tateishi and K. Fujiwara, *Influence of oxygen concentration and alkalinity on the hydrogen gas generation by corrosion of carbon steel*, Mat. Res. Soc. Symp. Proc. **663**, 497, 2001.

199 C.M. Hansson, *The corrosion rate of mild steel in deaerated synthetic cement pore solution*, SKB-1984-11-14, 1984.

200 P. Kreis, *Wasserstoffentwicklung durch korrosion von eisen und stahl in anaeroben, alkalischen medien im hinblick auf ein SMA-Endlager*, NAGRA-NTB-93-27, 1993.

201 F. Matsuda, R. Wada, K. Fujiwara, A. Fujiwara, *An evaluation of hydrogen evolution from corrosion of carbon steel in low/intermediate level waste repositories*, Scientific Basis for Nuclear Waste Management XVIII. Part I; Kyoto; Japan; 23-27 Oct. 1994. 719-726, 1994.

202 C. Andrade and C.M. Alonso, *Values of corrosion rate of steel in concrete to predict service life of concrete structures*, in: Application of accelerated corrosion tests to service life prediction of materials, ASTM 1194, p. 282, 1994.

203 C. Andrade, C. Alonso and J.A. Gonzalez, *Results of polarization resistance and impedance of steel bars embedded in carbonated concrete contaminated with chlorides, in* Electrochemical methods in corrosion research (3rd international symposium), Zurich (Switzerland), 12-15 Jul 1988, Mater. Sci. Forum, **44-45,** 329-335, 1989.

204 M.A. Baccay, N. Otsuki, T. Nishida and S. Maruyama, *Influence of cement type and temperature on the rate of corrosion of steel in concrete exposed to carbonation*, Corrosion/2005, Paper 05332, 2005.

205 H.T. Cao, L. Bucea and V. Sirivivatnanon, *Corrosion rates of steel embedded in cement pastes*, Cement and Concrete Research **23**(6), 1273-1282, 1993.

206 W-J. Chitty, P. Dillmann, V. L'Hostis and C. Lombard, *Long-term corrosion resistance of metallic reinforcements in concrete. A study of corrosion mechanisms based on archaeological artefacts*, Corrosion Science **47**(6), 1555-1581, 2005.

207 J.A. Gonzalez, W. Lopez and P. Rodriguez, *Effect of moisture availability on corrosion kinetics of steel embedded in concrete*, Corrosion **49**(12), 1004, 1993.

208 T.J. Hakkarainen, *Corrosion of reinforcing steel in concrete - electrochemical laboratory experiments*, Electrochemical Methods in Corrosion Research (3rd International Symposium), Mater. Sci. Forum **44-45**, 347-356, 1989.

209 W. Hauser and R. Köster, *Corrosion behaviour of nodular cast iron casks for low and intermediate level wastes*, p. 437 in Scientific Basis for Nuclear Waste Management **IX**, L.Werme (ed.), 1985.

210 D.J. Lee, *PETF Phase III Generic Studies. Generic report on the corrosion of mild steel in contact with cement pastes*, CPDG(88)P019, PETF(88)P39, 1988.

211 D.K. Lysogorski, P. Cros and, W.H. Hartt, *Performance of corrosion resistant reinforcement as assessed by accelerated testing and long term exposure in chloride contaminated concrete*, Corrosion/2005, paper 05258, 2005.

212 H. Saito, Y. Miyata, H. Takazawa, K. Takai, G. Yamauchi, *Corrosion rate measurements of steel in carbonated concrete*, Corrosion`95, NACE, Paper 544, 1995.

213 K.K. Aligizaki, *Assessing corrosion rates of steel in chloride contaminated concrete using different techniques*, NACE International Corrosion Conference and Expo, 2007.

214 S. P. Arredondo-Rea, R. Corral-Higuera, J. M. Gómez-Soberón, J.H. Castorena-González, V. Orozco-Carmona, J.L. Almaral-Sánchez, *Carbonation rate and reinforcing steel corrosion of concretes with recycled concrete aggregates and supplementary cementing materials*, Int. J. Electrochem. Sci. **7**, 1602–1610, 2012.

215 A. Boden and S. Pettersson, *Development of rock bolt grout and shotcrete for rock support and corrosion of steel in low-pH cementitious materials*, SKB Report R-11-08, 2011.

216 O Geng, Y Yuan and F Li, *Study on the corrosion rate of steel bars in concrete under high humidity conditions*, Int. J. Modeling, Identification and Control **7**(2), 2, 2009.

217 R.R. Hussein, *Time dependent electrochemical effect of saturated area in capillary and gel pores of concrete on the corrosion rate of embedded steel reinforcement*, Int. J. Electrochem. Sci. **7**, 1402 – 1411, 2012

218 H. Xu, Z. Chen, B. Xu and D. Ma, *Impact of low calcium fly ash on steel corrosion rate and concrete steel interface*, The Open Civil Engineering Journal **6**, 1-7, 2012.

219 M.Yokota, J-W. Kyung and H-S. Lee, *Environmental influence on the corrosion rate of steel bars embedded in concrete*, ISIJ International, **48**, 230-234, 2008.

220 Y Yuan, Y Ji and J Jiang, *Effect of corrosion layer of steel bar in concrete on time-variant corrosion rate*, Materials and Structures **42**, 1443-1450, 2009.

221 A.A. Bragard and H.E. Bronnarens, *Prediction at long terms of the atmospheric corrosion of structural steels from short term experimental data*, p. 339 in: S.W. Dean and E.C. Rhea (eds.), Atmospheric Corrosion of Metals, ASTM STP 767, 1980.

222 H.R. Copson, *Long-time atmospheric corrosion tests on low alloy steels*, ASTM Proceedings **60**, 650, 1960.

223 S. Feliu, M. Morcillo and S. Feliu Jr., *The prediction of atmospheric corrosion from meteorological and pollution parameters - I. Annual corrosion*, Corrosion Science **34**(3), 403, 1993.

224 S. Feliu, M. Morcillo and S. Feliu Jr., *The prediction of atmospheric corrosion from meteorological and pollution parameters - II. Long-term forecasts*, Corrosion Science **34**(3), 415, 1993.

225 D. Knotkova, K. Barton and B. Van Tu, *Atmospheric corrosion in maritime industrial atmospheres: laboratory research*, p. 290 in: S.W. Dean and T.S. Lee (eds.), Degradation of metals in the atmosphere, ASTM STP 965, 1988.

226 C.R. Shastry, J.J. Friel and H.E. Townsend, *Sixteen year atmospheric corrosion performance of weathering steels in marine, rural and industrial environments*, pg. 5 in: S.W. Dean and T.S. Lee (eds.), Degradation of metals in the atmosphere, ASTM STP 965, 1988.

227 D. de la Fuente, I. Díaz, J. Simancas, B. Chico and M. Morcillo, *Long-term atmospheric corrosion of mild steel*, Corrosion Science **53**, 604–617, 2011.

228 S.M. Morsy, S.M. El-Raghy, A.A. Elsaed and A.E. El-Mehairy, *Effect of cations on the corrosion of stainless alloys in saline water at elevated temperatures*, Arab Republic of Egypt Atomic Energy Establishment Report 232, 1979.

229 A.L. Alexander, C.R. Southwell and B.W. Forgeson, *Corrosion of metals in tropical environments, Part 5 - stainless steel*, Corrosion **17**(7), 345t, 1961.

230 S.M. Sharland and C.J. Newton, *The long term prediction of corrosion of stainless steel nuclear waste canisters*, in Scientific Basis for Nuclear Waste Management **XII**, W. Lutze and R.C. Ewing (eds.), Materials Research Society Symposium Proceedings, **127**, p. 373, 1989 and Nirex Report NSS/R136, 1989.

231 D.J. Blackwood, C.C. Naish, S.M. Sharland and A.M. Thompson, *An experimental and modelling study to assess the initiation of crevice corrosion in stainless steel containers for radioactive waste*, AEA Technology Report AEAT/ERRA-0300, 2002.

232 N.R. Smart and N.J. Montgomery, *The repassivation of carbon steel and stainless steel in deaerated alkaline conditions: an electrochemical and surface analytical investigation*, AEA Technology Report AEAT/R/ENV/0232, 2001.

233 S. Yoshida, H. Tanabe, T. Sakuragi, T. Nishimura, O. Kato and T. Tateishi, *Stainless steel corrosion rate under geological disposal conditions,* Draft paper 2013.

234 The Agency of Natural Resources and Energy of the Ministry of Economy, Trade and Industry of Japan, *Research and development of processing and disposal technique for TRU waste containing I-129 and C-14 (FY2012)*, 2013 (in Japanese).

235 J.F. McGurn and B.A. McKean, *Stainless steel for reinforcing bar in concrete*, in Environmentally induced cracking of metals, 39th Annual Conference of Metallurgists of CIM; Ottawa, Ontario; Canada; 20-23 Aug. 2000, 253-263, 2000.

236 D.J. Cochrane, *Stainless steel reinforcement for durability in concrete structures*, Nuclear Energy **37**(5), 331-5, 1998.

237 M.F. Hurley and J.R. Scully, *Threshold chloride concentrations of selected corrosion resistant rebar materials compared to carbon steel*, Corrosion/2005, paper 05259, 2005.

238 L. Bertolini, M. Gastaldi, T. Pastore, M.P. Pedeferri, *Corrosion behaviour of stainless steels in chloride contaminated and carbonated concrete*, International Journal for Restoration of Buildings and Monuments **6**(3), 273-292, 2000.

239 K. W. J. Treadaway, R. N. Cox and B. L. Brown, *Durability of corrosion resisting steel in concrete*, Proc. Inst. Civ. Engrs., Part 1 **86**, 305-331, 1989.

240 I.O. Wallinder, J. Lu, S. Bertling and C. Leygraf, *Release rates of chromium and nickel from 304 and 316 stainless steel during urban atmospheric exposure - a combined field and laboratory study*, Corrosion Science **44**(10), 2303-2319, 2002.

241 J.S. Lu, I. Odneval and C. Leygraf, *Atmospheric corrosion of 304 and 316 stainless steels*, Acta Metallurgica Sinica (English Letters) **12**(5), 958-961, 1999.

242 C.P. Jackson and N.R. Smart, *Assessment of pit propagation rates in stainless steel*, Serco Assurance Report SA/EIG/14921/C009, 2006.

243 F.M.I. Hunter and B.T. Swift, *An assessment of the generation of GDF-derived gas using the 2007 Derived Inventory*, AMEC Report AMEC/006255/001 Issue 3, 2013.

244 B.J. Little and F.B. Mansfeld, *The corrosion behaviour of stainless steels and copper alloys exposed to natural seawater*, Werkstoffe und Korrosion **42**, 331, 1991.

245 M.C. Juhas, R.D. McRight and R.E. Garrison, *Behaviour of stressed and unstressed 304L specimens in tuff repository environmental conditions*, Lawrence Livermore Report UCRL 91804, 1984.

246 M.K. Adler Flitton, and T.S. Yoder, *Underground corrosion of activated metals 6-year exposure analysis*, National Association of Corrosion Engineers Expo Annual Conference. INL/CON-05-00761 Preprint, 2006.

247 M.K. Adler Flitton, T. S. Yoder and P.K. Nagata, *The underground corrosion of selected type 300 stainless steels after 34 years*, National Association of Corrosion Engineers Expo. INL/CON-09-15408 Preprint, 2009.

248 S. Atashin, M. Pakshir and A. Yazdani, *Synergistic investigation into the marine parameters' effect on the corrosion rate of AISI 316 stainless steel*, Materials and Design **32,** 1315–1324, 2011.

249 Bechtel SAIC Company, *Aqueous corrosion rates for waste package materials*, ANL-DSD-MD-000001, 2004.

250 F. Casteels, G. Dresselaars and H. Tas, *Corrosion behaviour of container materials for geological disposal of high level waste*, Commission of the European Communities Report EUR 10398 EN, p. 3-40, 1986.

251 C. Cuevas-Arteaga and J. Porcayo-Calderón, *Electrochemical noise analysis in the frequency domain and determination of corrosion rates for SS-304 stainless steel*, Materials Science and Engineering A **435–436**, 439–446, 2006.

252 M. Pakshir, S. Atashin and A. Yazdani, *Synergistic analysis of seawater parameters' effect on corrosion rate of austenitic stainless steels 304 and 316*, Proceedings of the 29th International Conference on Ocean, Offshore and Arctic Engineering, OMAE2010, Shanghai, China, June 6-11, 2010, OMAE2010-20227.

253 J.R. Kearns, M.J. Johnson and I.A. Franson, *The corrosion of stainless steels and nickel alloys in caustic solutions*, paper 146, Corrosion '84, NACE Houston, 1984.

254 D.B. McDonald, M.R. Sherman, D.W. Pfeifer and Y.P. Virmani, *Stainless steel reinforcing as corrosion protection*, reprint from Concrete International, supplied by Nickel Development Institute, reprint number 14034, May 1995.

255 E. Rabald, *Corrosion Guide*, p. 134, Elsevier, 1968.

256 F.I. Rubinshtejn, D.E. Lashchevskaya, E. Rubinshtejn, L.M. Mamontava and V.A. Gulyaev, *Accelerated Testing of the Corrosion Resistance of Chromium-Nickel Steels in Model Environments Simulating the Manufacturing Conditions of the Synthetic Resin KFE*, Lakokras Mat. Primen, Moskau, No.3, p. 59, 1977.

257 R.C. Scarberry, D.L. Graver and C.D. Stephens, *Alloying for corrosion control. properties and benefits of alloy materials*, Materials Protection **6**(6) 54, 1967.

258 A.J. Sedriks, J.W. Schultz and M.A. Cordovi, *Inconel alloy 690 - a new corrosion resistant material*, Boshoku Gijutsu **28**, 82, 1979.

259 R.K. Swandby, *Corrosion charts: Guides to materials selection*, Chem. Eng. **69**, 186, 1962.

260 C.C. Naish, D.J. Blackwood, K.J. Taylor and M.I. Thomas, *The anaerobic corrosion of stainless steels in simulated repository backfill environments*, Nirex Report NSS/R307, 1995.

261 J.N. Wanklyn and D. Jones, *The corrosion of austenitic stainless steels under heat transfer in high temperature*, J. Nuc. Materials **2**, 154, 1959.

262 R. Fujisawa, T. Kurashige, U. Inagaki, and M. Senoo, *Gas generation behaviour of transuranic waste under disposal conditions*, Mat. Res. Soc. Symp. Proc. Vol. 556, 1999.

263 R. Wada and T. Nishimura, *Experimental study of hydrogen gas generation rate from corrosion of Zircaloy and stainless steel under anaerobic alkaline condition*, Radioactive Waste Management and Environmental Remediation, ASME 1999.

264 B. Sorensen, P.B. Jensen and E. Maahn, *The corrosion properties of stainless steel reinforcement*, p. 601 in C.L. Page, K.W.J. Treadaway and P.B. Bamforth (eds.), Corrosion of reinforcement in concrete, Elsevier, 1990.

265 E. Medina, A. Cobo and D.M. Bastidas, *Evaluation of structural behaviour and corrosion resistant of austenitic AISI 304 and duplex AISI 2304 stainless steel reinforcements embedded in ordinary Portland cement mortars*, Revista de Metalurgia **48**(6), 445-458, 2012.

266 E.A. Baker and T.S. Lee, *Long-term atmospheric corrosion behaviour of various grades of stainless steel*, p. 52 in S.W. Dean and T.S. Lee (eds.), Degradation of Metals in the Atmosphere, ASTM STP 965, 1988.

267 M.J. Johnson and P.J. Pavlik, *Atmospheric corrosion of stainless steels*, p. 461 in 'Atmospheric Corrosion' W.H. Ailor (ed.), 1982.

268 J.R. Kearns, M.J. Johnson and P.J. Pavlik, *The corrosion of stainless steels in the atmosphere*, p. 35 in S.W. Dean and T.S. Lee (eds.), Degradation of Metals in the Atmosphere, ASTM STP 965,1988.

269 J.S. Seewald, *Model for the origin of carboxylic acids in basinal brinces*, Geochem. Cosmochim. Acta 64, 3779-3789, 2001.

270 T.M. McCollom and J.S. Seewald, *Experimental studu of the hydrothermal reactivity of organic acids abd acid anions: II Acetic acid, acetate and valeric acid*, Geochem.Cosmochim. Acta 67, 3645-3664, 2003.

271 T. Yamaguschi *et al*., *A study of the chemical forms and migration of radionuclides in hull wastes*, Radioactive Waste Management and Environmental Remediation – ASME 1999.

272 H. Tanabe *et al*., *Characterisation of hull waste in underground condition*, in Proceedings of the NEA Workshop "Mobile Fission and Activation products in Nuclear waste disposal", La Baule, France 16-19, pp. 207-220, January 2007.

273 L.I. Hardy and R.W. Gillham, *Formation of hydrocarbons from the reduction of aqueous CO_2 by zero-valent iron*, Environ. Sci. Technol, **30**, 57-65, 1996.

274 T.J. Campbell, D.R. Burris, A.L. Roberts and J.R. Wells, *Trichloroethylene and tetrachoroethylene reduction in a metallic iron-water-vapour batch system*, Env. Toxicol. Chem. **16**, 625-630, 1997.

275 B. Deng, T.J. Campbell, and D.R. Burris, *Hydrocarbon formation in metallic iron/water systems*, Environ. Sci. Technol. **31**, 1185-1190, 1997.

276 Y. Hori, A. Murata and R. Takahashi, *Formation of hydrocarbons in the electrochemical reduction of carbon dioxide at a copper electrode in aqueous solution*. J. Chem. Soc., Faraday Trans. I, **85**, 2309-2326, 1989.

277 G. Henrici-Olive and S. Olive, *Fischer-Tropsch synthesis - molecular-weight distribution of primary products and reaction-mechanism*, Angewandte Chemie - International Edition **15**, 136-141, 1976.

278 M. P. Kaminsky, N. Winograd, and G.L. Geoffroy and M.A. Vannice, *Direct SIMS observation of methylidyne, methylidene and methyl intermediates on a Ni(111) methanation catalyst*, J. Am. Chem. Soc. **108**, 1315-1316, 1986.

279 M. Sasoh, *The study of the chemical forms of C-14 released from activated metals*, pp. 19-21 in NAGRA Working Report NAB 08-22, 2008.

280 Y. Yamashita, *A study on the analysis methods of C-14 chemical species*, presentation to AMEC and NDA RWMD on 12 September 2012.

281 R Takahashi, M. Sasoh, Yu. Yamashita, H. Tanabe and T. Sakuragi, *Improvement of inventory and leaching rate measurements of C-14 in hull waste, and separation of organic compounds for chemical species identification*, paper (draft) presented at MRS 2013.

282 A. Clacher, T.G. Heath, S.W. Swanton and C.A. Utton, *Leaching behaviour of low Ca:Si ratio CaO-SiO_2-H2O systems*, AMEC Report AMEC/D.003133/003 Draft Issue 2, 2013.

283 M. Sasoh, *Study on chemical behaviour of organic-14 under alkaline condition*, pp. 79-81 in NAGRA Working Report NAB 08-22, 2008.

284 N. Kogawa, *Migration of C-14 in activated metal under alkaline anaerobic condition*, pp. 99-105 in NAGRA Working Report NAB 08-22, 2008.

285 Y. Miyauchi, Y. Yamashita, J. Sakurai and M. Sasoh, *Nuclide release behaviour from activated stainless and measurement of Kd-value*, Atomic Energy Society of Japan Autumn Meeting, B23, 2011 (in Japanese).

286 *Metallic carbides*, Nature **54**, 357, 1896, doi:10.1038/054357a0.

287 J.S. Bates, *Assessment of carbide distribution in four steel samples*, Loughborough University Test Report EM/NIR/1117, to be published.

Appendix 1

Carbon-14 containing steel wastes in the UK

An assessment is made of the UK's radioactive waste inventory (RWI) on a three-year cycle. The 2013 UK RWI was published in 2014 [A1.1] and contains a best estimate for total carbon-14 of 10,743 TBq in the UK's higher activity wastes that are destined for geological disposal. The majority of this carbon-14 is associated with graphite, but some is associated with steel wastes. More detailed studies of carbon-14-bearing wastes have been undertaken by RWM's Carbon-14 Project [A1.2]. This section draws on work undertaken in 2013 and 2014 that will be published as a project report [A1.3].

Work undertaken by the RWM Carbon-14 Project has identified that the majority of the carbon-14 inventory in waste steels arises from seven distinct classes of reactor wastes, as summarised in Table A1.1. In general, the carbon-14 activities of the waste steels have been determined by activation calculations based on assumed concentrations of nitrogen-14 impurities in the steels concerned and either known or projected neutron fluxes and durations of reactor operation.

Further information concerning the UK's irradiated steel wastes, gathered by the RWM Carbon-14 IPT Project, is summarised in the following sub-sections.

ILW AGR stainless steel fuel cladding

This waste group comprises a single waste stream, 2F03/C, the encapsulated chopped and nitric acid-leached cladding from AGR fuel pins. AGR fuel cladding comprises austenitic stainless steel type 20Cr/25Ni/Nb and varies in thickness from 0.37mm to 0.46mm. This waste stream is projected to contribute 29 TBq of carbon-14 in the 2013 UK RWI. The activation calculations were based on a nitrogen precursor concentration of 100 ppm in the stainless steel.

Table A1.1: Carbon-14 activity in steel wastes from existing and legacy reactors destined for geological disposal in the UK.

Waste stream group	Carbon-14 activity (TBq) at 2200
ILW AGR stainless steel fuel cladding	29.4
ILW AGR stainless steel fuel assembly components	38.4
ILW AGR fuel stringer debris	99.5
ILW stainless steels from legacy reactor decommissioning	97.5
ILW other stainless steel reactor wastes	1.2
ILW other ferrous metal from legacy reactor decommissioning	124.3
ILW other ferrous metal reactor wastes	23.5
Total Carbon-14	**413.8**

Notes: These figures exclude about 101 TBq of carbon 14 in Scottish Policy wastes that may not be disposed to a GDF and a further 6,664 TBq of carbon-14 in stainless steel wastes that are projected to arise from a programme of new-build nuclear reactors in the UK.

ILW AGR stainless steel fuel assembly components

This waste group also comprises a single waste stream, 2F08, the stainless steel components (grids, braces and supporting guide tube) removed from AGR fuel assemblies during initial processing at the Sellafield plant. Fuel element grids and braces are reported to be made from 20Cr/25Ni/Ti stainless steel.

The specific activity data for this waste stream in the 2013 UK RWI is significantly higher than that for the AGR fuel cladding, which would be exposed to a similar neutron flux. This data is understood to be historic and there is no information available on the basis of its derivation. Therefore, the specific activity has been re-evaluated by RWM's Carbon-14 Project based on a nitrogen concentration of 100 ppm and a fuel burn up of 33 GWd/tU (Giga Watt days per tonne of uranium). The revised carbon-14 activity of 38 TBq for 2F08 is a 170 TBq reduction compared to the activity in the 2013 UK RWI.

ILW AGR fuel stringer debris

The waste streams (nine in total) comprising this category are classified as either miscellaneous activated components and/or fuel stringer debris, which are stored in vaults at the AGR stations. In addition to stainless steel, many of these waste streams contain lesser amounts of graphite and Nimonic alloy. Limited information is available on the stainless steel composition(s), but in some cases is stated to be 18Cr/9Ni/Nb; tie bars comprise Nimonic PE16 (high cobalt steel).

The nitrogen impurity concentrations used for the activation calculations are not known. Historically, the inventories of these waste streams combined the activities of the graphite and steel components. In the 2013 UK RWI, these two contributions have been separated, however, some inconsistencies have been found. Électricité de France Energy (EDFE) is currently re-evaluating the activities for all its AGR ILW vaults.

ILW stainless steels from legacy reactor decommissioning

This waste group comprises 18 waste streams that will arise principally from the final stage clearance of the UK's commercial Magnox (34.4 TBq) and AGR (11.1 TBq) reactors and the Sizewell B Pressurised Water Reactor (PWR, 35.3 TBq). It also includes waste streams from submarine reactors (7.1 TBq) and the Vulcan Naval Test Reactor at Dounreay (9.6 TBq).

The predominant grade of stainless steel in Magnox reactors is EN58B (equivalent to AISI Type 321, a titanium stabilised grade); other steels identified across the Magnox fleet include BS970-EN56; BS970-EN59; BS970-EN59F; BS970-321S12; BS980-CDS20; BS1631/1950 and BS1508-821[20]. No information is currently available concerning the relative quantities of these different steel grades; information in the 2013 UK RWI states that component thicknesses vary between a few mm and 25 mm.

[20] It has proved difficult to find accurate data for the compositions of these various grades of steel, because many of them are old grades and the information is not readily available.

For activation calculations, a nitrogen impurity concentration of 1,000 ppm was assumed for all grades of Magnox stainless steels with the exception of Bradwell, where 1,500 ppm was assumed. Magnox Limited is reported to have information supporting the use of these high concentrations in the calculations.

No details are available concerning the stainless steel types, component thicknesses or the nitrogen precursor levels used in activation calculations for AGR decommissioning wastes. Likewise no information is available concerning the types of stainless steels arising from the Sizewell B PWR (waste stream 3S306). The estimated carbon-14 activity for 3S306 of ~35 TBq in Table A1.1 comes from a recent review of carbon-14 activity data by EDFE and is based on a nitrogen impurity concentration of 500 ppm. This new estimate is significantly lower than the total carbon-14 activity of ~120 TBq for the waste stream in the 2013 UK RWI.

Stainless steels from nuclear submarines, including Vulcan, are reported to comprise austenitic and low-alloy steels.

ILW other stainless steel reactor wastes

This category consists of a single waste stream, 3SO3, spent cartridge filters from the Sizewell B PWR. The filters comprise 85% 304 stainless steel.

ILW other ferrous metal from legacy reactor decommissioning

Other ferrous metal waste streams comprise predominantly mild steels that will arise from final dismantling and site clearance (FDSC) of reactor structures, principally from Magnox (90 TBq) and AGR reactors (18 TBq) but with sizeable contributions (16 TBq) from other UK reactors.

For Magnox reactors, the 2013 UK RWI reports a range of standard steel grades including BS14, BS15, BS1501, BS592, COHLO (PV) steel and BS970 (1955)-EN3A and BS970 (1955)-EN5. Magnox Limited has reported in the 2013 UK RWI that metal thicknesses are likely to vary from a few mm to about 100 mm. Table A1.2 below presents grades and material thicknesses for mild steel components from the Calder Hall Magnox reactor

(waste stream 2A311) provided by Magnox Limited. The nitrogen impurity concentration assumed for all grades in activation calculations is 200 ppm.

Table A1.2: Mild steel reactor components from the Calder Hall Magnox reactors.

Component	Grade	Thickness (mm)
Main pressure vessel shell	COHLO 1 (or LOWTEM)	51
Vessel reinforcing plates	BS 1501-157B	114
Inlet/outlet ducts	Plate	13
Charge tubes	BS1507-151B	6
Diagrid	BS 15	10 - 32
Core support plates	BS 15	102
Gas flow fairings	Plate	6
Vessel support A frames	-	19 - 25
Thermal Shield Plates (on inside of bioshield)	-	152

No details are available concerning the types of other ferrous metal wastes, component thicknesses or the nitrogen precursor levels used in activation calculations for AGR FDSC wastes.

ILW other ferrous metal reactor wastes

This waste group comprises redundant or defective equipment from Magnox reactors including absorber bars, fuelling machine equipment (ropes and grabs), thermocouple wires, burst can detector equipment (pressure safety valves) and other debris, which are made predominantly from steels. However, no specific information is available concerning steel grades.

The activities of these components are calculated using neutron activation calculations, with an assumed nitrogen concentration of 200 ppm for mild steel and 1,000 ppm for stainless steel.

References

A1.1 See http://www.nda.gov.uk/ukinventory/, accessed on 23 May 2014.

A1.2 Nuclear Decommissioning Authority, *Geological Disposal. Carbon-14 Project – Phase 1 Report*, NDA/RWMD/092, December 2012.

A1.3 A.C. Adeogun, *Carbon-14 Project Phase 2: Inventory (Tasks 1& 2)*, AMEC Report AMEC/200047/003 (Pőyry/390936/Phase 2), to be published.

Appendix 2

KIT-INE corrosion studies relevant to CAST WP2

KIT-INE is dealing with waste forms and the barrier behaviour with respect to geochemical processes relevant for the long-term safety within the German Disposal Safety Case. KIT-INE is the owner of irradiated steel and irradiated Zircaloy cladding material and has full rights on the materials including the right of open publication of all results. The irradiation history of these materials is known.

In the period between 1980 and 2005, KIT-INE performed numerous corrosion studies with different metallic canister materials. At this time, a clear decision was taken in Germany to establish an HLW disposal facility in the Gorleben salt dome [A2.1]. Initially, only high level waste glass was considered as a heat-producing wasteform, but shortly after, the POLLUX cask was designed as the disposal cask for spent nuclear fuel elements [A2.2]. The POLLUX cask consists of a shielding cask with a screwed lid and an inner cask with bolted primary and welded secondary lid. The inner cask consists of fine-grained steel 15 MnNi 6.3, the thickness of the cylindrical wall is 160 mm according to mechanical and shielding requirements. The outer cask provides shielding. Its thickness is 265 mm and it consists of cast iron GGG 40. The weight of the inner cask (including spent fuel is 31 Mg, the weight of the outer cask is 34 Mg. In total 10 complete PWR fuel elements can be stored in a POLLUX cask. Another possibility is the accommodation of consolidated fuel rods (5.4 tHM).

For Gorleben, disposal of POLLUX casks was foreseen in horizontal galleries at distances of several meters between the galleries and between each cask. Afterwards, the galleries should be backfilled using crushed rock salt. As a consequence of the decision in Germany, most of the corrosion investigations have been directed towards the actively corroding fine-grained steels and the cast iron GGG 40. The investigations covered the temperature range up to 200°C and different salt brine compositions (Table A2.1).

Table A2.1: Composition of salt solution mainly applied in the corrosion studies.

Component	NaCl solution mol l^{-1}	$MgCl_2$ solution mol l^{-1}
Na	4.43	0.24
K	0.03	0.63
Ca	0.01	-
Mg	-	2.93
Cl	4.43	6.50
SO_4	0.03	0.12
H_2O	40.83	36.50
pH	5.70	4.00

In CAST WP2 KIT had intended to investigate the release of carbon-14 from irradiated Inconel samples under non-oxidising, acidic conditions. The samples originate from a spring in a test fuel rod designed for keeping the fuel pellet in close contact. However, recent information provided by Areva shows that fuel rods produced in the 1980s, the springs were not produced from Inconel but from stainless spring steel 1.4568. According to the steel key tables, this spring steel 1.4568 is an austenitic steel X7-CrNiAl-17-7-1 (0.07 % C, 17% Cr, 7% Ni, 1% Al). Characteristic data of the fuel rod segment where the spring was incorporated and its irradiation history are shown in Table A2.2. The KIT experiments will deliver the quantification and chemical speciation of carbon-14 in this material.

Table A2.2: Characteristic data of the fuel rod segment N0204 KKG-BS studied by KIT [A2.3].

Property	**Value**
initial enrichment:	3.8% ^{235}U
pellet diameter:	9.3 mm
pellet density:	10.41 g·cm^{-3}
rod diameter:	10.75 ± 0.05 mm
Zircaloy wall thickness:	0.725 mm
initial radial gap:	0.17 mm
number of cycles:	4
average burn-up:	50.4 GWd/t_{HM}
av. linear power:	260 W/cm
max. linear power:	340 W/cm
discharge date:	27. May 1989
duration of irradiation:	1226 days
storage time:	23 years

With respect to corrosion of stainless steels, in 1981 a report was published describing the corrosion behaviour and the mechanical testing of metallic materials considered for construction of containers for vitrified HLW [A2.4]. The investigations included the potential barrier properties of the materials in a disposal system. The tested materials are listed in Table A2.3.

Table A2.3: List of metallic materials considered for construction of containers for HLW glass.

No.	Registered Trade Name	Material No.	DIN ID
1		1.4306	X 3 CrNi 189
2		1.4417	X 2 CrNiMoSi 195
3		1.4439	X 3 CrNiMoN 17135
4		1.4462	X 2 CrNiMoN 225
5		1.4539	X 2 NiCrMoCu 25205
6	Incoloy 800 H	1.4558	X 2 NiCrAlTi 3220
7	Inconel 625	2.4856	NiCr22Mo9Nb
8	Incoloy 825	2.4858	NiCr21Mo
9	Hastelloy C4	2.4610	NiMo16Cr16Ti
10	Fine grained steel	1.0566	FStE 355
11	ELA-Ferrit	1.4591	X 1 CrMoTi 182
12	TIKRUTAN RT 12	3.7025.10	Ti99.7-Pd

Table A2.4: Comparison of the chemical composition of stainless steels investigated [A2.4] with the relevant spring steel 1.4568

Element	1.4568	1.4301	1.4306	1.4558
C	0.07	0.06	0.03	≤ 0.04 - 0.1
Cr	17	18.0 – 20.0	18.0 – 20.0	19-21
Ni	7	8.0 – 10.5	9.0 – 13.0	30-34
Al	1	-	-	0.15-0.6
Mn	2	2	2	
Fe	Bal.	Bal.	Bal.	Bal.

The stainless steels 1.4301 and 1.4306 have relatively similar compositions to the spring steel 1.4568; however for steels, the corrosion behaviour cannot be directly related to the elemental composition. In the case of stainless steels, chromium oxide forms as a

protective layer onto the surface. This chromium oxide layer is unstable in the presence of chloride in attacking solutions. Chromium also reacts with carbon forming chromium carbide onto the grain boundaries. This effect may give rise to inter-crystalline corrosion processes. The materials shown in Table A2.3 were analysed with respect to mass losses, pitting and crevice corrosion, corrosion susceptibility by stress cracking and inter-crystalline corrosion. Relevant for CAST are the integral mass loss rates. The mass loss rates were determined using samples where the corrosion products have been removed by application of appropriate etchants. The corrosion tests were performed in $MgCl_2$ solutions (Table A2.1) at 170°C and atmospheric pressure. For example, the following maximum and minimum corrosion rates were obtained [across the range of materials studied]:

- for the material ELA-Ferrit (steel 1.4591), the average mass loss rate was extremely high and in the range of 7840 $mg \cdot m^{-2} \cdot d^{-1}$ after 40 days, decreasing to 2700 $mg \cdot m^{-2} \cdot d^{-1}$ after 135 days [these are equivalent to about 1 µm d^{-1} at 40 days and 0.34 µm d^{-1} after 135 days, assuming uniform corrosion];
- for the Ti-Pd alloy (TIKRUTAN RT 12), very low corrosion rates were determined: 1 mg m^{-2} d^{-1} after 33 days and 0.3 $mg \cdot m^{-2} \cdot d^{-1}$ after 130 days.

Hastelloy C4, a nickel-based material, was investigated in more detail. Experiments were performed in salt brines as well as under γ irradiation between 10 to 1000 Gy h^{-1}. It was found that Hastelloy C4 alloys showed corrosion from the passive state [A2.5]. Hastelloy C4 was resistant to stress corrosion cracking between 1 Gy h^{-1} and 100 Gy h^{-1} in the absence of irradiation and its general corrosion rates were low (0.1 to 0.4 µm yr^{-1}). Moreover, after 12 months exposure at 1 Gy h^{-1}no local corrosion attack had been measured. At 10 Gy $h^{-1}$and 100 Gy h^{-1}, however, pitting and crevice corrosion occurred with a maximum rate of penetration of 20 µm. At 90°C and a gamma dose rate of 1000 Gy h^{-1}general corrosion rates of Hastelloy C4 in salt brines were much higher than in the absence of irradiation. Moreover, heavy pitting and crevice corrosion up to 1 mm yr^{-1} has been observed on Hastelloy C4.

The results for relevant stainless steels and the nickel alloys 1-8 in Table A2.3, as published in reference [A2.4], are shown in Figure A2.1. Apart from steels 1.4417 and 1.4439, the mass losses were in the range of 80 to 100 $g \cdot m^{-2} \cdot yr^{-1}$ at 170°C in $MgCl_2$ solution [this is equivalent to between 10 and 13 µm yr^{-1} assuming uniform corrosion].

These corrosion rates of the chromium-nickel steels are in many cases not applicable [to uniform corrosion], as these steels undergo local corrosion phenomena such as pitting or crevice corrosion resulting in much deeper penetration into the materials than would be expected from linear mass loss rates.

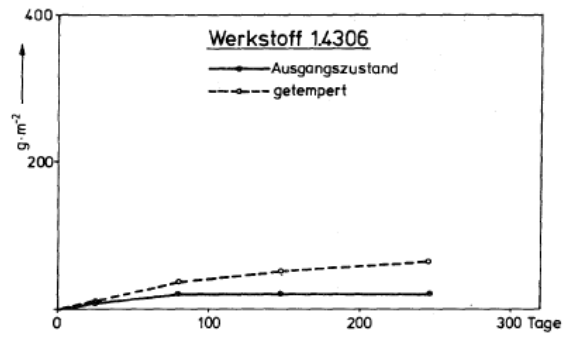

Fig. 1 Mass loss of steel 1.4306

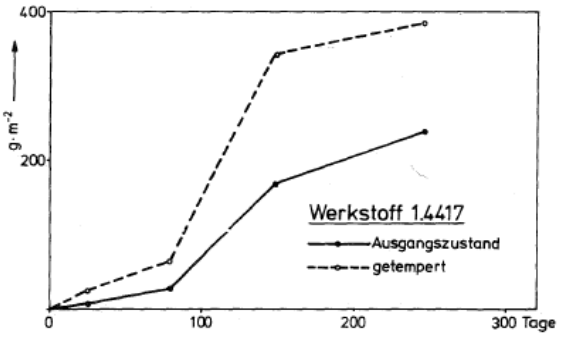

Fig. 2 Mass loss of steel 1.4417

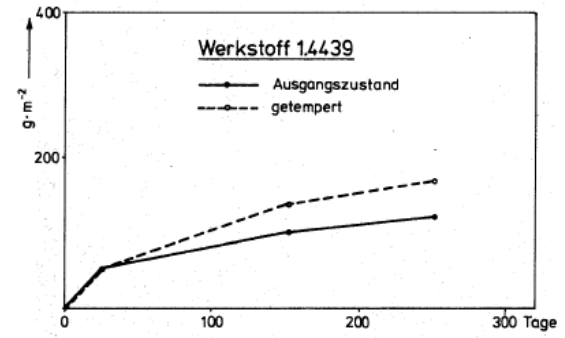

Fig. 3 Mass loss of steel 1.4439

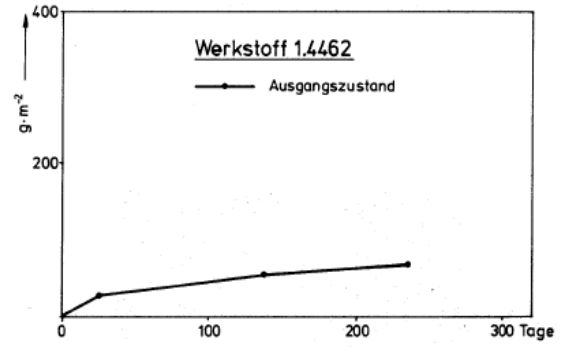

Fig. 4 Mass loss of steel 1.4462

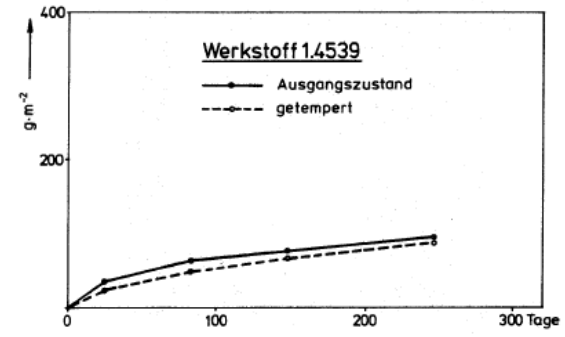

Fig. 5 Mass loss of steel 1.4539

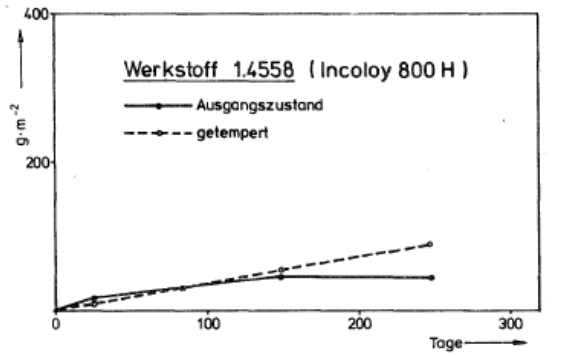

Fig. 6 Mass loss of steel 1.4558

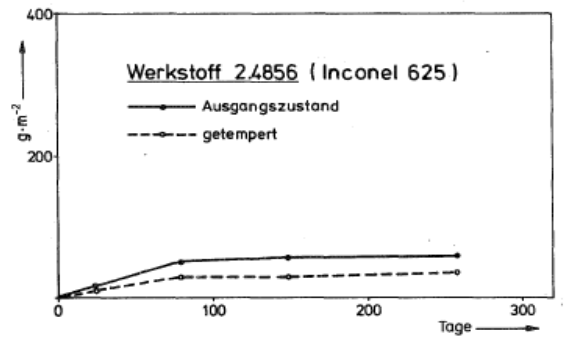

Fig. 7 Mass loss of steel 2.4856

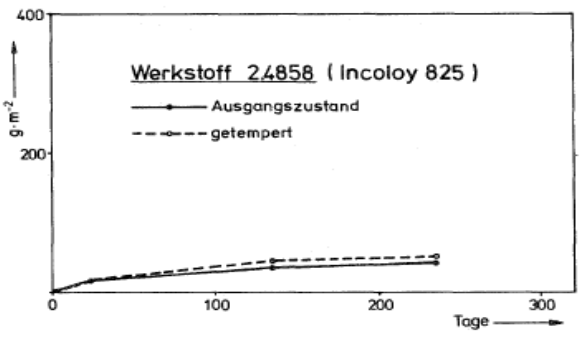

Fig. 8 Mass loss of steel 2.4858

Figure A2.1: Mass loss corrosion data for a range of stainless steel and nickel alloys obtained in $MgCl_2$ solution at 170°C

References

A2.1 H. Röthemeyer, *Site investigation and conceptual design for the repository in the nuclear "Entsorgungszentrum" of the Federal Republic of Germany*, in International symposium on underground disposal of radioactive wastes, *IAEA-SM-243/48*, Otaniemi, Finland, July 2-6, 1980.

A2.2 H. Spilker, *Status of the development of disposal casks and prospects in Germany*, in *Proc. DisTec'98, September 9-11, 1998*, pp. 301-302, Kontec, Hamburg, 1998.

A2.3 B. Kienzler, V. Metz, L. Duro, and E. A. Valls, *1st Annual workshop proceedings of the collaborative project 'FIRST-Nuclides'*, Karlsruhe Institute of Technology (KIT), Karlsruhe KIT-SR 7639 2013.

A2.4 E. Smailos, W. Stichel, and R. Köster, *Korrosionsuntersuchungen und mechanische prüfungen an metallischen werkstoffen zur auslegung von behältern für verglaste hochradioaktive abfälle als barriere im endlager*, Forschungszentrum Karlsruhe KfK 3230, 1981.

A2.5 E. Smailos, W. Schwarzkopf, R. Köster and K.H. Gruenthaler, *Advanced corrosion studies on selected packaging materials for disposal of hlw canisters in rock salt*, in 'Corrosion problems related to nuclear waste disposal', European Federation of Corrosion Publication number 7, p. 23, Institute of Materials, 1992.